# PROVENANCE OF THE NAM DUK FORMATION AND IMPLICATIONS FOR THE GEODYNAMIC EVOLUTION OF THE PHETCHABUN FOLD BELT

**Kitsana Malila**

**A Thesis Submitted in Partial Fulfillment of the Requirements for the Degree of Doctor of Philosophy in Geotechnology**

**Suranaree University of Technology**

**Academic Year 2005**

**ISBN 974-533-545-2**

# การศึกษาแหล่งกำเนิดตะกอนในหมวดหินน้ำดุกเพื่ออธิบายวิวัฒนาการด้านธรณีวิทยาแปรสัณฐานของแนวหินคดโค้งเพชรบูรณ์

นายกิจษณะ มลิลา

วิทยานิพนธ์นี้เป็นส่วนหนึ่งของการศึกษาตามหลักสูตรปริญญาวิศวกรรมศาสตรดุษฎีบัณฑิต
สาขาวิชาเทคโนโลยีธรณี
มหาวิทยาลัยเทคโนโลยีสุรนารี
ปีการศึกษา 2548

ISBN 974-533-545-2

**PROVENANCE OF THE NAM DUK FORMATION AND IMPLICATIONS FOR THE GEODYNAMIC EVOLUTION OF THE PHETCHABUN FOLD BELT**

Suranaree University of Technology has approved this thesis submitted in partial fulfillment of the requirements for the Degree of Doctor of Philosophy.

Thesis Examining Committee

_____

(Asst. Prof. Thara Lekuthai)

Chairperson

_____

(Dr. Chongpan Chonglakmani)

Member (Thesis Advisor)

_____

(Prof. Dr. Feng Qinglai)

Member

_____

(Asst. Prof. Dr. Aim-orn Tassanasorn)

Member

_____

(Dr. Tawisak Silakul)

Member

_____ _____

(Assoc. Prof. Dr. Saowanee Rattanaphani) (Assoc. Prof. Dr. Vorapot Khompis)

Vice Rector for Academic Affairs Dean of Institute of Engineering

กิจษณะ มลิลา : การศึกษาแหล่งกำเนิดตะกอนในหมวดหินน้ำดุกเพื่ออธิบายวิวัฒนาการด้านธรณีวิทยาแปรสัณฐานของแนวหินคดโค้งเพชรบูรณ์ (PROVENANCE OF THE NAM DUK FORMATION AND IMPLICATIONS FOR THE GEODYNAMIC EVOLUTION OF THE PHETCHABUN FOLD BELT) อาจารย์ที่ปรึกษา : ดร.จงพันธ์ จงลักษมณี, 163 หน้า. ISBN 974-533-545-2

บริเวณด้านทิศตะวันตกของที่ราบสูงโคราชถูกขนาบด้วยแนวเทือกเขา อายุพาลีโอโซอิกตอนปลายจนถึงอายุควาเทอร์นารี แนวเทือกเขานับจากแม่น้ำโขงทางด้านทิศเหนือจนถึงบริเวณจังหวัดสระบุรีและจังหวัดนครราชสีมาทางด้านทิศใต้ รวมระยะทางประมาณ 400 กิโลเมตร แนวเทือกเขานี้รู้จักกันในชื่อแนวหินคดโค้งเลย (Loei Fold Belt; Bunopas, 1981) อยู่ทางด้านขอบตะวันตกของแผ่นทวีปอินโดไชน่า มีทิศทางการวางอยู่ในแนวเหนือ-ใต้ ประกอบไปด้วยหินที่มีการลำดับชั้นและธรณีวิทยาโครงสร้างที่หลากหลาย มีนักวิจัยหลายท่านได้ศึกษาสภาพการเปลี่ยนลักษณะของแนวหินคดโค้งเลยหรือแนวหินคดโค้งเพชรบูรณ์ (Phetchabun Fold Belt) อย่างไรก็ตามความชัดเจนของสภาพภูมิศาสตร์บรรพกาล (paleogeography) ในช่วงอายุพาลีโอโซอิกตอนปลายยังขาดความชัดเจน จึงทำให้เกิดความหลากหลายของมุมมองทางด้านธรณีวิทยา ด้วยข้อจำกัดนี้เองการเพิ่มเติมข้อมูลใหม่จากงานวิจัยนี้ จะช่วยแปลความหมายทางด้านธรณีวิทยาในบริเวณพื้นที่ศึกษา และบริเวณภูมิภาคเอเชียตะวันออกเฉียงใต้มีความชัดเจนมากยิ่งขึ้น

งานวิจัยนี้ทำการวิเคราะห์แหล่งกำเนิดตะกอนจากหินตะกอนของหมวดหินน้ำดุก (Nam Duk Formation) และหินตะกอนอายุเพอร์เมียนบริเวณพื้นที่จังหวัดเลย สระบุรี และนครราชสีมา โดยวิธีธรณีเคมี (geochemical analysis) และเทคนิค Cathodoluminescence เพื่อศึกษาวิวัฒนาการด้านธรณีวิทยาแปรสัณฐานของแอ่งน้ำดุก และแนวหินคดโค้งเพชรบูรณ์ ผลการศึกษาสรุปได้ดังนี้

จากผลการศึกษาธรณีเคมีของธาตุออกไซต์หลัก (major elements) และธาตุหายาก (trace elements) พบว่าหน่วยหินเพลาจิก (pelagic sequence) ของหมวดหินน้ำดุก ตกตะกอนในมหาสมุทรบริเวณแนวรอยต่อระหว่างหมู่เกาะรูปโค้งในมหาสมุทร (oceanic island arc) และ หมู่เกาะรูปโค้งภาคพื้นทวีป (continental island arc) และบ่งชี้ว่าแหล่งจ่ายตะกอนหลักมาจากหินเมตาเบสิก (metabasic) จากการศึกษาเม็ดตะกอนควอตซ์ (quartz grain) ที่ตกตะกอนในหินปูน allodapic โดยวิธี Cathodoluminescence ให้สีน้ำเงินแสดงถึงแหล่งกำเนิดที่มาจากหินภูเขาไฟ (volcanic) หน่วยหินฟลิช (flysch sequence) และหน่วยหินโมลาสส์ (molasse sequence) ซึ่งประกอบไปด้วยตะกอนซิลิซิคลาสติก (siliciclastic sediments) ชั้นหนา ตกตะกอนในลำดับ

ต่อมา จากแผนผังการจำแนกลักษณะการแปรสัณฐานโดยวิธีธรณีเคมีและลักษณะของธาตุหายาก พบว่า หน่วยหินทั้งสองมีลักษณะทางเคมีที่คล้ายคลึงกันโดยมีแหล่งกำเนิดตะกอนที่สำคัญได้แก่ หินอัคนีชนิดเมฟิก (mafic igneous) หินเมตาเบสิก (metabasic) หินแกรนิติกไนต์ (granitic gneiss) และหินแปรที่มีซิลิกาต่ำ อย่างไรก็ตามหน่วยหินโมลาสส์ มีองค์ประกอบของเม็ดตะกอนควอตซ์จากหินภูเขาไฟมากกว่าหน่วยหินฟลิช โดยหน่วยหินทั้งสองตกตะกอนในบริเวณหมู่เกาะรูปโค้งภาคพื้นทวีป (continental island arc)

เมื่อเทียบลำดับความสัมพันธ์กับหินอายุพาลีโอโซอิกตอนปลายบริเวณ แนวตะเข็บน่าน-อุตรดิตถ์ (Nan-Uttaradit Suture Zone) และบริเวณแนวหินคดโค้งเพชรบูรณ์ พบว่าลำดับชั้นการตกตะกอนมีความต่อเนื่อง ซึ่งสามารถสร้างภาพการแปรสัณฐานในอดีตได้ โดยเริ่มจากลำดับการตกตะกอนของหินอัคนีในมหาสมุทร และหินเชิร์ต บริเวณแนวตะเข็บน่าน-อุตรดิตถ์ ต่อเนื่องมายังหินเพลาจิก หินทรายเกรแวคกระแสน้ำขุ่นของหน่วยหินฟลิช และหินคลาสติกน้ำตื้นของหน่วยหินโมลาสส์ ในช่วงอายุคาร์บอนิเฟอรัสต่อเนื่องถึงอายุเพอร์เมียน

ในด้านธรณีวิทยาแปรสัณฐาน ตะกอนในแอ่งน้ำดุกพัฒนามาจากการเปิดของแอ่งทางด้านทิศตะวันตกของแผ่นทวีปอินโดซิเนีย (Indosinia craton) ซึ่งเป็นผลมาจากการปิดตัวของทะเลเลย (Loei Ocean) ในช่วงอายุระหว่างดีโวเนียนถึงคาร์บอนิเฟอรัส (Intasopa and Dunn, 1994) การเปิดของแอ่งน้ำดุกคาดว่าเริ่มพัฒนาในช่วงอายุคาร์บอนิเฟอรัสตอนกลาง (Kozar et al., 1992) โดยมีตะกอนของหน่วยหินเพลาจิกซึ่งเป็นตะกอนที่เกิดในแอ่งน้ำลึกในมหาสมุทร โดยคาดว่าการสะสมของตะกอนเพลาจิก อาจเริ่มตั้งแต่ช่วงคาร์บอนิเฟอรัสตอนกลางถึงตอนปลายต่อเนื่องจนถึงเพอร์เมียนตอนต้น โดยมีแนวสะสมตะกอนลานหินปูนผานกเค้าและเขาขวาง (Pha Nok Khao and Khao Khwang Platforms) ซึ่งในอดีตอาจเป็นแนวเดียวกัน วางตัวอยู่ทางทิศตะวันออกหรือทางด้านทิศตะวันตกของแผ่นทวีปอินโดไชน่า ในช่วงบนเพอร์เมียนตอนกลาง แผ่นทวีปอินโดไชน่า (Indochina craton) ได้เคลื่อนตัวมุดชนกับแผ่นทวีปฉาน-ไทย (Shan-Thai craton) ทางด้านทิศตะวันตก โดยจ่ายตะกอนประเภทหินอัคนีเมฟิก และอัลตราเมฟิก ให้กับหน่วยหินฟลิช ในบริเวณแนวการพอกพูนซับซ้อน (accretionary complex) และตกตะกอนในสภาพแวดล้อมบริเวณด้านนอกของร่องโค้ง (outer or a fore-arc environment)

การเปลี่ยนสภาพการตกตะกอนจากหินตะกอนของหน่วยหินฟลิช ไปสู่ตะกอนของหน่วยหินโมลาสส์ อันเนื่องมาจากการปิดตัวลงของแอ่งน้ำดุก โดยมีตะกอนของหน่วยหินโมลาสส์ปิดทับบริเวณแอ่งรอบส่วนหน้าของแผ่นดิน (peripheral foreland basin) ซึ่งในช่วงเวลานี้เองคือการสิ้นสุดลงของแอ่งมหาสมุทรโดยที่การแปรสัณฐาน หรือการเปลี่ยนลักษณะได้เกิดขึ้นอย่างสูงสุด

หรือที่เรียกว่าบรรพตรังสรรค์ช่วงปลายวาริสกัน (Late Variscan orogeny; Helmcke and Lindenberg, 1983)

สาขาวิชา เทคโนโลยีธรณี
ปีการศึกษา 2548

ลายมือชื่อนักศึกษา_____
ลายมือชื่ออาจารย์ที่ปรึกษา_____
ลายมือชื่ออาจารย์ที่ปรึกษาร่วม_____

KITSANA MALILA : PROVENANCE OF THE NAM DUK FORMATION AND IMPLICATIONS FOR THE GEODYNAMIC EVOLUTION OF THE PHETCHABUN FOLD BELT. THESIS ADVISOR : CHONGPAN CHONGLAKMANI, Ph.D. 163 PP. ISBN 974-533-545-2

NAM DUK FORMATION/NAN-UTTARADIT SUTURE/PROVENANCE/ SILICICLASTIC/PERMIAN/TECTONIC

The huge “Khorat Plateau” is bordered to the west by a belt of rock that reflects a complex Late Paleozoic to Quaternary history. It includes mountain ranges that stretch from the Mekong River in the north to Saraburi and Nakhon Ratchasima in the south, a distance of approximately 400 km. These mountain belts are known as the Loei Fold Belt (Bunopas, 1981) which is located on the western margin of the Indochina plate. These N-S elongated mountain ranges are characterized by a series of different stratigraphic sequences and varying structural histories. Various researchers have studied on the deformation history of the Loei or Phetchabun Fold Belt. The paleogeographic situation of the region during Late Paleozoic time is still not clearly understood. Different scenarios have to be explored and it is expected that new data will provide a solution. This solution must be compatible with the wider geological interpretation of mainland SE Asia.

Provenance analyses of the siliciclastic sediments in the Nam Duk Formation and Permian sequences in Loei and Saraburi areas have been done based on geochemical and cathodoluminescence analysis. The geodynamic evolution of the

Nam Duk Basin and the Phetchabun Fold Belt are proposed and discussed. The results can be summarized as follows;

The pelagic sequence of the Nam Duk Formation was formed in an oceanic setting between oceanic island and continental island arc environments according to the result of major and trace elements analyses. The source of the quartz detritus in the allodapic limestone was from metabasic and volcanic provenance as indicated by geochemical and blue luminescence family quartz. The subsequent deposition of flysch and molasse sequences consists of thick siliciclastic sediments. Tectonic setting discrimination diagrams and trace elements characteristics of flysch and molasse siliciclastic sediments indicate similar geochemical characteristics. The most important sources for both flysch and molasse were from mafic igneous, metabasic, granitic gneiss, and low-silica metamorphic sources. However, the molasse contains more volcanic quartz grains and recycled sediments than the flysch. Both sequences were deposited in a continental island arc setting.

Correlation of the Late Paleozoic strata in the Nan-Uttaradit suture zone and the Phetchabun Fold Belt reveals a continuous sedimentary sequence which can be used for the paleotectonic reconstruction. An idealized vertical sequence from oceanic igneous rocks and chert (ophiolite sequence) passing upward through pelagic, greywacke turbidite (flysch) to shallow marine clastic (molasse) deposits have been proposed.

Tectonically, the Nam Duk Basin was formed as a back arc basin after the closure of small oceanic basin (Loei Ocean) in Indosinia continent during the Devonian-Carboniferous (Intasopa and Dunn, 1994). This basin rifting probably occurred in Middle Carboniferous (Kozar et al., 1992) and subsequently the pelagic

sediments were accumulated during Middle – Late Carboniferous to lower Middle Permian in a deep sea basin. The Pha Nok Khao and the Khao Khwang Platforms (or probably one coherent unit) were located in the eastern side of the Nam Duk Basin or the western margin of the Indochina plate. The subduction of Indochina beneath the Shan-Thai cratons (on the west) towards west was started in the upper Middle Permian. The provenance signature of the flysch sequence shows the mafic-ultramafic igneous source which is interpreted as being derived from the accretionary complex and it was in an outer or a fore-arc environment.

After the Nam Duk remnant ocean was closed, a peripheral foreland basin was formed with molasse sedimentation. The changing of flysch to molasse sediments as the result of the termination of the oceanic basin indicates the maximum deformation or disturbance which is known as the Late Variscan orogeny (Helmcke and Lindenberg, 1983).

School of Geotechnology

Academic Year 2005

Student's Signature _____

Advisor's Signature _____

Co-advisor's Signature _____

# ACKNOWLEDGEMENTS

First and foremost, I would like to express my gratitude to all those who gave me the possibility to complete this thesis. With a deep sense of gratitude, I wish to express my sincere thanks to my supervisors, Dr. Chongpan Chonglakmani (SUT), Prof. Dr. Dietrich Helmcke (GZG), and Prof. Dr. Feng Qinglai (CUG), for their immense help in planning and executing the works in time. Financial support for this research was provided by a grant from the Royal Golden Jubilee (RGJ) No. PHD/0140/2545 and the DAAD Scholarships which have made my stay and study in China and Germany possible.

Specials thanks to Dr.Chongpan Chonglakmani, who encouraged me to learn geology and provided me with the opportunity to work and study on an integrated multidisciplinary topic in geosciences. Over six year for field work in Thailand and China and a journey through various schools of geosciences provide me a valuable experience.

I express my indebtedness to Prof. Dr. Dietrich Helmcke, who advised and stimulated me on tectonic and supported me during my stay in Germany. Prof. Dr. D. Helmcke provided a motivating, enthusiastic and critical atmosphere during the many discussions we had. It was a great pleasure to me to conduct this thesis under his supervision. However, it was a hard shocking to learn that he had caught a serious illness during the beginning of January, 2004 on a fieldwork in northern Thailand. He passed away on April 1$^{st}$, 2004.

I am greatly appreciation to Prof. Dr. F. Qinglai, who made arrangement for me to work at the laboratory for ICPMS at the China University of Geosciences (Wuhan) and for having facilitated my interaction with a group of geologist from Yunnan during a fieldwork in southwest Yunnan and northern Thailand.

Mrs. Rucha Ingavat-Helmcke should receive indebtedness thanks for encouraging me and taking care of my life in Germany and Thailand.

My sincere thanks are due to Dr. Bent T. Hansen, Director of GZG, University of Göttingen, for providing me constant encouragement. I specially thanks Dr. A.M. Kerkhof for the help extended to me for cathodoluminescence analysis when I approached him and the valuable discussion that I had with him during the course of research. Special thanks are due to Ms. F. Doreen for timely help in every think during my stay in Germany. The cooperation I received from other peoples of this department is gratefully acknowledged. I will be failing in my duty if I do not mention the laboratory staff and administrative staff of this department for their timely help. Please receive my indebted sincere thank.

The episode of acknowledgement would not be complete without the mention and comment of my thesis committee Asst. Prof. Thara Lekuthai, Asst. Prof. Aim-orn Thassanasorn, and Dr. Taweesak Sirakul from the School of Geotechnology, Institute of Engineering, Suranaree University of Technology. I would also like to gratefully acknowledge the support of some very special individuals. They helped me immensely by giving me encouragement and friendship during a fieldwork in

Phetchabun and Loei; Mr. Mana Jatuwan, Mr. Piboon Phetchum, and Mr. Noppadon Chukorn.

I am grateful to Miss Wiyada Wong-ammart for the inspiration and moral support she provided throughout my research work and her patience was tested to the utmost by a long period of my study. My personally grateful to Khun Adul Harnsongkham for his suggestion and care.

Lastly I am grateful to thank my parent, who taught me the value of hard work by their own example. I would like to share this moment of happiness with my mother, father, brothers and sister. They rendered me enormous support during the whole tenure of my research.

Finally, I would like to thank all whose direct and indirect support helped me completing my thesis.

Kitsana Malila

# TABLE OF CONTENTS

**PAGE**

# TABLE OF CONTENTS (Continued)

**PAGE**

# TABLE OF CONTENTS (Continued)

**PAGE**

# TABLE OF CONTENTS (Continued)

**PAGE**

# TABLE OF CONTENTS (Continued)

**PAGE**

# LIST OF TABLES

**TABLE** **PAGE**

# LIST OF FIGURES

**FIGURE** **PAGE**

# LIST OF FIGURES (Continued)

**FIGURE** **PAGE**

# LIST OF FIGURES (Continued)

**FIGURE** **PAGE**

# LIST OF FIGURES (Continued)

**FIGURE** **PAGE**

# LIST OF FIGURES (Continued)

**FIGURE** **PAGE**

# LIST OF FIGURES (Continued)

**FIGURE** **PAGE**

# LIST OF FIGURES (Continued)

**FIGURE** **PAGE**

# LIST OF FIGURES (Continued)

**FIGURE** **PAGE**

# LIST OF FIGURES (Continued)

**FIGURE** **PAGE**

# CHAPTER I

# INTRODUCTION

In this Chapter, the author likes to briefly describe the geological setting of Thailand and the results of geological investigations on the evolution of the mountain belt bordering the huge Khorat Basin of Northeastern Thailand to the west. This mountain belt is known in Thai as “Dong Phaya Yen”. Due to the formerly little developed infra-structure and the wide distribution of primary jungles in this mountainous region most of the data discussed here were collected only during the past 25 years. The main intention of this summary of data obtained till now is to characterize the open questions and problems which cause the ongoing scientific controversy, and to indicate necessary directions of future research.

## 1.1 The physiographic and geological setting of Thailand

The physiography of Thailand is the consequence of the long complex geodynamic evolution during Phanerozoic time except for the Khorat Basin in northeastern part. According to recent geological interpretation, it is believed that two micro-continental blocks named Shan-Thai in the west and Indochina in the east welded together along the Nan-Uttaradit suture (Bunopas and Vella, 1978; Bunopas and Vella, 1983). The Shan-Thai terrane comprises eastern Myanmar, western Thailand, western peninsular Malaysia and northern Sumatra. The Indochina terrane comprises eastern Thailand, Laos, Cambodia and parts of Vietnam. A brief review of

the geology of both terrane are given here for the understanding and introducing of the study area. A physiographic region of Thailand is given in Figure 1.1. A simplify geological map of Thailand is given in Figure 1.2.

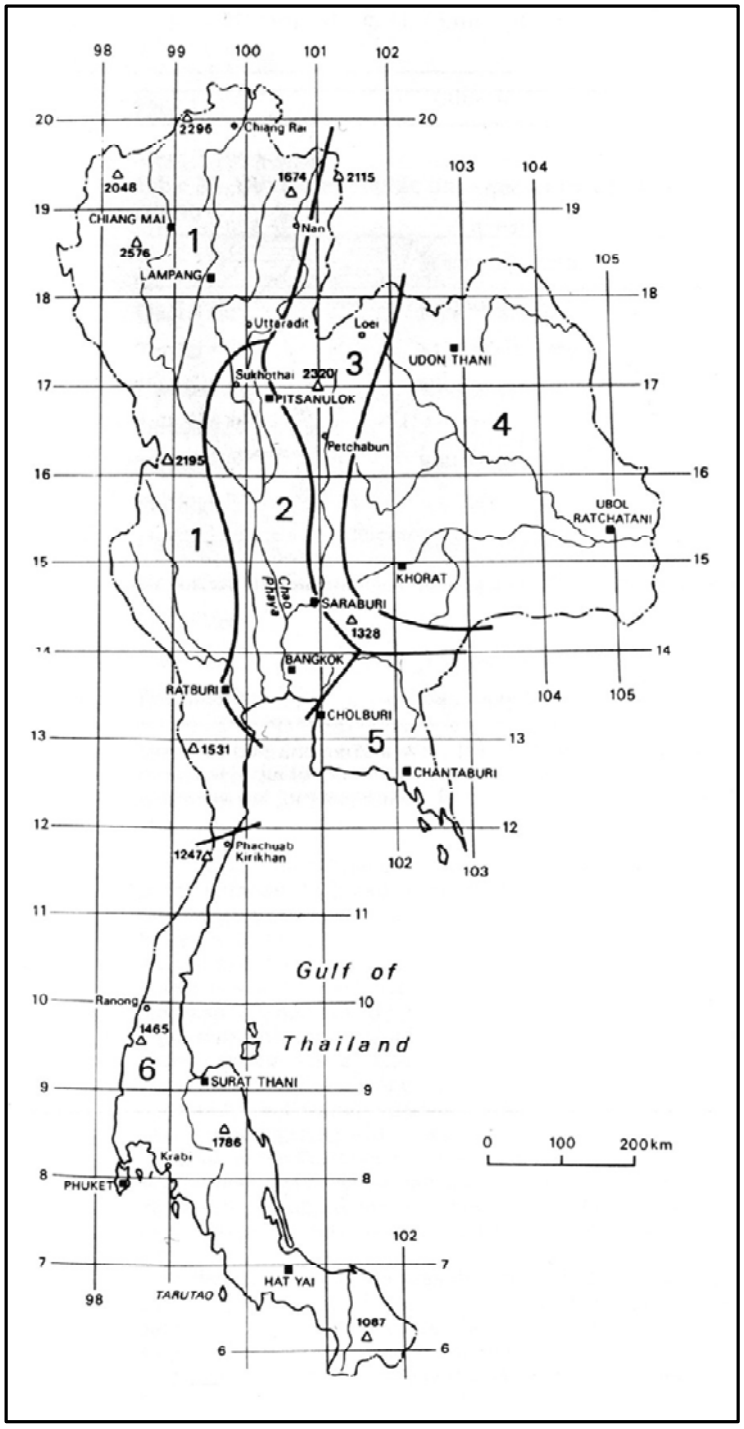


**Figure 1.1** Map of Thailand showing physiographic regions. (1 = Northern and Western mountains; 2 = Central plains; 3 = East-central hill ranges; 4 = Khorat Plateau; 5 = Southeast; 6 = South peninsular).

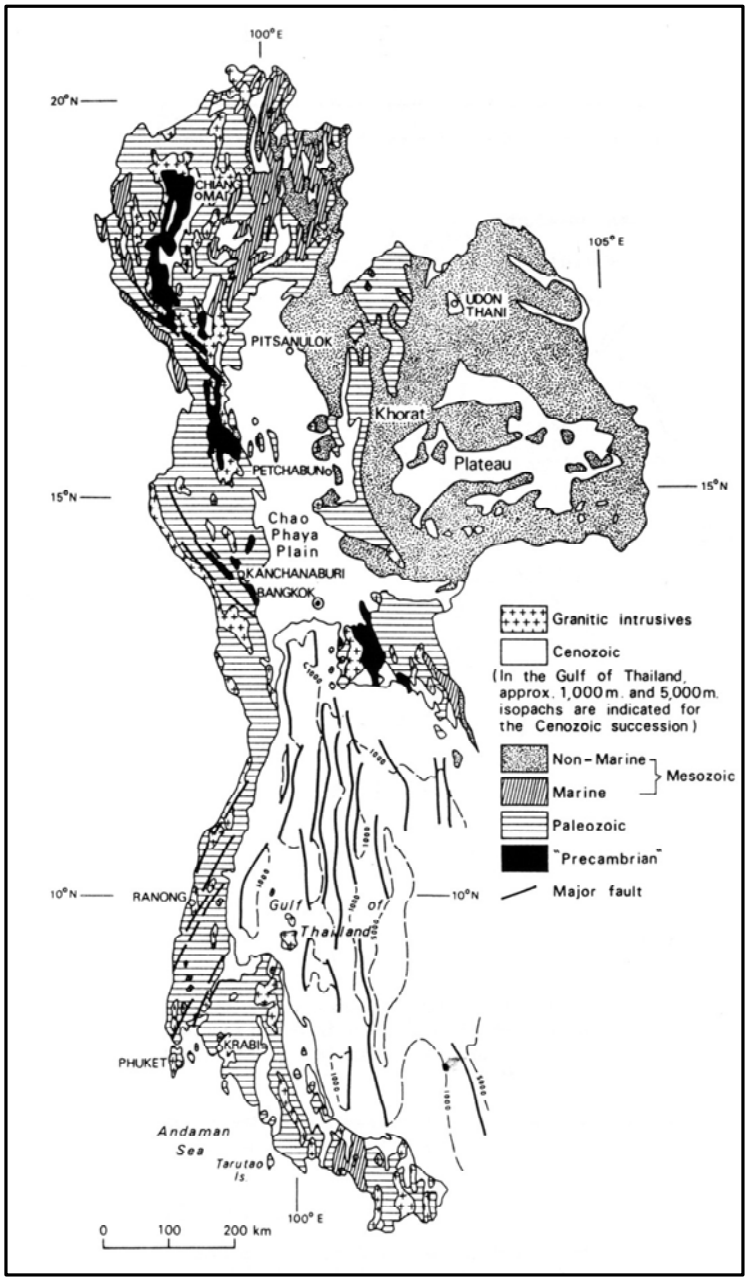


**Figure 1.2** Simplified geological map of Thailand (simplified from Geological Survey Division, Bangkok, 1987).

### 1.1.1 The Precambrian

Only Shan-Thai terrane contains the Precambrian rocks. In northwest Thailand, the first mention of "well-bedded quartzites up to 500 m thick lie stratigraphically below Ordovician limestones" belonging to the Precambrian age is reported by Baum et al. (1970). Since then, all the high grade metamorphic rocks in the western mountain range which are characterized by evidences of migmatization, were all mapped as Precambrian or inferred Precambrian rocks (Mantajit, 1975; Dheeradilok, 1975; Mantajit, 1997).

### 1.1.2 The Paleozoic

The Paleozoic rocks are divided into three parts as lower, middle and upper Paleozoic. According to Mantajit (1997), the Lower Paleozoic rocks in Thailand are well exposed in the south and on the main western range of the Shan-Thai terrane. There is no record of the Lower Paleozoic rocks in the Indochina terrane in northeast Thailand. On Shan-Thai terrane, the lower Paleozoic rocks are divided into two conformable rock units: a lower siliciclastic unit, the Tarutao Group and the upper carbonate unit, the Thung Song Group. They are closely associated with the Precambrian rocks and have often been repectively equated to the Cambrian and Ordovician. The red sandstone and shale of the Tarutao Group is a shallow-shelf sequence periodically subjected to storm (Akerman, 1986) whereas the limestone of the Thung Song Group is a shallow to deep carbonate ramp deposit (Wongwanich and Burrett, 1983; Wongwanich et al. 1983).

The Middle Paleozoic rocks of Thailand during the Silurian to Devonian can be differentiated into three rock units from the west to the east: the

Thong Pha Phum Group, The Sukhothai Group (of Shan-Thai terrane) and the Pak Chom Formation (Mantajit, 1997). The Thong Pha Phum Group is composed of back shale, chert, sandstone, siltstone and variegated nodular limestone and was deposited on shelf to back arc basin (Dheeradilok et al. 1992). The Sukhothai Group (in Sukhothai fold belt) is composed mainly of metamorphic and metavolcanic rocks including amphibolite, mica schist, agglomerate, fine-grained tuff, marble and bedded chert (Bunopas, 1992). The Pak Chom Formation (in Loei fold belt), the latest Silurian to Devonian sequence, crops out in east of Loei and west of Nong Bua Lam Phu and Udon Thani. They consist of the Silurian schist, phyllite, quartzite, metatuff, and fossiliferous limestone and unconformably overlie metamorphic rocks of the Namo Group.

The Upper Paleozoic rocks consist of Carboniferous and Permian siliciclastics and limestones which lie conformably over the Middle Paleozoic and are widely distributed throughout Thailand. In the west and the peninsula, the Thong Pha Phum Group continues from its uppermost Ordovician-Silurian-Devonian to Carboniferous without a break (Wongwanich et al. 1990 and Bunopas, 1991). The pebbly sandstone and mudstone belonging to the Thong Pha Phum Group are named the Kaeng Krachan Group by some authors (Piyasin, 1975 and Raksaskulwong and Wongwanich, 1993). In the north, the Mae Hong Son Formation is proposed for chert, sandstone and shale deposited near the cratonic axis whereas the sandstone, shale, graywacke and agglomerate of the Dan Lan Hoi Group were deposited in shallow marine condition further offshore. The Wang Sapung Formation Formation is proposed for the nearshore siliciclastics rocks interbedded with limestone along western edge of the Khorat Plateau. The Permian rocks of Thailand are dominantly

limestones and range in age from Lower to Upper Permian and can be subdivided into three Groups. The Permian karstic limestones in the west and the Peninsular are referred to as the Ratburi Group and in the north the Ngao Group. These two Groups belong to the Shan-Thai terrane. Whereas the limestones interbedded with siliciclastic rocks and chert along western and southern edges of the Khorat Plateau are known as the Saraburi Group of the Indochina terrane (Bunopas, 1992).

### 1.1.3 The Mesozoic

The Mesozoic sequences in Thailand can be lithologically suddivided into two main facies: the marine facies and the non-marine continental facies. Chonglakmani (2002) divided the Triassic sedimentary rocks into four main facies as the continental facies, the continental platform facies, marine intra-arc facies and deep marine and oceanic facies. The continental facies is widely exposed in northeastern Thailand along the edge of the Khorat Plateau. The facies consists predominently of siliciclastics rocks deposited in alluvial fan, fluvial, and lacustrine environments. It is known as the Huai Hin Lat Formation and was dated by fossils as *Dictyophyllum-Clathropteris* warm climate flora (Kon'no and Asama, 1973). The continental platform facies consists of shallow marine clastics and carbonates. It has no volcanic rocks. The facies was deposited in two separate terranes, the Shan-Murgui and Chiang Mai terranes. The marine intra-arc facies occurs only in the western part of the Sukhothai-Indosinia terrane. It consists of shallow marine siliciclastic and carbonate strata, basinal turbidites, and rhyolitic and andesitic volcanic rocks. These sequences are represented by the Scythian-Early Norian Lampang Group in the north. The deep marine and oceanic facies occurs in two linear belts. One belt is discontinuous between the Chiang Mai and Sukhothai-Indosinia terranes. This belt originates in

Chiang Rai, where it occurs as isolated sheets of pelagic Fang Chert overthrust on shallow marine carbonate and siliciclastic strata of the Chiang Mai terrane.

The marine Jurassic rocks are exposed on the western and southern parts of Thailand. Marine Jurassic strata are well exposed in the Mae Sot and Umphang areas and less extensively near Mae Hong Son, Kanchanaburi, Chumphon and Nakhon Si Thammarat in the north, west and south respectively (Meesook and Grant-Mackie, 1997). The continental facies Khorat Group covers northeastern and some part of northern Thailand. It consists of six formations in ascending order as Nam Phong, Phu Kradung, Phra Wihan, Sao Khua, Phu Phan and Khok Kruat Formations ranging from Latest Triassic to Upper Cretaceous. In general, the group consisting predominantly of red sandstone, siltstone, and mudstone. In Upper Cretaceous, the remarkable giant evaporite deposits occurred in the Maha Sarakham Formation.

### 1.1.4 The Cenozoic

The Tertiary basins in Thailand are mainly N-S trending fault-bounded grabens which were developed by conjugate strike-slip faults orientating in NW-SE and NNE-SSW directions and by clockwise rotation of the Southeast Asia crustal blocks (Polachan and Sattayarak, 1991). Over sixty Cenozoic basins are distributed in various parts of Thailand, both onshore and offshore except in the northeastern part, and are grouped in five main geographic regions: the Andaman Sea, Gulf of Thailand, Peninsular, Central and Northern Thailand (Chaodumrong et al.1983; Polachan et al. 1991).

## 1.2 Geographic setting of study area

The Khorat Plateau covers an area of about 155,000 square km. Surface elevations on the Plateau range from about 320 m in the northwest to about 100 m in the southeast and the range of elevation is about 90-200 m above sea level. The terrain is rolling, and the hilltops generally slope to the southeast in conformity with the tilt of the land. This tilting created ranges of low hills, small lakes and mountains along the western edges of the plateau. The plateau is drained by the Chi and Mun rivers and is bounded by the Mekong River (north and east on the Laos border). The Khorat Plateau was formed by uplifting along the western and southern parts. As a result, the underlying sedimentary rocks were tilted rather than uniformly uplifted. The escarpments of these uplands overlook the plain of the Chao Phraya basin (central plain) to the west and the Cambodian plain to the south.

The Phetchabun mountain range forms a barrier between the Khorat Plateau and the lower northern region and the central plains. The central part of this region is on the Pa Sak river basin with mountain ranges running along both the western and eastern sectors. The name “Khao Kao” is made up of mountain ranges to the northwest of Phetchabun province about 1174 metres above mean sea level covered mainly by deciduous plants. To the south of Phetchabun province, the continuity of mountain range covering the area of Lop Buri, Saraburi, Nakhon Ratchaisma, Prachin Buri, and Nakhon Nayok is locally named “Khao Yai” or “Khao Yai National Park”. The Khao Yai National Park covers an area of over 2,000 square km and includes one of the largest intact monsoon forests in mainland Asia. There are also several mountains of around 1000 meters including Khao Khieo and Khao Phaeng Ma.

The study area is easily accessible from Bangkok by using highway No. 1 to Saraburi province. At Saraburi junction, the study area starts when turning to highway No. 21 to the north and highway No. 2 to the east. The highway No. 21 starts from Saraburi to Lom Sak and runs parallel with highway No. 201 from Nakhon Ratchasima to Loei. Both highways are crossed cut by the highway No. 205, 225, and 12 from south to north in west-east direction respectively. The geographical information is given in Figure 1.3, provincial boundary and highway network is given in Figure 1.4.

## 1.3 Subdivision of the Loei-Phetchabun mountain belt

The mountain ranges to the west of the Khorat Plateau comprise the area of Loei, Phetchabun, Phitsanulok, Chaiyaphum, Lop Buri, Saraburi, Nakhon Ratchasima and Nakhon Nayok provinces. In this thesis, we mention only the rocks bordering the Khorat Plateau to the west. They are composed of marine Paleozoic and continental Mesozoic rocks. The continental red beds which formed the plateau to the east are cropped out as outliers in these mountain ranges.

The study area comprises two fold belts, the Phetchabun fold and thrust belt in Phetchabun province and the Loei fold and thrust belt in Loei province. The term Phetchabun fold and thrust belt is one sector of the Pak Lay-Laung Prabang and Phetchabun fold belt as proposed by Workman (1975). According to Workman (1975), this fold belt includes the areas around the Lom Sak-Chum Phae highway and the area between Muak Lek and Pak Chong in Saraburi and Nakhon Ratchasima provinces. The term Loei fold and thrust belt covers the region of Loei including the area around the Chiang Khan-Pak Chom-Sang Khom highway.

The author has divided this region into seven parts as following, the mountain region NE of Loei, the mountain region NE of Phetchabun, the mountain region of Chon Dan, the mountain region of Nakhonthai, the mountain region of Saraburi, the area east of Phetchabun along Pa Sak River, and the area of Central Plain. The geological and paleogeographical terms are based on the previous works, e.g., the Pha Nok Khao Platform (Wielchowsky and Young, 1985), the Khao Khwang Platform (Wielchowsky and Young, 1985), the Nam Duk Basin (Helmcke and Kraikhong, 1982), the Phetchabun Basin (Chaodumrong et al. 1983), and the Nakhonthai terrane (Sattayarak et al. 1989).

The Pha Nok Khao Platform covers the area of Loei, Chaiyaphum and some part of Phetchabun provinces. To the west of Pha Nok Khao Platform, the Nam Duk Basin exposes extensively along N-S direction covering the area of Phetchabun and western part of Loei provinces. To the west of Nam Duk Basin, the Khao Khwang Platform is located and covers the area of Phetchabun, Lop Buri, and Saraburi. The Tertiary Phetchabun Basin is located between the Nam Duk Basin and the Khao Khwang Platform blanketed by Quaternary sediments. To the north of Khao Khwang Platform, the Mesozoic Nakhonthai terrane is located and covers the eastern part of Phitsanulok and western part of Loei provinces.

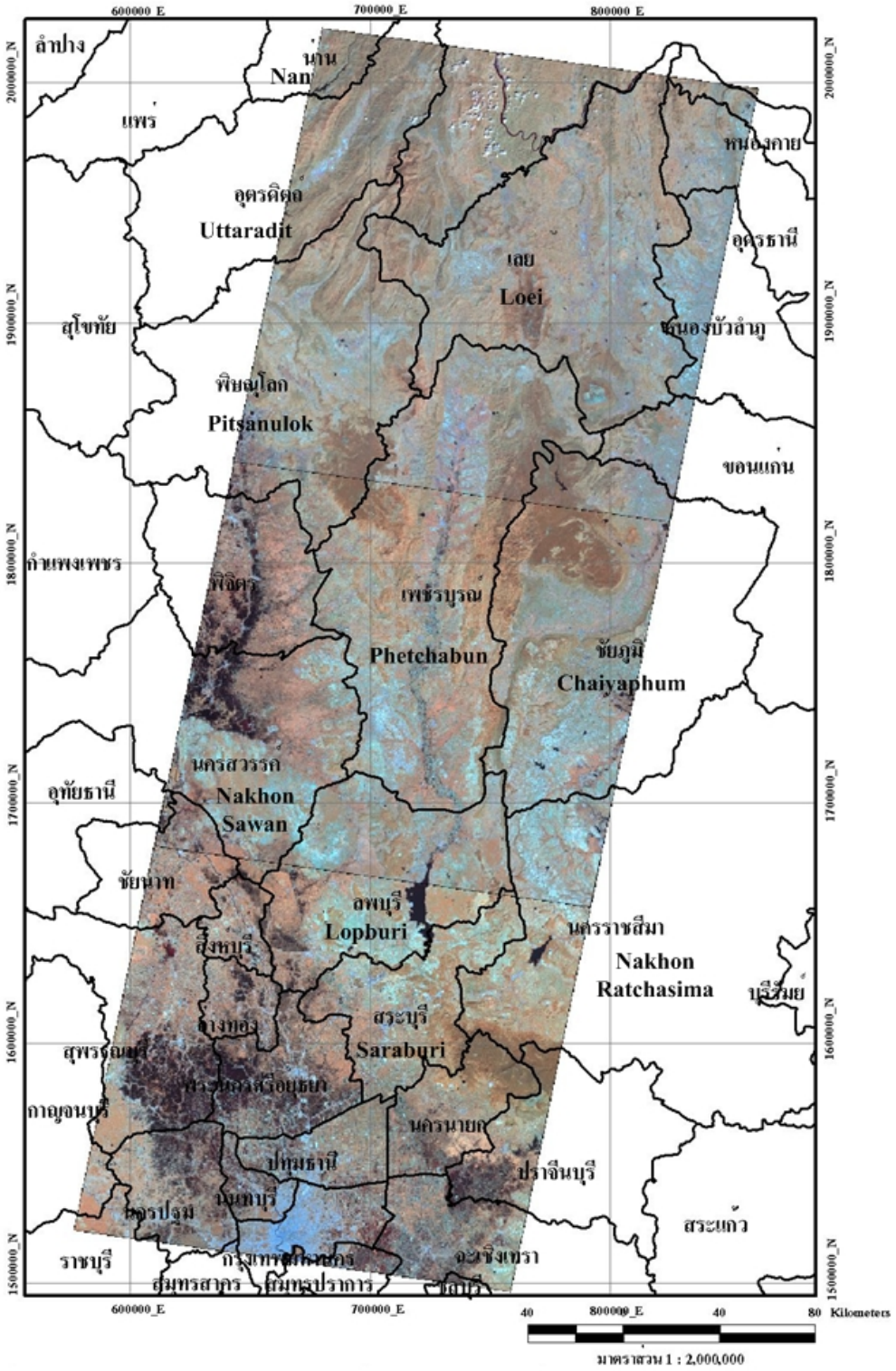


**Figure 1.3** Simplified geographical map along the western margin of the Khorat Plateau (yellow flame, not to scale).


**Figure 1.4** Provincial boundary and highway network in Thailand and adjacent area.

## 1.4 Research objectives

The objectives of this study are as follows;

1.4.1 To study the stratigraphy, sedimentology, and geologic structures of the Late Paleozoic sequences within the Phetchabun Fold Belt.

1.4.2 To establish the provenance of the Late Paleozoic siliciclastic sediments (Nam Duk Formation).

1.4.3 To characterize and interpret the tectonic setting of pelagic, flysch, and molasse facies of Late Paleozoic age within the Phetchabun Fold Belt.

1.4.4 To consider the paleogeography and geodynamic evolution of Thailand in relation to mainland Southeast Asia.

1.4.5 To discuss implications for potential mineral resources within the Phetchabun Fold Belt.

## 1.5 Scope and limitations of the study

The study area comprises the N-S elongated mountain belts located west of the Khorat Plateau and east of the Central Plain. This study is focused mainly on the stratigraphy, sedimentology, provenance, and structural geology of Late Paleozoic sequences and associated volcanics, with a view to establish more coherent and definitive interpretation of the geological and tectonic history of the Phetchabun Fold Belt.

## 1.6 Research methodology

Research strategies and activities will be carried out in Thailand, Germany and China as follows:

1.6.1 Field surveys in northeastern and adjacent area in Thailand to investigate the stratigraphic sequences and to collect rock samples. Selected areas of stratigraphic, structural, and tectonic importance will be examined.

1.6.2 Sample preparation and thin-sections for sedimentological analysis will be done. Provenance analysis will be carried out by the cathodoluminescence method.

1.6.3 Geochemical analysis of sedimentary rocks (of the Nam Duk Formation) for clarifying its tectonic setting will be done.

1.6.4 The results of all data will be compiled and interpreted for reconstruction of the paleogeography and geodynamic evolution of this region.

## 1.7 Area of study and localities of collected samples

Field work and sample collection were carried out on the exposures of the Nam Duk Formation along the highway No. 12 and the Permian section to the north in Loei province and to the south in Saraburi-Nakhon Ratchasima provinces. Figure 1.5, 1.6, and 1.7 shows a simplified geological map and localities of collected samples.

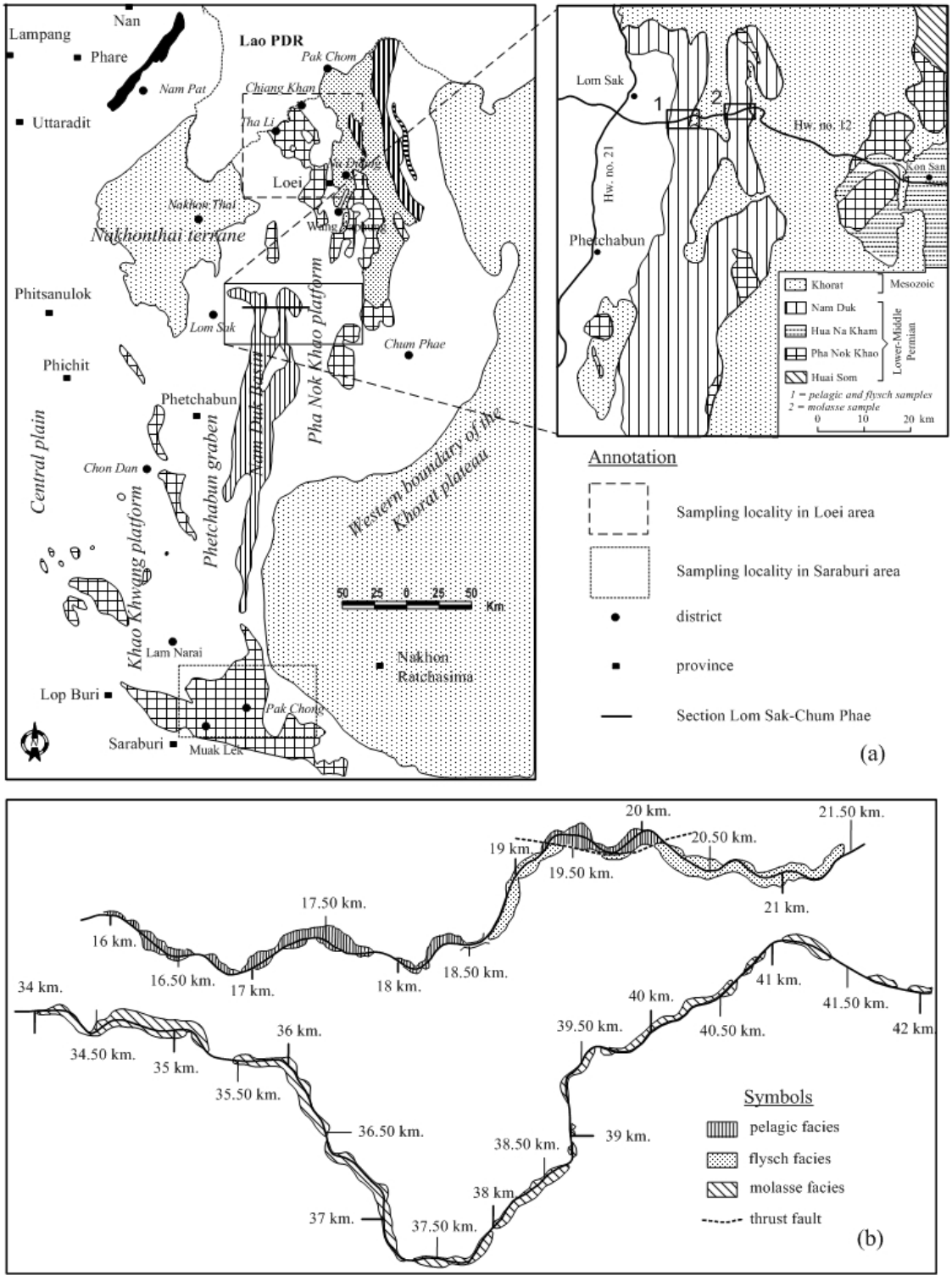


**Figure 1.5** (a) Simplified geological map of collected samples (modified from DMR, 1998; Chonglakmani and Sattayarak, 1978). (b) Section of the Nam Duk

Formation along highway No. 12 (modified from Helmcke et al., 1985). Sample numbers for geochemistry and CL are indicated by milestone.

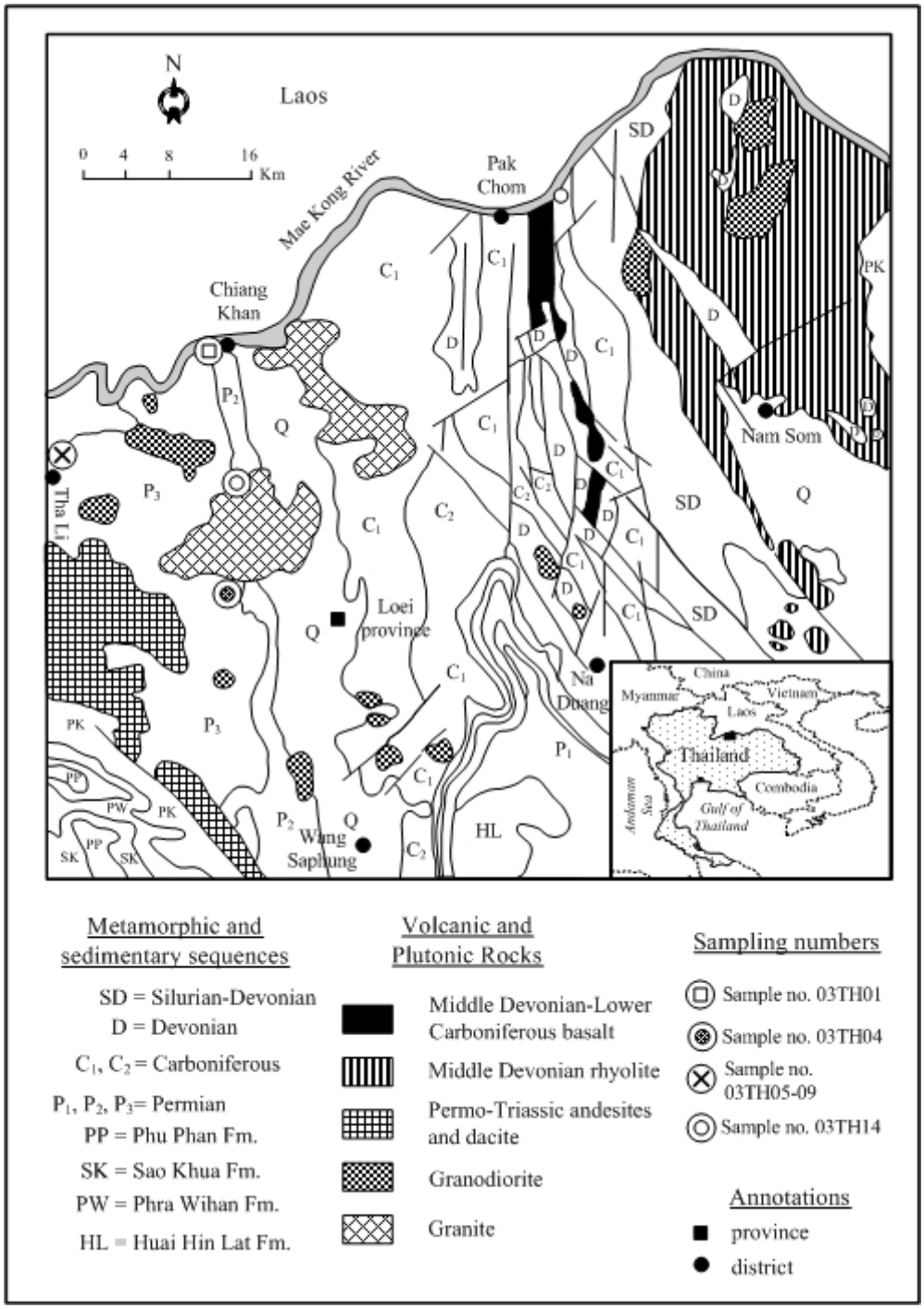


**Figure 1.6** Geological map of the Loei area showing the distribution of rock types and sample localities (modified after Geological Survey Report No. 95, 1989).

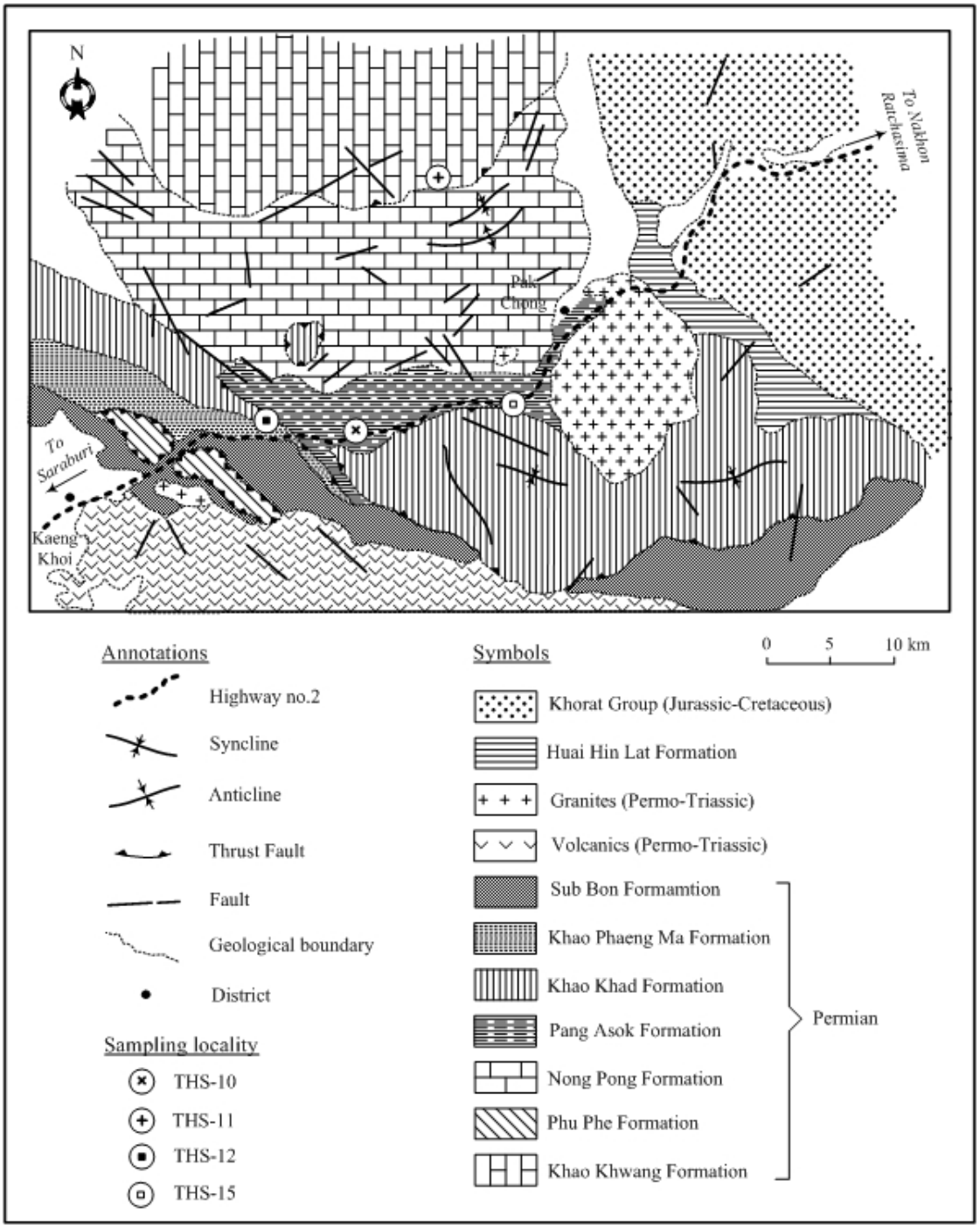


**Figure 1.7** Geological map of the Saraburi-Pak Chong area and sample localities (modified from Hinthong, et al., 1976; Chonglakmani, 2001).

# CHAPTER II
# GEOLOGICAL SETTING AND PLATE TECTONIC REVIEW

The geological study of northeastern Thailand was recorded more than forty years ago. The mountain belts bordering the Khorat Plateau to the west are highly complex during Upper Paleozoic to Tertiary time. Many researchers have proposed the geodynamic evolution, the timing of the amalgamation and geo-history of these mountain belts. To clearly understand the geological history of the region, the review of geological setting bordering the Khorat Plateau will be presented.

## 2.1 Geological setting

According to general geological subdivision in Chapter 1, more detail of each area is presented here and in Figure 2.1. The Late Paleozoic stratigraphic correlation of mentioned area is given in Figure 2.2.

### 2.1.1 The area NE of Loei (including Pha Nok Khao Platform)

The oldest rocks in this region belong to the Na Mo Group (Bunopas, 1981). They form the metamorphic basement and are composed of low grade metamorphic rocks of the upper green-schist facies (phyllite, chlorite and pelitic schists, metatuff, and quartzite). The quartzites and phyllites were obviously affected by tectonic deformation and metamorphism much more intensively than all other rocks in this region (Chairangsee et al. 1990). The Na Mo Group conformably

underlies the siliciclastics Silurian-Devonian Pak Chom Formation and is considered to be pre-Silurian in age.

The Pak Chom Formation comprises sediments deposited in a marine sedimentary basin on the metamorphic basement. It consists of sediments deposited in shallow to deep marine environments. Shallow marine strata are characterized by platform carbonates and shelf clastics (graywacke, shale and conglomerate). Patches of coral reef represented by massive limestones of Devonian to Early Carboniferous age are also recorded in this sequence (Chairangsee et al. 1990). Thin-bedded cherts, yielding radiolarian with intercalated tuffs, siliceous shale and siltstone, represent deep-sea sediments. Basaltic lava characterized by pillow structures is found associated with the chert. The chert is interpreted as oceanic sediment and was obducted as thrust sheets onto the platform sediments as a result of the Variscan Orogeny.

The Carboniferous Wang Sapung Formation has been proposed for the nearshore sandstone, shale, and limestone along western edge of the Khorat Plateau distributed mainly in Loei and some part of Udon Thani Provinces. The Nam Maholan Formation (equivalent to the Pha Nok Khao Formation) has been proposed for the Lower Permian sequence located in the area southeast of Loei province. At Ban Na Duang, east of Loei, the outcrops of Lower-Middle Permian were recorded by rich faunal assemblage (Fontain and Suteethorn, 1992). It has been noted that, the boundary between the Permian and Carboniferous appears to be located in limestone (Fontaine, 2002; Charoentitirat, 1999). This sequence was interpreted to have been deposited in the passive continental margin.

To the east of Nam Duk Basin, the Permian sediments are represented by the Pha Nok Khao and the Hua Na Kham Formations. The Pha Nok Khao Formation consists predominantly of massive to thick-bedded, gray limestone and dolomite. Thin- bedded gray shale and black, nodular or thin-bedded chert may occur locally. They had been studied extensively from outcrops. It represents all the main environments of shallow carbonate deposition, from reef to back reef, shoal, bio-hermal, lagoonal, intertidal and tidal flat, beach deposits and supratidal environments. They range from Asselian to Middle Permian (Murgabian) (Yanagida, 1966; 1976; Igo, 1972; 1974; Kobayashi and Hamada, 1979; Fontain and Suteethorn, 1992; Ueno et al., 1993).

The Hua Na Kham Formation overlies conformably the Pha Nok Khao Formation and has been informally named the “Upper Clastics” (Mouret, 1994). It consists of intercalated light and dark gray siltstone, sandstone, claystone, and limestone. The fossil content and sedimentary structures suggest a shallow platform marginal marine environment of deposition. Fusulinids from the limestone indicate Middle to early Upper Permian ages.

Altermann et al. (1983) pointed out that the sedimentation of the limestones (Pha Nok Kao Formation) ceased in Bolorian time and was followed by the sedimentation of the thick sequence of shallow marine clastics of the Hua Na Kham Formation of Bolorian to Kubergadian age. This remarkable change in sedimentation is therefore older than the typical molasse strata (the Nam Duk Basin, a more detailed discussion will follow) of the area east of Lom Sak which are of Murgabian to Midian age.

The outcrop of the thin-bedded fine-grained clastic sequence with predominant dark shale and siltstone representing the Pha Dua Formation is mapped by Chairangsee et al. (1990). It yields a Late Permian floral assemblage (Asama et al. 1968) and conformably overlies the E-lert Formation (equivalent to the Hua Na Kham Formation). It is about 213 m thick and uncomfortably underlies the Late Triassic Phu Lop Formation (equivalent to the Huai Hin Lat Formation). The basal part rests conformably on the Hua Na Kham Formation. The unit comprises predominantly siltstone and claystone, often tuffaceous, with rare thin beds of sandstone, coal, and limestone (Mouret, 1994). It was deposited mainly in upper delta to alluvial plain environments, with minor interruption of lower delta plain and bay facies.

In Pak Chom area, the radiometric age dating of basalts and rhyolites was reported by Intasopa and Dunn (1994). They proposed two magmatic episodes at approximately 374 and 361 Ma. The trace element and isotopic compositions of the rhyolites suggest that they were generated by partial melting of continental crust at 374 Ma. The ocean floor tholeiites basalts belong to a younger magmatic episode at 361 Ma and located to the west of Devonian rhyolites (Fig. 15, page 178 in Intasopa and Dunn, 1994).

### 2.1.2 Subsurface data underneath the Khorat Plateau

During the last twenty five years, the prospecting activities were performed for hydrocarbon exploration within the sedimentary basins especially in the Permian limestone underneath the formations of the Khorat Group. A number of deep wells have been drilled during the past years, mainly in the Khorat Basin. The data from the wells and seismic interpretation have improved and provided much information on the geological history of the region.

The Early Carboniferous rocks were drilled below the Variscan unconformity encountered undifferentiated volcanic, granite (329±3 Ma), meta-sediments, and sedimentary rocks (Kozar et. al 1992 and Sattayarak et al. 1989). According to Kozar et al. (1992), they proposed the rifting probably began during the Late Carboniferous as the region was subjected to back-arc extension and the extension continued through Middle Triassic. However, the rifting may have abated during the Late Permian time, and probably was rejuvenated in Early Triassic. This rejuvenation allowed the Early to Middle Triassic sediments to deposit in the area. During the Permian, the rift system was fully developed in back arc setting and appeared to consist of three major deep grabens with intervening high stable horst blocks. These high platforms were vital locations for the carbonate accumulations.

The stratigraphy of Middle Carboniferous to Middle Triassic was complied by Mouret (1994) based on data from drilled wells. The rocks comprise the Middle Carboniferous-Lowermost Permian (Asselian) “Lower Clastics”, the Permian Pha Nok Khao Carbonate, and the Upper Permian to Lower (?) Triassic “Upper Clastics” respectively. The Lower Clastics have been drilled in the eastern end of the Phu Phan range by ESSO Non Sung-1 well. The total thickness is 263 m and it shows thin beds of low energy sandstones and limestones scattered among siltstones and shales. Tuffs or lavas form isolated 1 meter thick beds. The Pha Nok Khao Carbonate known in TOTAL Phu Lop-1X well is thrust-truncated at the base. The massive 132 m thick section was dated Murgabian to Midian, late Middle to early Upper Permian by fossil faunas. The Sakmarian to Guadalupian Carbonate was reported in other well by Kozar et al. (1992).

The Upper Clastics are overall regressive as shown by the 791 m thick sequence in TOTAL Phu Lop-1X. The lowermost 95 m are shallow marine limestone interbeded with coal and organic shale both deposited in a lower delta plain to bay setting. Above, 600 m of grey beds with a few thin intercalations of reddish brown beds at the top are comprised of alternated volcano-sedimentary sandstones, rare sandstones with no volcanic component, siltstones and shales both tuffaceous to a variable extent, organic shale and coal. They were deposited in lower delta plain/bay grading upward to upper delta/alluvial environments. Alluvial red beds (96 m) form the top of the formation, mostly siltstone and shale with some volcano-sedimentary sandstone. The Dzulfian to Dorashamian (Upper Permian) age of the limestone and the huge thickness of the formation strongly suggest a Triassic age for the higher part of the section, especially Lower Triassic.

However, Mouret (1994) did not report the strong tectonic event during the Middle Carboniferous to Late Permian. Only Middle Permian movement in the Phetchabun area represented by the relative sea level fall and some minor uplift was mentioned (Fig. 2, page 135 in Mouret, 1994).

### 2.1.3 The Phetchabun Fold Belt (Nam Duk Basin)

Based on Helmcke and Kraikhong (1982), the statigraphic succession in Permian Nam Duk Basin is composed of three units; pelagic facies, flysch facies and molasse facies related to pre-orogenic, syn-orogenic and post-orogenic events (Figure 2.3). These facies are exposed between milestone 16.00-20.20, 20.20-21.30, and 34.0-42.20 respectively on highway No. 12 from Lom Sak to Chum Phae.

According to Helmcke and Lindenberg (1983), the oldest unit of rock comprises mainly cherts, tuffs, shales, and allodapic limestones. The allodapic

limestones were transported from south and north in the direction of the axis of the basin (Winkel et al., 1983). This facies represents a deep-sea depositional environment. The second unit of rocks consists of greywackes alternated with shales. In the greywackes all features of the Bouma-cycle can be found, characterizing them as turbidites. The third unit of rocks comprises a very thick sequence of clastic rocks, mainly sandstones and shales. Some beds are very rich in fossil and plant remains. In the upper part of this section limestone layers are intercalated. These limestones are generally rich in foraminifers and sometimes contain corals. Towards the east the limestones become thicker and more prominent. The foraminiferal fauna in the limestone is certainly autochthonous. The fauna can be assigned to a Middle to Upper Permian age.

Winkel et al. (1983) studied facies and stratigraphy of the lower Lower Permian strata of Phetchabun fold belt in central Thailand. They found that the turbiditic limestones (pelagic facies) were derived from carbonate-platforms which are located in the eastern as well as in the western parts of the Phetchabun fold belt (Pha Nok Kao limestone of Chonglakmani and Sattayarak, 1978 and Khao Khwang platform of Wielchowsky and Young, 1985). They proved that the pelagic regime encompasses the time interval of Upper Carboniferous? - Lower Permian to Lower Murgabian.

Altermann et al. (1983) proposed the timing of sudden onset of flysch sedimentation as upper part of Middle Permian. From paleontological data, they also proved that the molasse sediments comprise not only Murgabian but also part of Midian, i.e. the molasse sedimentation prevailed into the lower part of the Upper Permain. The study of fusulinoidean biostratigraphy by Charoentitirat (2002)

confirms that the molasse unit is in Midian age. Coalification study by Tassanasorn (1990) indicated that high vitrinite reflectance in the flysch facies is likely due to subsidence to great depth and decreasing from west to east (flysch to molasse facies). This study also indicated that the coalification in the Nam Duk Formation was mainly before the deposition of Mesozoic Khorat Group.

Thanomsap (1992) studied the structural development on the Khorat Plateau and its adjacent western region. From aerial photograph interpretation, he reported the thrust of Nam Duk Formation over the Khorat red beds occurred probably in the Cretaceous (?). Heggemann (1994) mapped the Nam Duk Formation which thrusted on the Nam Phong Formation (Lower Jurassic) at kilometer 24 on highway 12 Lom Sak-Chum Phae. Toward the west at kilometer 21, the cleavages were generated in sandstone (Nam Phong Formation) and the deformation was dated by K/Ar age in mineral fractions at 97 Ma (Ahrendt et al., 1993).

### 2.1.4 The area of Chon Dan (Khao Khwang Platform)

To the west of the Nam Duk Basin, the Khao Khwang platform is distributed in this area (Wielchowsky and Young (1985). In Chon Dan, Chonglakmani et al. (1983) and Chonglakmani and Fontaine (1992) reported a very similar startigraphic section to those of Loei area. The section starts from volcanic and chert layers. The sediments are composed of limestone interbedded with shale and sandstone ranging from lower Visean to Lower Permian. To the southwest of Chon Dan, massive limestones and clastic sediments are predominantly represented. They range from Lower Permian to lower Upper Permian. Fossil woods have been reported from this area and have been identified as *Dadoxylon* (Chonglakmani and Fontaine, 1992). Altermann (1989) pointed out that the strata in Chon Dan area were

generally younger from west to east. At least two shallowing upward sequences are exhibited first in the Visean and second in the Visean to Lower Permian.

Charoentitirat (2002) reported the fusulinoidean zonations established in the Phetchabun, Lop Buri, and Saraburi ranging in age from middle-late Asselian, early Yakhtashian, and Murgabian to Midian, with some straigraphic breaks. Altermann (1989) also reported the Permian sandstones and conglomerates conformably overling the Murgabian massive limestone at Khao Khi Nok west of Wichianburi. He proposed a coarsening upward sequence and an increase of hydrodynamic energy towards the top of this unit by the more likely regressive than the transgressive processes.

Fontaine et al. (1999) reported the new Carboniferous fossils at Ban Bo Nam north of Khao Somphot and east of Lam Narai. They consist of calcispherids, algae, foraminifers and corals indicating mainly a late Moscovian age and locally extending to early Kasimovian. Moreover, the interesting new information shows that the stratigraphic range of the sedimentary rocks of this area extends in continuity from Middle Carboniferous to the top of Middle Permain. Altermann (1989) indicated that the massive limestones at Khao Somphot are in the stratigraphic range from Asselian to Midian. Wielchowsky and Young (1985) reported the stratigraphic breaks by the lowstand sea level in the early Artinskian and again in the Ochoan (lower Upper Permian). During that period, the carbonate accumulation apparently decreased.

### 2.1.5 The Phetchabun Graben

The Phetchabun Basin is located within a fold belt in the central portion of Thailand. The basin comprises a series of five half and full grabens located in a narrow, elongate (30 kilometres by 120 kilometres) intermontaine rift. In general,

the Tertiary sediments are blanketed by Quaternary alluvial deposits and alkaline basalt flows throughout the basin and few outcrops are known. The basin was formed in the Late Oligocene as a result of simple shear tectonics associated with right lateral movement on the NW-SE trending Mae Ping and Three Pagodas faults and left lateral movement along NNE-SSW trending conjugate strike-slip faults (Remus et al. 1993).

Following the Carnarvan Petroleum Report (2002), the subsidence of the basin began in the Late Oligocene as a broad rift valley. Initial deposits included alluvial and fluvial sediments deposited in a river system ancestral to the present day Pa Sak river. By the beginning of the Miocene, increased rates of subsidence resulted in the formation of a series of lakes in the valley floor. Thick, highly organic rich shales were deposited in the lakes proper, while deltas and alluvial fans encroached from the lake margins. A period of tectonic activity at the end of the Early Miocene was followed by extensive fluvial deposition. A second phase of tectonism and igneous activity marked the end of the Middle Miocene. Lacustrine conditions were re-established throughout the basin. Subsidence was halted by Pliocene time, and a fluvial system was established that persists to the present day.

### 2.1.6 The Saraburi region

In Saraburi-Pak Chong area, Hinthong et al. (1976) subdivided the Permian rocks into six formations; the Sab Bon, the Khao Khad, the Pang Asok, the Nong Pong, the Khao Khwang, and the Phu Phe Formations respectively in descending order ranging in age from Lower to early Upper Permian. Dawson and Racey (1993) proposed the Permian strata of central Thailand as a sequence of supratidal to outer platform facies comprising a Lower-upper Middle Permian transgressive/regressive carbonate platform succession.

Chonglakmani (2001), studied in detail of the Saraburi Group in the Saraburi-Pak Chong area. He recognized the various facies belts representing the shelf or platform, basin margin and deep basin environments. The platform facies comprises the Phu Phe, the Khao Khad, and the Khao Khwang Formations. The Sap Bon, the Pang Asok and part of the Nong Pong Formations represent slope or basin margin facies. The deep basin or basin plain facies are characterized mainly by fine-grained sediments. They consist of thin-bedded shales, cherts, argillaceous micrites and allodapic limestones which are typical of the Nong Pong Formation.

The Permo-Triassic Khao Yai Volcanics are distributed as dikes and sills in the Permian country rocks in the area south of Saraburi (Hinthong, 1981). To the east of Pak Chong, the calcalkaline I-type granites with typical Rb/Sr dates of 260 Ma are exposed (Beckinsale et al. 1979; Cobbing et al. (1986). Charusiri et al. (1999a, quoted in Chutakositkanon et al., 2000) dated the hornblende from andesitic dikes which crosscut the Permian rocks close to Khao Pun area (north of Kaeng Khoi) by $^{40}Ar/^{39}Ar$ indicating the Early Jurassic age. It probably indicates the younger phase of the more widely exposed Permo-Triassic plutonics (Phra Ngam Diorite, Hinthong, 1981) and volcanics (Khao Yai Volcanics).

### 2.1.7 The Nakhonthai region

Nakhonthai terrane (Sattayarak et al., 1989) or Nakhon Thai Block (Charusiri et al. 1999b; quoted in Chutakositkanon et al., 2000) covers the Dan Sai, Na Haew and Nakhonthai Districts. The Mesozoic Khorat Group conformably overlies the Upper Triassic Huai Hin Lat Formation. The continental facies consists of six formations in ascending order as Nam Phong, Phu Kradung, Phra Wihan, Sao Khua, Phu Phan and Khok Kruat Formations. They formed the synclinorium

structure and were more deformed than those of the Khorat Plateau. On top of this section these formations are overlain by unnamed conglomerate and Phu Tok Formations respectively in asscending order (Heggemann, 1994).

### 2.1.8 The Central Plains

The large part of central Thailand is blanketed by Quaternary fluvial sediments which conceal a number of Tertiary Basins underneath. This region consists of a number of north-south trending half grabens and grabens which are believed to be originated in the Late Oligocene (Chaodumrong et al., 1983). More than ten small basins can be observed by seismic exploration. These basin were formed in response to dextral shear on the Mae Ping and Three Pagodas Fault Zone systems during the Late Tertiary (Cooper et al., 1989).

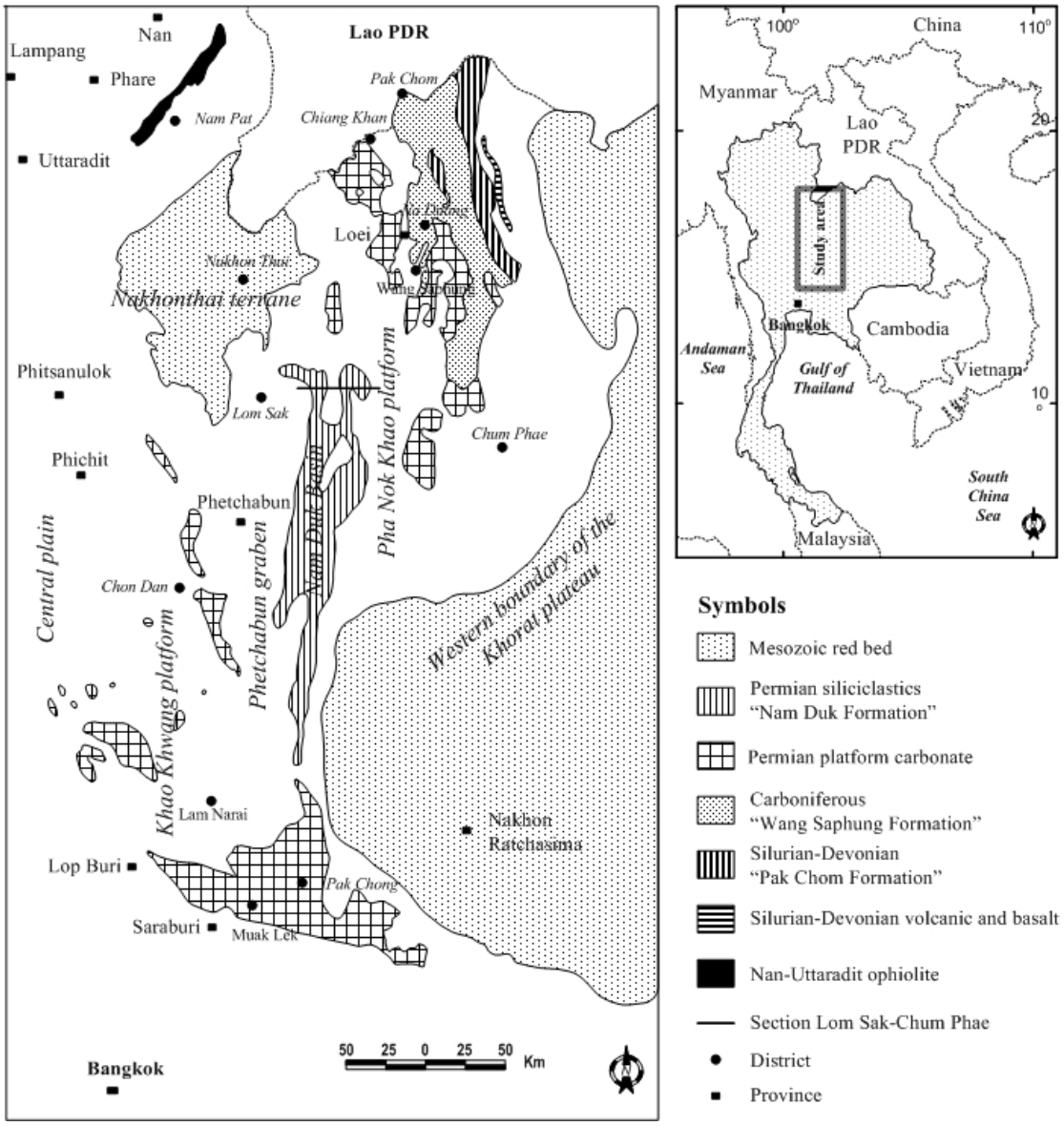


**Figure 2.1** Simplified geological map showing Late Paleozoic rock units and geological setting of the study area (modified from DMR. 1998).

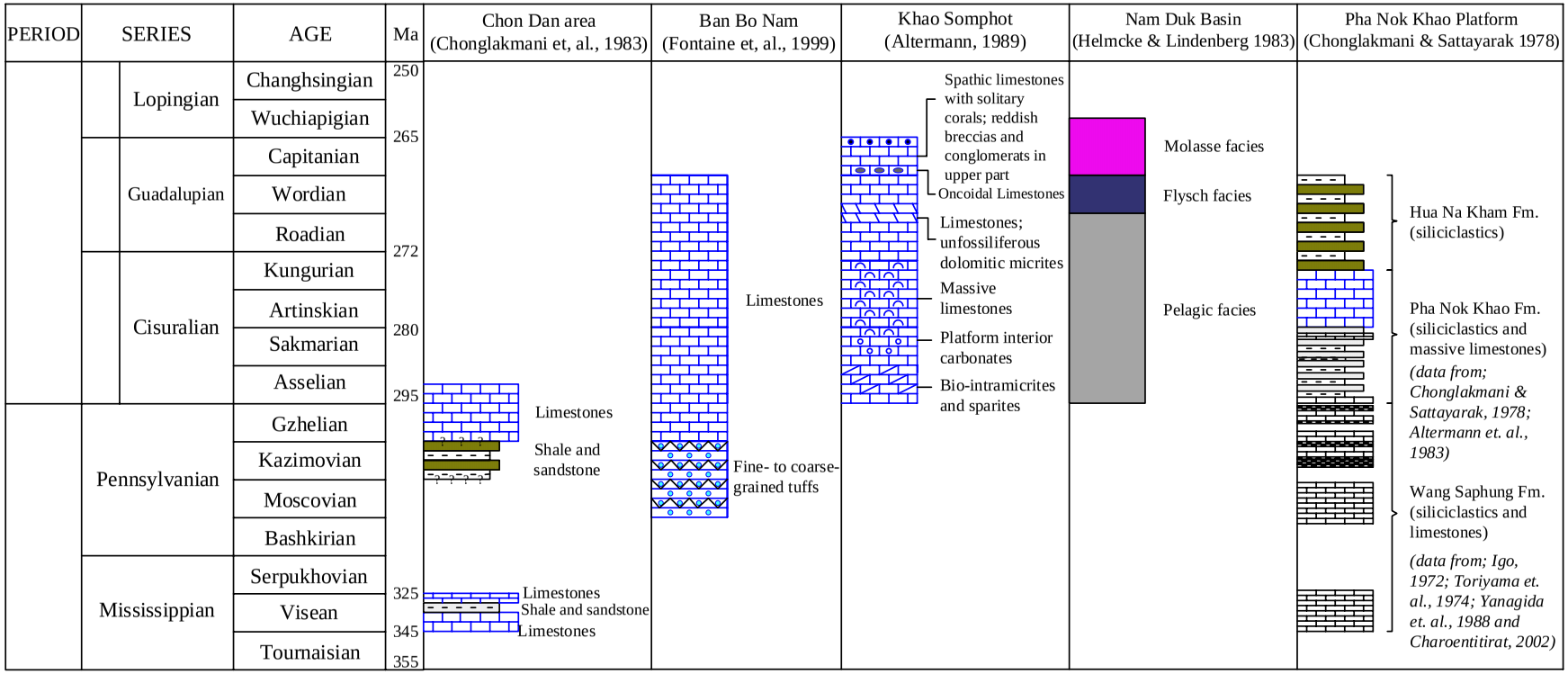


**Figure 2.2** Carboniferous – Permian stratigraphic correlation between Central Plain and Northeast Thailand.

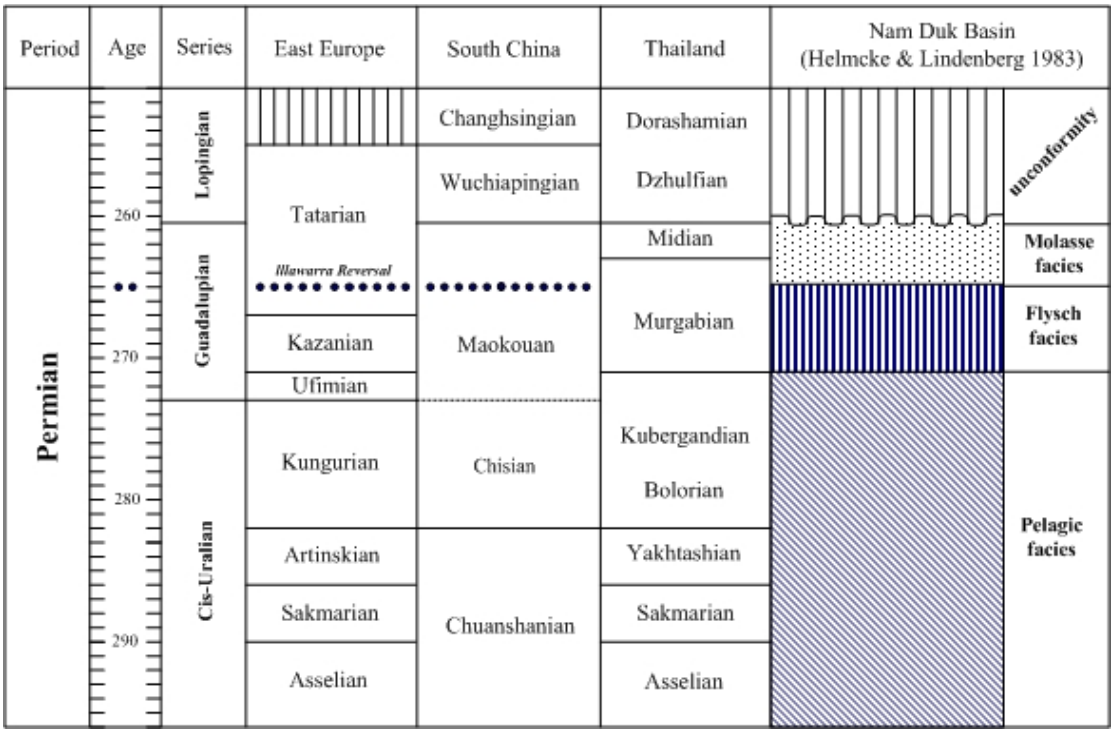


**Figure 2.3** Stratigraphic succession of Permian "Nam Duk Formation" in Phetchabun-Loei area.

## 2.2 Plate tectonic review

International research during the last three decades has led to the recognition that the geological backbone of Southeast Asia consists of a series of continental fragments. All fragments are derived from the ancient continent of Gondwanaland. After breaking off from the Gondwanaland continent in the Early Paleozoic, slices of continental crust moved northwards creating a succession of basins with attendant collision, rotation, accretion, and amalgamation at their respective present positions. The physiography of Thailand is the result of a long complex geodynamic evolution during Phanerozoic time. According to modern geologic interpretation, it is believed

that two micro-continental blocks named Shan-Thai in the west and Indochina in the east welded together along the Nan-Uttaradit suture (Figure 2.4; Bunopas and Vella, 1978; Bunopas and Vella, 1983). The mountain belts formed in response to convergent tectonics of the Shan-Thai and Indochina plates during closure of the Paleo-Tethys ocean during Middle Permian to Late Triassic time based on various argument (Helmcke and Kraikhong, 1982; Helmcke and Lindenberg, 1983; Sengör, 1985; Sattayarak et al. 1989; Cooper et al. 1989; Kozar et al. 1992; Mouret, 1994).

The Shan-Thai terrane comprises eastern Burma, western Thailand, western peninsular Malaysia and northern Sumatra. This terrane is an elongate continental block trending north-south and its basement consists of Precambrian rock. The fossiliferous glaciomarine siliciclastic rocks of the Early Carboniferous to Early Permian Phuket Group (equivalent to Kaeng Krachan Group) of southern Thailand suggest that the Shan-Thai terrane did not rift from Gondwanaland until the Early Permain (Metcalfe, 1988; Hills, 1989; Shi and Waterhouse, 1991; Singharajwarapan and Berry, 2000). The Indochina terrane comprises eastern Thailand, Laos, Combodia and parts of Vietnam. It is also an elongate stable blocks and is composed mainly of Paleozoic and early Mesozoic marine strata, with a younger Mesozoic continental cover succession.

Plate tectonic models accounting for the collision between Shan-Thai and Indochina terranes have been proposed by a number of workers. The timing of collision and the geometry of plate convergence are still debated. In the recent literatures four main scientific hypothesises can be distinguished (Figure 2.5).

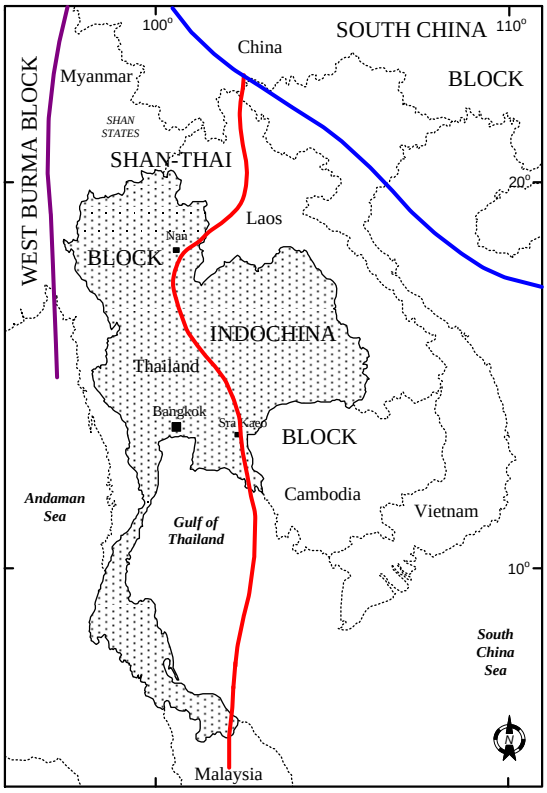


**Figure 2.4** Map showing main tectonic elements in Thailand (after Bunopas and Vella, 1978).

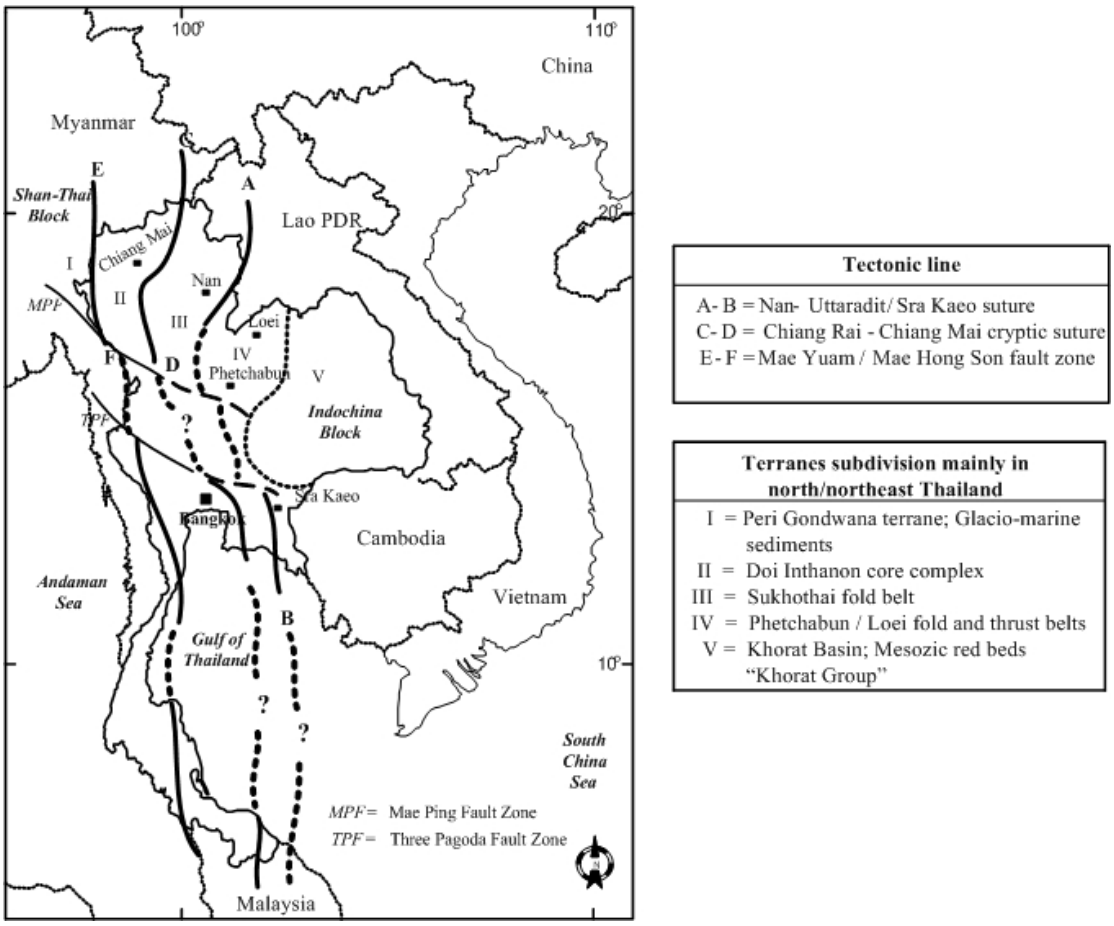


**Figure 2.5** Tectonostratigraphic terranes and proposed suture lines of Thailand.

**2.2.1 Nan-Uttaradit Suture as the main Paleo-Tethys located between Shan-Thai and Indochina Cratons.**

This scenario is based on the geological concept of "Gondwana" and "Cathaysia" or "Eurasia" provenance of mainland Southeast Asia. According to this theory, part of Burma, Thailand, Malaysia and Sumatra (Sibumasu Continent, Burret and Stait, 1985; Cimmerian Continent, Sengör, 1985; Shan-Thai Craton, Bunopas, 1981) drifted away most probably from NW Australian part of Gondwanaland in the Upper Paleozoic. After crossing the Main Paleo-Tethys Ocean, this sub-continent collided with Cathaysia or Eurasia in the Triassic to Jurassic which caused the Indosinian orogeny. This interpretation was based on the occurrence of the oceanic ribbon-bedded chert and shale sequences that have yielded graptolites, conodonts and radiolarians ranging in age from Lower Devonian to Upper Triassic. These fauna can be traced from the Bentong-Raub suture zone of Peninsular Malaysia, the Nan-Uttaradit/Sra Kaeo suture zone of Thailand and the Changning-Menglian suture zone of South China (Liu et al., 1996; Metcalfe, 1997; Spiller, 2002).

**2.2.2Nan-Uttaradit Suture is a branch of the main Paleo-Tethys.**

In this scenario, based on the scientists who did not accept that the Late Triassic "Indosinian orogeny" is the main orogenic event in Thailand and mainland Southeast Asia (Helmcke and Kraihong, 1982; Helmcke and Lindenberg, 1983; Helmcke, 1985). According to their theory, Southeast Asia was formed by the Variscan orogeny during the Permian time. For example, the orogenic event of Middle Permian age affected large areas of mainland Southeast Asia and the P.R. of China. Nan-Uttaradit suture zone shows evidence of compressional deformation and subsequent uplift to an erosional level in the short period of Middle Permian

represented by the Nam Duk Formation of the Phetchabun fold and thrust belt (Helmcke and Kraikhong, 1982; Helmcke and Lindenberg, 1983).

The correlation of tectonopaleogeographic units of northern and northeastern Thailand with southern Yunnan was attempted (Chonglakmani et al., 2003). The Ailaoshan and Nan-Uttaradit sutures were considered to be the same orogenic belt to the east of Simao and Lampang-Phrae basins. Recently, the discovery of an angular unconformity outcrop in Yunxian of Simao region is best fit for the orogenic event of Permian time (Qinglai and Helmcke, 2001). The outcrop shows strongly deformed Carboniferous to Lower Permian sediments which were deposited in a deep basin and are separated by an angular unconformity from the overlying shallow marine strata of upper Middle Permian age (Qinglai and Helmcke, 2001).

### 2.2.3 Chiang Mai "Cryptic" Suture is the main Paleo-Tethyan Ocean

The cryptic suture first proposed by Cooper et al. (1989) corresponds to the terms "Chiang Mai Volcanic Belt" (Macdonald and Barr, 1978; Barr et al., 1990), "the Inthanon Zone" of Barr and Macdonald (1991) and "the Chiang Mai Suture" of Metcalfe (2002). This suture proposed for the boundary between the Shan-Thai and Sukhothai/Indosinian terranes to the east and bounded by Mae Yum Fault zone which corresponds to western I+S type granites line proposed by Cobbing et al. (1986) to the west. The suture characterized by a metamorphic-plutonic basement with a structurally detached sedimentary cover of mainly Paleozoic age (Barr and Macdonald, 1991). The discoveries of oceanic and seamount rocks associations in the Chiang Mai-Chiang Dao area of western Thailand ranging in age from Devonian to Triassic are interpreted by Metcalfe (2002) as representing the main Paleo-Tethys

Suture. However, original stratigraphic succession was destroyed by various phases of metamorphism of the metamorphic core complex concept by several authors (Dunning et al., 1995). The closing time of the basin and the geodynamic evolution of this belt are still debated.

### 2.2.4 The main Paleo-Tethys located along the western-most part of Thailand

For this scenario, the candidate for the main Paleo-Tethys ocean is located west of the cryptic suture as mentioned above. This interpretation is based on the different faunas which are associated with the Gondwana and the Cathaysian domains (Figure 2.6). The boundary is recognized by the stratigraphic sequence of Devonian-Early Permian glacio-marine diamictites with Gondwana-related brachiopod faunas (Phuket Group) succeeded by Middle to Late Permian carbonates (Ratburi Group) with poor foraminifera (*Monodiexodina*, *Eopolydiexodina*, and *Shanita*) and rare coral (Chonglakmani, 2002). This boundary extends northwestward from the Three Pagoda Fault in western Thailand to Mae Sariang-Mae Hong Son and Mandalay in eastern Myanmar (Figure 2.7). Recent study of radiolarian faunas in Mae Sariang area range in age from Early Carboniferous to Late Triassic (Caridroit, et al., 1993; Kamata et al., 2002; Qinglai et al., 2004). The radiolarian results from Mae Sariang-Mae Hong Son suggest that there was a pelagic basin between the Shan-Thai terrane and the Gondwanaland during the Early Carboniferous until Late Triassic. However, the distributions of Devonian-Late Triassic radiolarian chert in northern Thailand (not only Mae Sariang-Mae Hong Son area) seem to be in conflict with this scenario. This problem was explained by the tectonic slices concept which some

sheets were translated eastward from the western part of the Shan-Thai block (Chonglakmani, 2002).

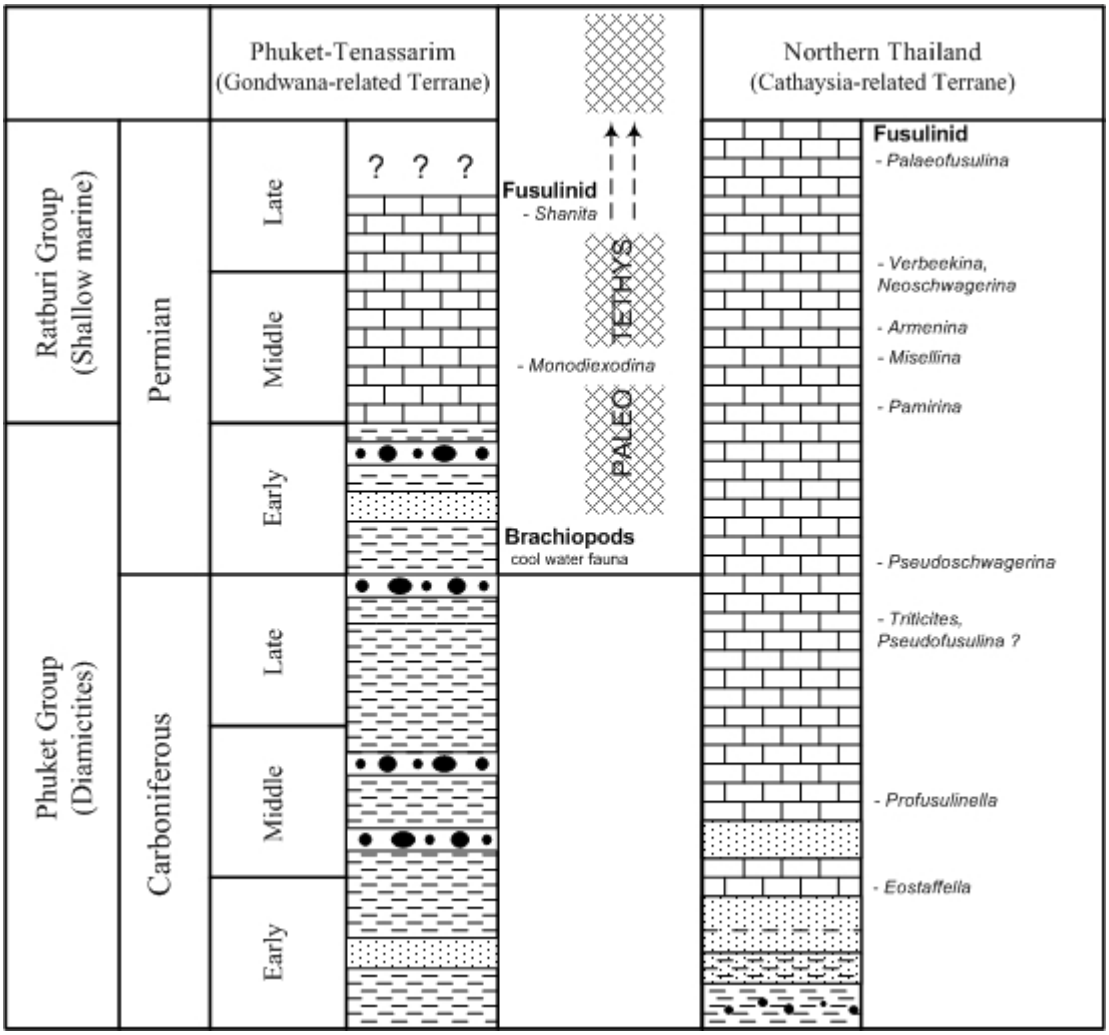


**Figure 2.6** Comparisons of sedimentary facies and fauna between the Phuket-Tenassarim Terrane and Inthanon (Northern Thailand) Terrane (From Toriyama, 1944; Konishi, 1953; Hahn and Siebenhuner, 1982; Fontaine and Suteethorn, 1988; Vachard et al., 1992; Ueno and Igo, 1997).

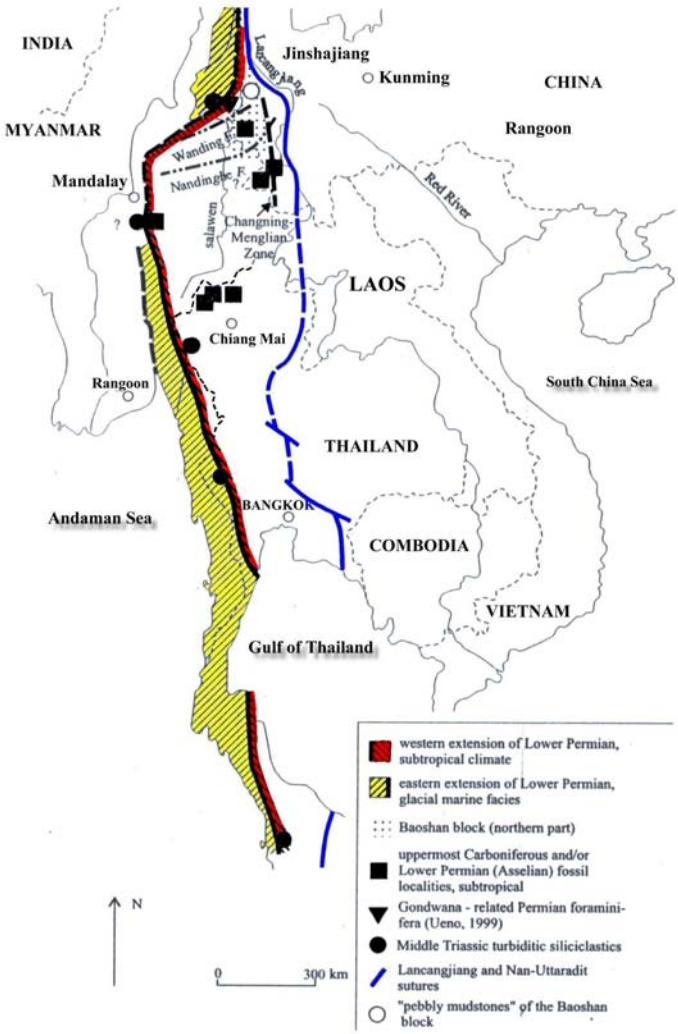


**Figure 2.7** Map showing Paleo-Tethyan Belt dividing Cathaysia from Gondwana-related terranes (Modified from Min et al., 2001).

# CHAPTER III

# GEOCHEMICAL AND

# CATHODOLUMINESCENCE TECHNIQUES

In this chapter, the author would review the methodology of geochemical and cathodoluminescence (CL) techniques on the siliciclastic sedimentary rocks.

## 3.1 Geochemical analysis

Determination the provenance of clastic sedimentary rocks is often an important component of an investigation of any sedimentary sequences. The composition of clastic sediments is controlled by many complex factors. Detritus from the sources are rarely uninterrupted, because the path of clastic sediments from source rock to sedimentary rock formation is composed of several stages, including tectonic movement, weathering, erosion, transportation, and deposition.

It is generally accepted that certain geochemically immobile trace and rare earth elements are quantitatively transferred into siliciclastic sediments and thus preserve the record of the average upper crustal element abundances. As far as sandstones are concerned considerable efforts have been made to extract provenance information from compositional and textural features of sandstone, and a thorough review of the subject is given by Folk (1974), Pettijohn et al. (1987). Standard petrographical approaches to the identification of source rock of sandstones are

investigation of types of feldspar present (Pittman, 1970) and rock fragments (Pettijohn et al. 1987). Tectonic setting can be determined from the relative proportion of quartz, feldspar, and rock fragments (Dickinson, 1982; 1985).

### 3.1.1 Equipments and Analytical Method

The samples were crushed and splitted before grinding and sieving for powder. Geochemical analyses were performed for major and trace elements. Thirty samples of sandstone and shale of flysch and molasse sequences were analyzed for major elements by X-ray fluorescence spectrometer (XRF) at the laboratory of Suranaree University of Technology. XRF using fusion discs prepared according to the method of Norrish and Hutton (1969). Thirty-three samples of sandstone, shale, and allodapic limestone of all sequences were analyzed for trace element and rare earth elements by inductively coupled plasma mass spectrometry (ICPMS) at the Key Laboratory of the Lithosphere and Crustal Evolution, China University of Geosciences (Wuhan).

### 3.1.2 Major Elements

Major elements comprise of $SiO_2$, $TiO_2$, $Al_2O_3$, $Fe_2O_3$, MnO, MgO, CaO, $Na_2O$, $K_2O$, $P_2O_5$, and $SO_3$. The major element composition of siliciclastic sediments of the Nam Duk Formation at the type section and the sections further north and south of the Phetchabun Fold Belt are compiled in Appendix A. The commonly used geochemical criteria of sediment maturity are the $SiO_2$/ $Al_2O_3$ ratio (Potter, 1978), which reflecting the abundance of quartz and the clay and feldspar content. According to Herron (1988), the $Fe_2O_3$/ $K_2O$ ratio is more successfully classified shale and sandstone and is also a measure of mineral stability, for ferromagnesian minerals they tend to be amongst the less stable minerals during weathering. The $SiO_2$/ $Al_2O_3$

and $Fe_2O_3$/ $K_2O$ ratios of the siliciclastic samples are plotted in order to distinguish the terrigeneous siliciclastic sediments in each formation.

### 3.1.3 Trace Elements

The geochemical data of trace elements for all rock units are tabulated in Appendix A. Taylor and McLennan (1985), and Bhatia and Crooks (1986) regard REE, Y, Th, U, Sc, and Co as the most useful elements in determining upper crustal abundances from clastic sedimentary rocks and as discrimination of tectonic settings. This is because both strongly incompatible elements (LREE, Th, U) and strongly compatible elements (Sc, Co) are represented in this group. All these elements tend to have low concentrations in ocean and river water, and residence times in the oceans are similarly low. When these features are combined with the observation that they are not affected by diagenesis and metamorphism (Rollinson, 1993), the ratios of incompatible elements can serve as an index of differentiation (Taylor and MaLennan, 1985).

### 3.1.4 Rare Earth Elements (REE)

The rare earth elements (REE) are the most useful of all trace elements and REE studies have important applications in igneous, sedimentary and metamorphic petrology. The REE comprise the series of metals earth atomic numbers 57 to 71 (La-Lu). REE are not easily fractionated during sedimentation and diagenesis, thus sedimentary REE patterns reflect the REE pattern of the sources (Taylor and McLennan, 1985; McLennan, 1989; Condie, 1991). It is generally accepted that mixing of various provenance components results in remarkable uniformity of the REE patterns in fine-grained sedimentary rocks (McLennan et al., 1993; Singh and Rajamani, 2001). Therefore, the REE's are particularly useful in

provenance investigation and concentration in sedimentary rocks is usually normalized to a sedimentary standard such as North American shale composite (NASC), European shale, Post Archaean average Australian Shale (PAAS), and Upper crust.

### 3.1.5 Tectonic setting and Provenance

Several studies including Bhatia (1983) and Roser and Korsch (1986), led to the recognition of major elements that are useful discriminating parameters. The discrimination diagram for sandstone, based upon a bivariation plot of $TiO_2$ and ($Fe_2O_3$ + MgO), was proposed by Bhatia, (1983). The fields display oceanic island arc, continental island arc, active continental margin, and passive margin. Tectonic-setting discrimination diagram using $K_2O$/ $Na_2O$ ratio and $SiO_2$ content (Roser and Korsch, 1986) are applied. The diagrams are suitable for sandstone-mudstone and show the fields of a passive continental margin, an active continental margin and an island arc. Ti and Al are generally considered to be chemically immobile constituents of weathering profiles, sediments and sedimentary rocks (Maynard, 1992), and may be used as provenance indicators (Young and Nesbitt, 1998). The $TiO_2$ versus $Al_2O_3$ plot showing fields of alkali granite, granodiorite, and peridotite is presented. A discrimination function diagram has been proposed by Roser and Korsch (1988) to distinguish between sediments whose provenance is primarily mafic, intermediate or felsic igneous and quartzose sedimentary rocks. A plot of two discriminate functions, based upon the oxides of Ti, Al, Fe, Mg, Ca, Na, and K, differentiates most effectively the four provenances.

Trace elements, concentrations of trace element and their ratios can be useful discriminators of tectonic settings because some trace elements are considered to be immobile during sedimentation (Bhatia and Crook, 1986). A simple two-

component mixing model (ratio-ratio plots Co/Th vs La/Sc, Co/Th vs Sc/Th) using incompatible and compatible elements are plotted. The ferromagnesian trace elements, Ni, Cr, and V are generally abundant in mafic and ultramafic rocks, and their enrichment in sedimentary rocks may be indicative of the presence of these rocks in the provenance area (McLennan, et al., 1993). The abundance of mafic and ultramafic rocks in the provenance can be further tested by Y/Ni ratios. Cr/V ratios can also indicate the presence of chromite among the heavy minerals (McLennan, et al., 1993).

Amount of La, Th, Ba, Sc, Co, Cr and their element ratios such as La/Sc, Th/Sc, Ba/Sc, La/Cr, Th/Cr are useful indicators for discriminating basic and felsic source rocks (Andre et al., 1986; Cullers el al., 1988; Culler, 1994). The immobile elements have also been used for the same proposed as major elements. In general, there is a systematic increase in the light rare-earth elements (La, Ce, and Nd), in Th and Nb, and in a La/Y ratio; and a decrease in V and Sc in greywackes from oceanic island arc to continental island arc, to active continental margin and to passive continental margin. The trace elements discriminators of tectonic settings and source composition of Nam Duk Formation are compared to those well study of Bhatia and Crook (1986) and Culler (1994). Distinctive fields for four environments; oceanic island arc, continental island arc, active continental margin and passive margin are recognized on the ternary plots of La-Th-Sc, Th-Sc-Zr/10 and Th-Co-Zr/10. However, on a La-Th-Sc plot, the fields of active continental margin sediments and passive margin sediments are overlapped, but the Th-Sc-Zr/10 shows distinct separation.

## 3.2 Cathodoluminescence analysis

Cathodoluminescence (CL) is the visible light emitted by the surface of a mineral when bombarded with electrons in a vacuum. The term cathodoluminescence designates the luminescence induced by electron bombardment. The interaction of the electron beam with the sample gives rise to a number of effects: the emission of secondary electrons (SE), back-scattering of electrons (BSE), electron absorption ("sample current"), characteristic X-ray, and CL emission (Figure 3.1). Most energy of the beam is converted into heat. The penetration depth of electrons and accordingly, the excitation depth depend on the energy of the electrons (10-20 keV) and are in the range of 2-8 μm (e.g. Marshall, 1988).

### 3.2.1 Cathodoluminescence Microscope (HC3-LM)

The commercially produced hot-cathodoluminescence microscope (HC1-LM) after Neuser et al. (1995) is provided with a high-vacuum chamber ($<10^{-5}$ mbar) and uses an accelerlation voltage of 14 keV (Figure 3.2). The HC1-LM is a development of the prototype constructed at the IGDL Göttingen in 1987 (Neuser, 1988) according to the model of Zinkernagel (1978). The electron gun operates as a "hot cathode", i.e. the electrons are emitted from a heated filament. The hot-cathode technique provides a considerably greater beam stability and CL intensity and thus is suitable for investigation of the weakly luminescent quartz. The electron gun directs a focused beam upwards onto an inverted thin section; the CL is viewed through the sample from above. The electron beam with a diameter of ca. 4.8 mm irradiates the thin section surface with a current density of ca. 10 $mA/mm^2$. The basis of the HC3-LM is a polarization microscope model OLYMPUS BX30M with some modifications, for instance, the vacumm sample chamber is mounted in place of the sample stand.

The polarization objectives have a magnification/numerical aperture of 5x/0.15, 10x/0.30, and 20x/0.40. The high vacumm of the sample chamber is attained by a Diffstak oil diffusion pump combined with an Edwards rotary vane pump.

### 3.2.2 Sample Preparation

The samples used for CL measurement need the extremely smooth and highly polished thin section without cover slips. The first stage of sample preparation consists of cutting the section, which was mounted on a glass slide with epoxy resin. Subsequent polishing was carried out with progressively finer grades of abrasive. The final stage involves polishing with diamond paste with a grade of 0.3 μm. The samples were thoroughly cleaned. The polished surface was mounted on a standard glass slide (48x24x2.8 nm) with Akemi Mamorkitt 1000. The other glass slide was removed and the procedure of polishing was repeated until a section thickness of 250 μm was reached. For sample temperature measurements during CL and FTIR spectroscopy the section was removed from the glass slide with Xylol. In addition, a number of thin sections were chemically polished with a OP-S suspension of different granularities (1 μm and 3 μm) in order to test the effect of the surface quality on the CL properties.

Quartz being a non-conductor requires a conductive coating to prevent charging under electron bombardment. The preferred coating for CL studies is carbon. The coating was done at standard conditions to a thickness of about 15 μm to avoid variations in CL intensity. The instruments and thin sections preparation were done at the Center of Geosciences, University of Göttingen, F. R. Germany.

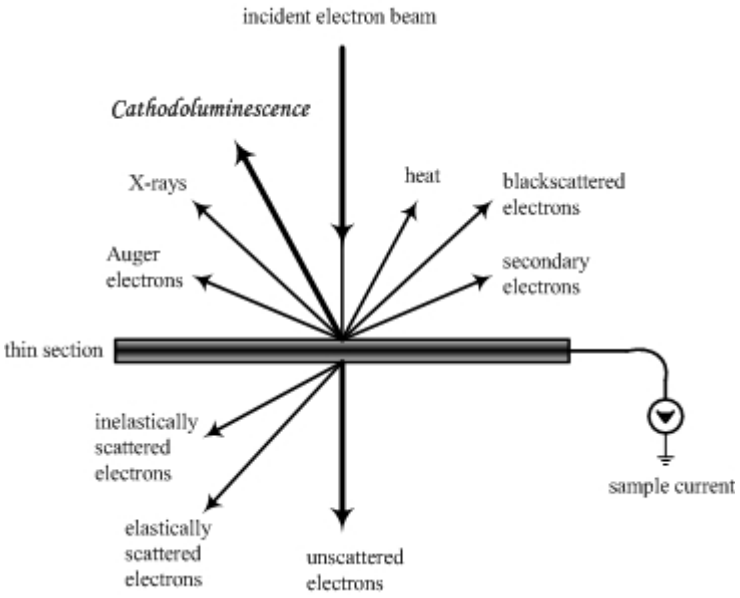


**Figure 3.1** Schematic representation of processes resulting from electron bombardment (modified after Potts et al. 1995). Note that the emissions come from different depths e.g. CL and X-ray are emitted from deeper section levels than secondary electrons.

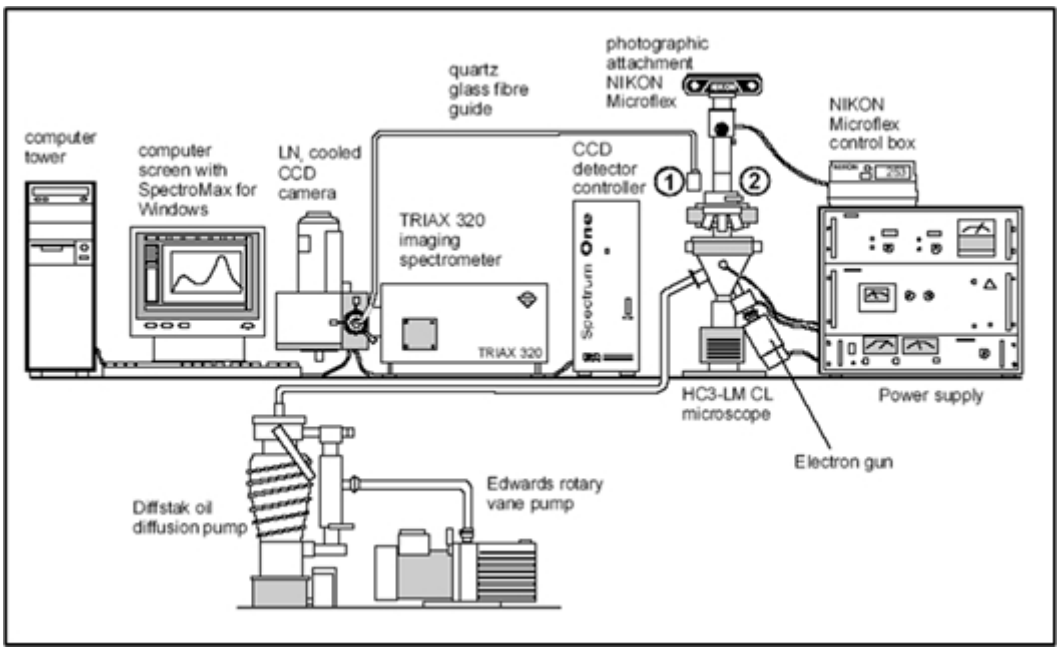


**Figure 3.2** Cathodoluminescence equipment HC3-LM with TRIAX 320 spectrography and photographic Microflex attachment at the Center of Earth Sciences, Göttingen, (1) configuration for spectral analysis, (2) configuration for photographic documentation (after Müller, 2000).

### 3.2.3 Geological Application

Cathodoluminescence petrography is now a routine technique that can provide essential information on provenance, growth fabrics, diagenetic textures and mineral zonation, in addition to enabling more precise quantification of constituents and fabrics. This CL method is very informative for trace element identification in minerals. From the geological point of view, there are two main applications of CL. The first is the differentiation of detrital from diagenetic phase and the second provide information on mineral paragenesis.

### 3.2.4 Provenance Interpretation of Quartz from CL

The CL color of quartz and feldspar in sandstone may provide a signature of the source rock from which individual grains, or populations of grains, were derived. This information, in concert with conventional petrography, study of accessory minerals, and geochemistry, provided a broad base upon which to infer petrogenetic relations (such as shared source regions), provenance, and to some extent, paleotectonic setting (Owen, 1991).

Provenance studies of detrital quartz are one of the most important of CL on sandstone petrography (Zinkernagel, 1978; Matter and Ramseyer, 1985; Owen, 1991; Götze and Simmerle, 2000; Richter et al. 2003). However, there are three critical assumptions for interpretation which must be made before CL can provide legitimate provenance information (Owen, 1991). (1) CL color is characteristic of the grain and does not change with time or exposure to the sedimentary environment. (2) CL color is invisible to sedimentary processes such that grains are not segregated appreciably based on their CL color. (3) stratigraphic units under consideration are sufficiently well mixed so that CL color distributions are sensibly uniform over a broad area.

Owen (1991) defined the assumptions discussed above as “the relative abundance of quartz CL colors should remain essentially unchanged for a sand population as it experiences one or several cycles of uplift, erosion, and deposition. In this way, the sand’s identity is preserved in a manner similar to the preservation of blood types or languages among migrating groups of people. If sands become mixed with other sands during transportation, their petrogenetic signals will become mixed as well”.

Based on his pioneering work, Zinkernagel (1978), presented an extensive discussion of quartz CL, with well reproduced color plates. He defined three types of quartz, based on CL and original occurrence as follow: *Violet-luminescing quartz*, from plutonic, volcanic, and contact metamorphic rocks or rocks which have undergone fast cooling; *Brown-luminescing quartz*, from low-grade metamorphic rocks, or from high-grade metamorphic rocks which have been slowly cooled; and *Nonluminescing quartz*, from authigenic. The recent general classification of the CL behavior of the CL detrital quartz (Götze and Simmerle, 2000) distinguishes the following criteria: *blue or violet*, plutonic quartz as well as quartz phenocrysts in volcanic rocks, and high grade metamorphic quartz; *red*, matrix quartz in volcanic rocks; *brown*, quartz from regional metamorphic rocks; *non or weakly luminescent*, authigenic quartz; *short-lived green or blue*, hydrothermal and pegmatitic quartz.

Müller (2000) studied CL properties of magmatic quartz and has subdivided it into (1) euhedral quartz phenocrysts showing stable, dominantly blue CL and growth zoning related to Ti distribution and (2) anhedral matrix quartz with unstable red-brown CL and homogeneous trace element distribution. Rhyolitic and granitic quartz phenocrysts also show similar growth textures. Hydrothermal quartz shows similar growth patterns as magmatic quartz, but stepped zoning is dominant. The application of scanning cathodoluminescence (SEM-CL) imaging to characterize volcanic, plutonic, and metamorphic quartz was proposed (Seyedolali et al., 1997; Kwon and Boggs, 2002). According to Seyedolali et al., (1997), the volcanic quartz is characterized by well-developed zoning in CL images. Plutonic quartz may also be zoned, but much plutonic quartz is unzoned. Metamorphic quartz is more complex; its characteristics depend upon whether metamorphism has been largely thermal (contact

metamorphism) or has resulted from regional tectonic forces. Thermally metamorphosed quartz typically displays few internal features in CL images, other than a few late-stage fractures, or it has a kind of indistinct, ill-defined, mottled texture.

### 3.2.5 CL of carbonate mineral

For carbonate minerals, when activated, can exhibit intense CL. The important ions affecting luminescence intensity in carbonate are $Mn^{2+}$ and $Fe^{2+}$, with the manganese activating luminescence and the iron quenching it. Hence, variations in luminescence intensity usually reflect a variation in the ratio of $Mn^{2+}$ to $Fe^{2+}$ in a crystal. The CL measurement of the various carbonate minerals usually ranges in color from green to red. For example, calcite or dolomite cement often stands out clearly from the other minerals in a sedimentary sample. One of widespread use of CL in carbonate studies is in cement stratigraphy using zoned cements. The CL intensity which is an expression of the possible iron and manganese content may be used as a guide to deciding whether the sedimentary carbonate was formed under oxidizing or reducing conditions. The uniformity or non-uniformity of conditions during deposition and post tectonic deformation can be revealed.

### 3.2.6 Statistical Analysis for Quartz Provenance

CL reveals petrogenetic relations between candidate sands (or sandstones) by demonstrating statistically significant similarity between their distributions of CL colors. This is conceptually identical to linking two sands by means of modal analysis, except that CL may rely upon fewer variables (Owen, 1991). When comparing sandstones for possible a genetic connection, multiple CL point counts are required from each candidate stratigraphic unit. Each point count,

consisting of CL color determination of grains per thin section, reduces to single value. If one chooses the simple brown-blue CL color distinction, a value of "percent brown CL quartz" represents each thin section (Owen and Carozzi, 1986). The collection of data sets for each formation or sampling site is amalgamated into a frequency histogram that shows the range and abundance of values held by each parameter.

As mentioned above, combination of all criteria to identify and interpret the provenance of detrital quartz grains are presented. The statistical analysis by point counting was used. CL point counts are required from each candidate stratigraphic unit. Each point count, consisting of CL color determination of grains per thin section, reduces to single value.

# CHAPTER IV

# GEOCHEMICAL RESULT AND INTERPRETATION

This chapter presents the result of the geochemical analysis of the siliciclastic sediments from the Nam Duk Formation at the types section and the sections further to the north and south of the Phetchabun Fold Belt.

## 4.1 Nam Duk Formation

### 4.1.1 Nam Duk Formation at Phetchabun

Field work and samples collection were carried out on the exposures of Nam Duk Formation along the highway cut across the forestry area of the Phetchabun and Loei provinces. Samples are collected from the sequences of pelagic, flysch, and molasse at the localities indicated by the number of milestone from Lom Sak to Chum Phae Highway (Figure 1.5 in Chapter 1).

***Major elements***

All the flysch samples fall in the field of Fe-sand in the plots of $SiO_2$/ $Al_2O_3$ and $Fe_2O_3$/ $K_2O$ (Figure 4.1). Similarly the samples of molasse sequence are scattered and fall into the field of Fe-sand with somce in Wacke (Figure 4.2). Both sequences have very high $TiO_2$ and $Fe_2O_3$, but low $Al_2O_3$, and a wide range of CaO and $K_2O$. However, an average concentration of $TiO_2$, $Fe_2O_3$, and $Al_2O_3$ of flysch samples are lower than molasse samples. It seems to be less $Na_2O$ content than molasse samples, only a few ppm (two samples) can be detected.

The tectonic-setting discrimination diagram using $K_2O/ Na_2O$ ratio and $SiO_2$ content (Roser and Korsch, 1986) was applied to flysch and molasse sequences. Due to small $Na_2O$ content in molasse sequences, only the data obtained from flysch sequence are plotted. They show indication of oceanic island arc margin to active continental margin setting (Figure 4.3). The discrimination diagram based upon a bivariation plot of $TiO_2$ and ($Fe_2O_3$ + MgO) is plotted. Due to the high $TiO_2$ content, only half of samples from flysch sequence can be plotted and they fall into the field of oceanic arc setting (Figure 4.4). The provenance signature of siliciclastic sandstones from flysch and molasse are plotted by using discrimination diagram of Roser and Korsch (1988). Scattering plots of both sequences show dominantly mafic igneous provenance (Figure 4.5). The best-fit line of the $TiO_2$ versus $Al_2O_3$ of flysch and molasse passes through the estimated peridotite end member which indicates an ultramafic-mafic provenance (Young and Nesbitt, 1998; Figure 4.6 and 4.7).

***Trace elements***

The trace elements of pelagic, flysch, and molasse sequences are compiled in Appendix A. In the pelagic sequence, shales and micritic-limestones have been chosen for ICPMS. Sandstones and shales are more prominent in flysch and molasse sequences and are used for trace elements analysis. The plots of incompatible and compatible elements of La vs Sc, Th vs Sc, La vs Nb, and Th vs U, all samples show variable degrees of correlation (Figure 4.8). The best correlation is recorded between Th and U. Correlation trends of bivariate plots in sediments demonstrate that the detritus was well mixed especially in flysch and molasse samples. The Y/Ni and Cr/V elemental ratios which are used to identify mafic-ultramafic sources are plotted in Figure 4.9 (Hiscott, 1984). Cr/V ratios of flysch and

molasses samples are higher than 1 which indicates the presence of chromite among the heavy mineral during deposition. Y/Ni ratios in the flysch and molasse are low which confirms that the mafic and ultramafic rocks were abundantly present in the source area of the Nam Duk Formation. Cr/V versus Y/Ni ratios is analyzed and they indicate mainly the ultramafic sources, although some samples are scattered. The plots of the pelagic samples are scattered. Some of them are similar to Post Archaean average Australian Shale (PAAS). Two samples plotted are close to the field of ultramafic and one sample plotted close to the granite member.

Chondrite normalized REE and trace elements abundance patterns of pelagic, flysch, and molasse samples are plotted and compared with the sedimentary composition standard as shown in Table 4.1 (Figure. 4.10). Flysch and molasse samples have higher concentration of Cr, Sr, Zr, Ba, and light rare earth elements (LREE, La through Eu) similar to pelagic samples but they have lower average values (Figure 4.11, 4.12, and 4.13). Comparison of REE plot from well known source and the Nam Duk Formation including chert sample from Nan-Uttaradit Suture Zone is shown in Figure 4.14. Summation of rare earth elements increases from oceanic island arc to continental island arc, and it is the highest in an Andean-type margin and a passive margin (Bhatia, 1985). Summation of REE of the flysch is higher than molasse and is nearly the same as pelagic samples (Table 4.1). In addition, these values are also less than the average summation of REE from NASC, PAAS, Upper Crust, and European shale. The result indicates that the Nam Duk Basin was not derived from the Upper Crust and should have been deposited in the oceanic to continental island arc environments.

According to the comparison data in Table 4.2, flysch and molasse samples show similarity of continental island arc setting (Bhatia and Crook, 1986) and indicate low-silica metamorphic sources (Culler, 1994). Pelagic samples are not clearly defined. They show values between oceanic to continental island arc setting and indicate low-silica metamorphic sources. A La-Th-Sc and Th-Sc-Zr/10 ternary diagrams are plotted to discriminate tectonic setting and composition of source rocks as shown in Figure 4.15, 4.16, and 4.17 (Bhatia and Crook, 1986: Cullers, 1994). However, on a La-Th-Sc plot, the fields of active continental margin and passive margin sediments are overlapped, but the Th-Sc-Zr/10 shows distinct separation. For pelagic sequence, the result of a La-Th-Sc ternary diagram plot falls into the field of oceanic island arc and continental island arc setting and it is derived mainly from metabasic source. The sediments of flysch and molasse sequences are derived from mixed sources from metabasic and granitic gneiss and fall into the field of continental island arc setting. In consideration of the Th-Sc-Zr/10 plots, most of pelagic samples fall into the fields of oceanic island arc and continental island arc setting. On the contrary, only the field of continental island arc setting is plotted in flysch and molasse sequences. This result is consistent with the low La, Th, U, Zr, and Nb concentrations in the sandstones and shales.

**Table 4.1** Standard sedimentary compositions and Permian siliciclastic sediments from Phetchabun and Loei Fold Belt including Nan-Uttaradit suture zone used for normalizing the REE concentration in sedimentary rocks (in ppm).

| | NASC | PAAS | Upper crust | ES | Pelagic | Flysch | Molasse | Tha Li | Chiang Khan | Muak Lek | Khon San | Chert, Nan |
|---|---|---|---|---|---|---|---|---|---|---|---|---|
| (REE) | *1* | *2* | *3* | *4* | *5* | *6* | *7* | *8* | *9* | *10* | *11* | *12* |
| La | 31.10 | 38.20 | 30.00 | 41.10 | 19.29 | 20.83 | 24.62 | 27.10 | 20.93 | 26.26 | 27.78 | 2.17 |
| Ce | 67.03 | 79.60 | 64.00 | 81.30 | 33.08 | 36.88 | 46.20 | 50.80 | 37.66 | 51.20 | 49.44 | 2.97 |
| Pr | | 8.83 | 7.10 | 10.40 | 5.00 | 5.02 | 5.95 | 6.60 | 5.03 | 6.63 | 6.40 | 0.48 |
| Nd | 30.40 | 33.90 | 26.00 | 40.10 | 20.47 | 18.39 | 22.19 | 23.80 | 18.87 | 24.83 | 23.02 | 1.79 |
| Sm | 5.98 | 5.55 | 4.50 | 7.30 | 4.81 | 3.71 | 4.53 | 4.60 | 4.16 | 5.10 | 4.48 | 0.50 |
| Eu | 1.25 | 1.08 | 0.88 | 1.52 | 1.05 | 0.81 | 1.00 | 1.00 | 0.98 | 1.12 | 0.89 | 0.16 |
| Gd | 5.50 | 4.66 | 3.80 | 6.03 | 4.45 | 3.23 | 4.01 | 4.10 | 3.92 | 4.72 | 3.92 | 0.41 |
| Tb | 0.85 | 0.77 | 0.64 | 1.05 | 0.77 | 0.54 | 0.69 | 0.70 | 0.67 | 0.80 | 0.65 | 0.08 |
| Dy | 5.54 | 4.68 | 3.50 | | 4.21 | 3.03 | 3.86 | 3.80 | 3.67 | 4.20 | 3.56 | 0.40 |
| Ho | | 0.99 | 0.80 | 1.20 | 0.87 | 0.60 | 0.77 | 0.80 | 0.76 | 0.77 | 0.66 | 0.09 |
| Er | 3.28 | 2.85 | 2.30 | 3.55 | 2.24 | 1.68 | 2.11 | 2.20 | 1.99 | 2.10 | 1.88 | 0.28 |
| Tm | | 0.41 | 0.33 | 0.56 | 0.33 | 0.25 | 0.33 | 0.30 | 0.29 | 0.30 | 0.28 | 0.04 |
| Yb | 3.11 | 2.82 | 2.20 | 3.29 | 2.32 | 1.78 | 2.28 | 2.40 | 2.12 | 2.11 | 1.95 | 0.28 |
| Lu | 0.46 | 0.43 | 0.32 | 0.58 | 0.39 | 0.29 | 0.37 | 0.40 | 0.35 | 0.34 | 0.32 | 0.04 |
| Sum | 154.50 | 184.77 | 146.37 | 197.98 | 99.28 | 97.04 | 118.91 | 128.60 | 101.40 | 130.47 | 125.22 | 9.70 |

*1* *North American shale composite (Gromet et al., 1984)*
*2* *Post Archaean average Australian sedimentary rock (McLennan, 1981)*
*3* *Average upper continental crust (Taylor and McLennan, 1981)*
*4* *Average European shale (Haskin and Haskin, 1966)*
*5* *Average Pelagic sequence of the Nam Duk Formation (this study)*
*6* *Average Flysch sequence of the Nam Duk Formation (this study)*
*7* *Average Molasse sequence of the Nam Duk Formation (this study)*
*8* *Average Permian siliciclastic sediments sequence from Tha Li, Loei (this study)*
*9* *Permian siliciclastic sediments from Chiang Khan, Loei (this study)*
*10* *Permian siliciclastic sediments from Pang Asok Formation, Muak Lek, Saraburi (this study)*
*11* *Permian "Upper Clastic" from Hw.12 Km. 84+530, Khon San, Chaiyaphum (this study)*
*12* *Permian "Chert" from Nan-Uttaradit Ophiolitic sequence (this study)*

**Table 4.2** Trace element discriminators of tectonic settings and source composition.

| | Graywackes, Bhatia and Crook (1986) | | | | Culler (1994) | | Nam Duk Formation (this study) | | |
|---|---|---|---|---|---|---|---|---|---|
| Trace ele. | Passive margin | Active continental margin | Continental island arc | Oceanic island arc | high-silica metamorphic sources | low-silica metamorphic sources | Molasse (ave) | Flysch (ave) | Pelagic (ave) |
| Discriminators decreasing toward oceanic island or low silica sources | | | | | | | | | |
| Pb | 16.00 | 24.00 | 15.10 | 6.90 | | | 14.99 | 12.18 | 11.11 |
| Th | 16.70 | 8.80 | 11.10 | 2.27 | 17.00 | 8.00 | 9.40 | 6.88 | 3.50 |
| Zr | 298.00 | 179.00 | 229.00 | 96.00 | | | 210.36 | 185.98 | 159.35 |
| Hf | 10.10 | 6.80 | 6.30 | 2.10 | 12.20 | 6.90 | 6.08 | 5.26 | 4.66 |
| Nb | 7.90 | 10.70 | 8.50 | 2.00 | | | 9.44 | 7.58 | 6.47 |
| La | 33.50 | 33.00 | 24.40 | 8.72 | 57.00 | 45.50 | 24.62 | 20.83 | 33.98 |
| Ce | 71.90 | 72.70 | 50.50 | 22.53 | 127.00 | 87.00 | 46.20 | 36.88 | 54.86 |
| Nd | 29.00 | 25.40 | 20.80 | 11.36 | | | 22.19 | 18.39 | 35.37 |
| Rb/Sr | 1.19 | 0.89 | 0.65 | 0.05 | | | 0.353 | 0.133 | 0.078 |
| La/Y | 1.31 | 1.33 | 1.02 | 0.48 | | | 1.134 | 1.188 | 0.757 |
| La/Sc | 6.25 | 4.55 | 1.82 | 0.55 | 20.00 | 1.80 | 2.484 | 2.584 | 1.598 |
| Th/Sc | 3.06 | 2.59 | 0.85 | 0.15 | 7.00 | 0.33 | 0.949 | 0.854 | 0.285 |
| Th/U | 5.60 | 4.80 | 4.60 | 2.10 | | | 4.159 | 3.865 | 2.340 |
| Ba/Sc | | | | | 268.00 | 29.50 | 19.037 | 17.019 | 10.557 |
| La/Cr | | | | | 3.70 | 0.98 | 0.029 | 0.023 | 0.116 |
| Th/Cr | | | | | 1.10 | 0.11 | 0.011 | 0.008 | 0.021 |
| Discriminators increasing toward oceanic island or low silica sources | | | | | | | | | |
| Ti | 0.22 | 0.26 | 0.39 | 0.48 | | | | | |
| Sc | 6.00 | 8.00 | 14.80 | 19.50 | 4.50 | 31.00 | 9.910 | 8.060 | 12.070 |
| Co | 5.00 | 10.00 | 12.00 | 18.00 | | | 13.700 | 14.250 | 11.470 |
| Zn | 26.00 | 52.00 | 74.00 | 89.00 | | | 67.990 | 59.440 | 65.380 |
| Cr | | | | | 18.50 | 113.00 | 840.760 | 899.050 | 166.890 |
| Ti/Zr | 6.74 | 15.30 | 19.60 | 59.80 | | | | | |
| Zr/Hf | 29.50 | 26.30 | 36.30 | 45.70 | | | 34.599 | 35.357 | 36.342 |
| Zr/Th | 19.10 | 9.50 | 21.50 | 48.00 | | | 22.379 | 27.029 | 29.052 |
| La/Th | 2.20 | 1.77 | 2.36 | 4.26 | | | 2.619 | 3.028 | 5.608 |
| Sc/Cr | 0.16 | 0.30 | 0.32 | 0.57 | | | 0.012 | 0.009 | 0.072 |

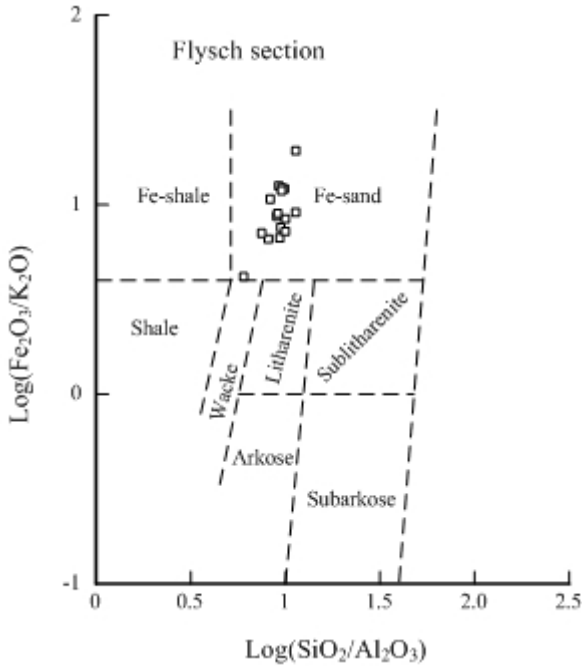


**Figure 4.1** Classification of terrigeneous sandstones and shales of flysch samples (after Herron, 1988). The plots fall into the field of Fe-sand.

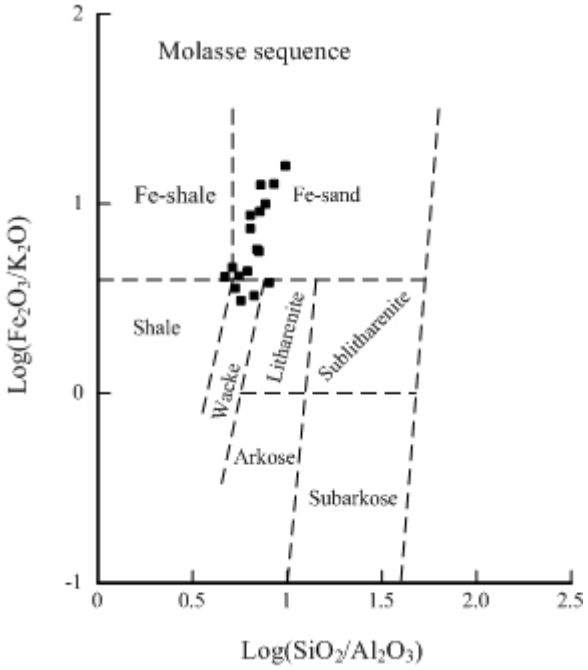


**Figure 4.2** Classification of terrigeneous sandstones and shales of molasse samples (after Herron, 1988). The plots fall into the field of Fe-sand and Wacke.

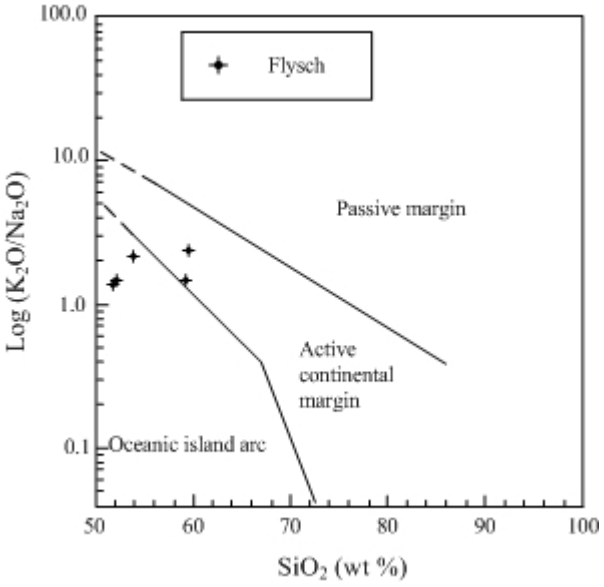


**Figure 4.3** Discrimination diagrams of Roser and Korsch (1986) for flysch sandstones showing the field of oceanic island arc to active continental margin.

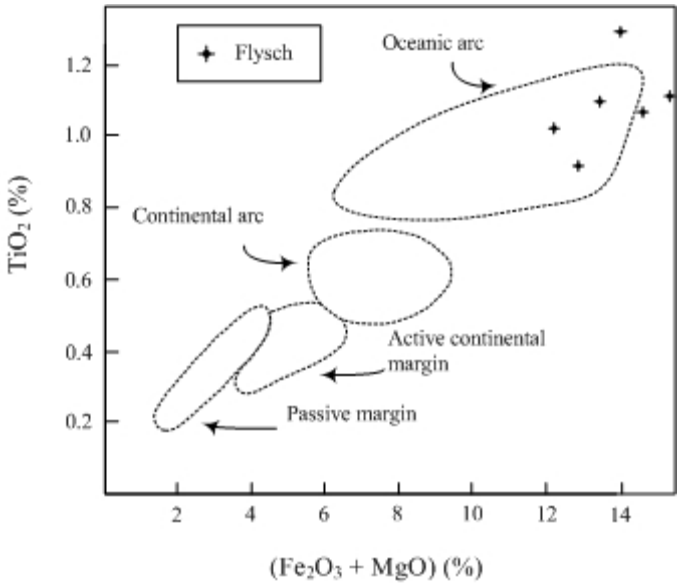


**Figure 4.4** Discrimination diagram for flysch sandstones based upon a bivariation plot of $TiO_2$ versus ($Fe_2O_3$ + MgO) after Bhatia (1983).

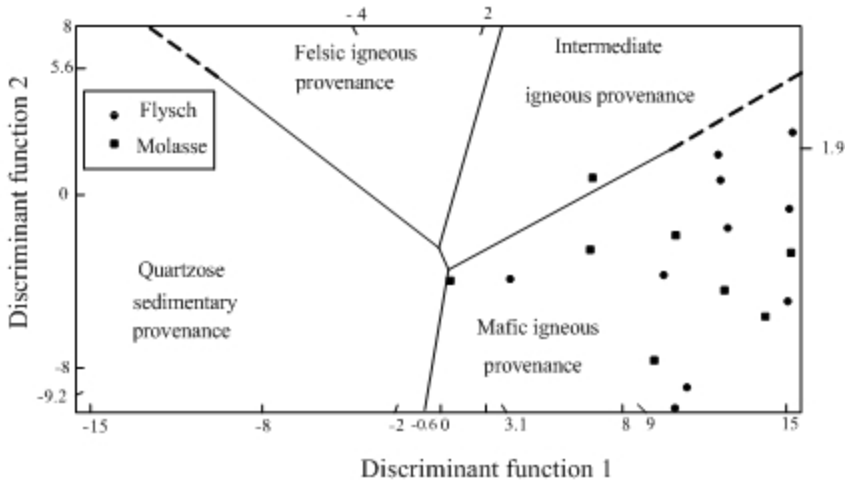


**Figure 4.5** Provenance signature of flysch and molasse siliciclastic sediments using major elements indicates a mafic igneous source of flysch and molasse sections (modified from Roser and Korsch, 1988).

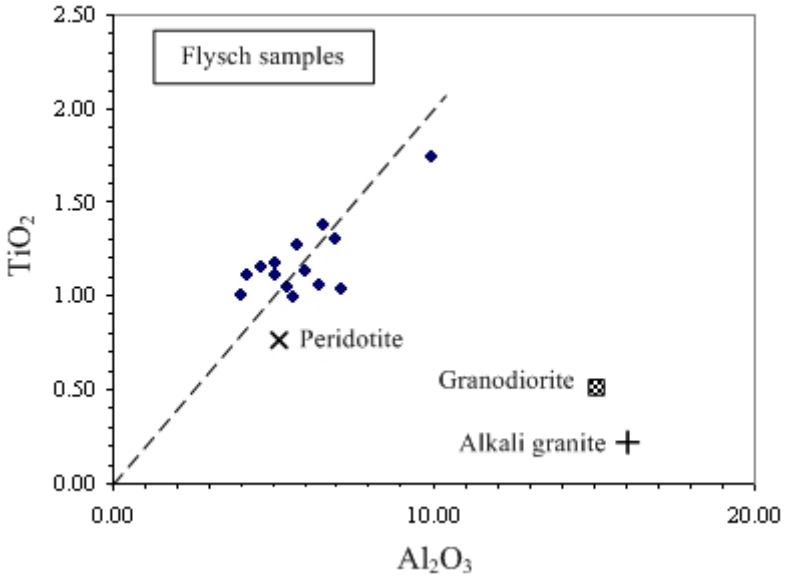


**Figure 4.6** $TiO_2$ versus $Al_2O_3$ plot for the flysch samples shows a positive correlation trend with peridotite end member (Young and Nesbitt, 1998).

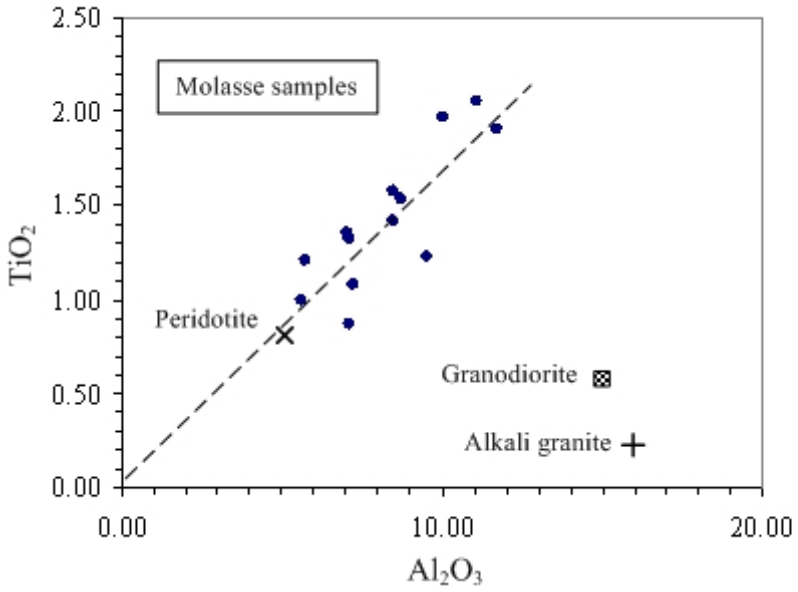


**Figure 4.7** $TiO_2$ versus $Al_2O_3$ plot for the molasse samples shows a positive correlation trend with peridotite end member (Young and Nesbitt, 1998).

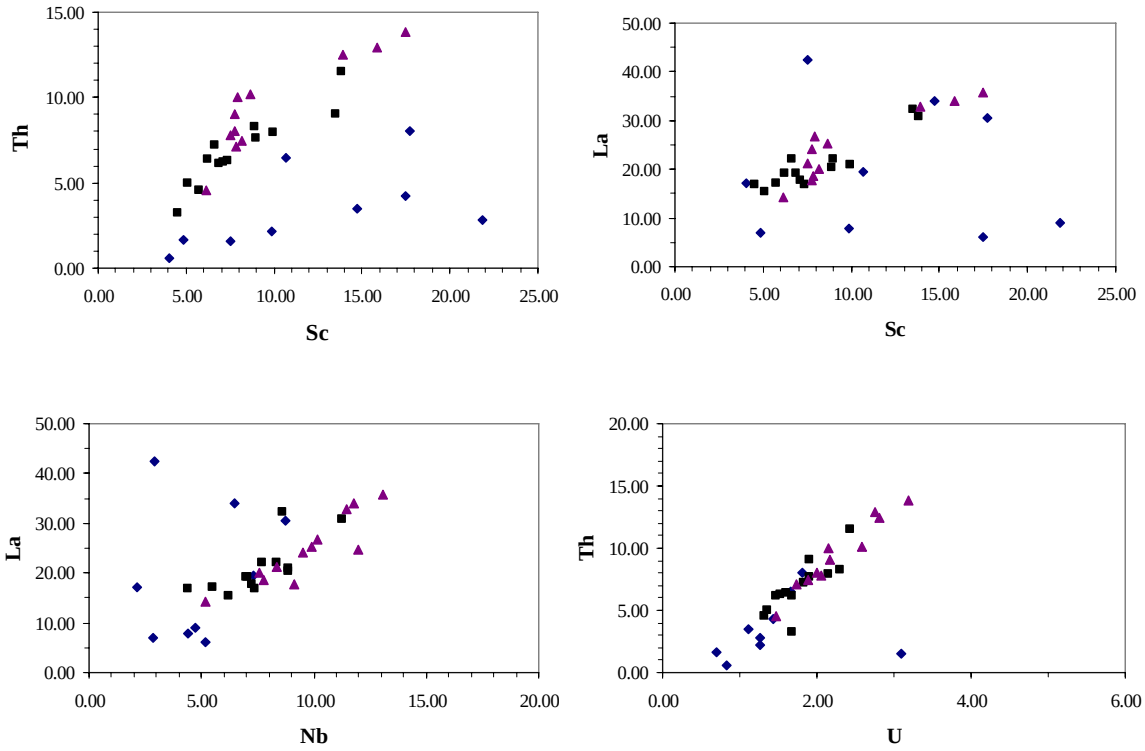


**Figure 4.8** Bivariate plots of incompatible versus compatible trace elements of the Nam Duk Formation (explanation; rhombic = pelagic, square = flysch, triangle = molasse).

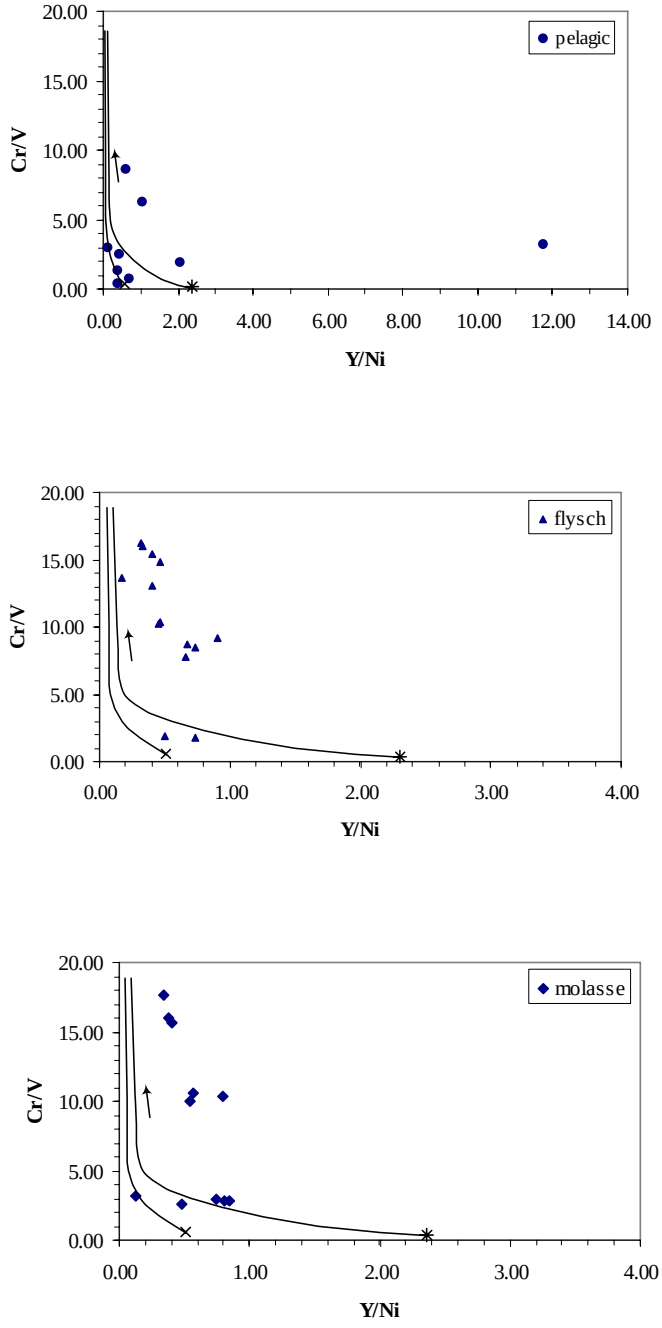


**Figure 4.9** Cr/V vs. Y/Ni diagrams of flysch and molasse samples show an ultramafic end member as indicated by high Cr/V and low Y/Ni ratios. Pelagic samples show scattering plot (Hiscott, 1984).

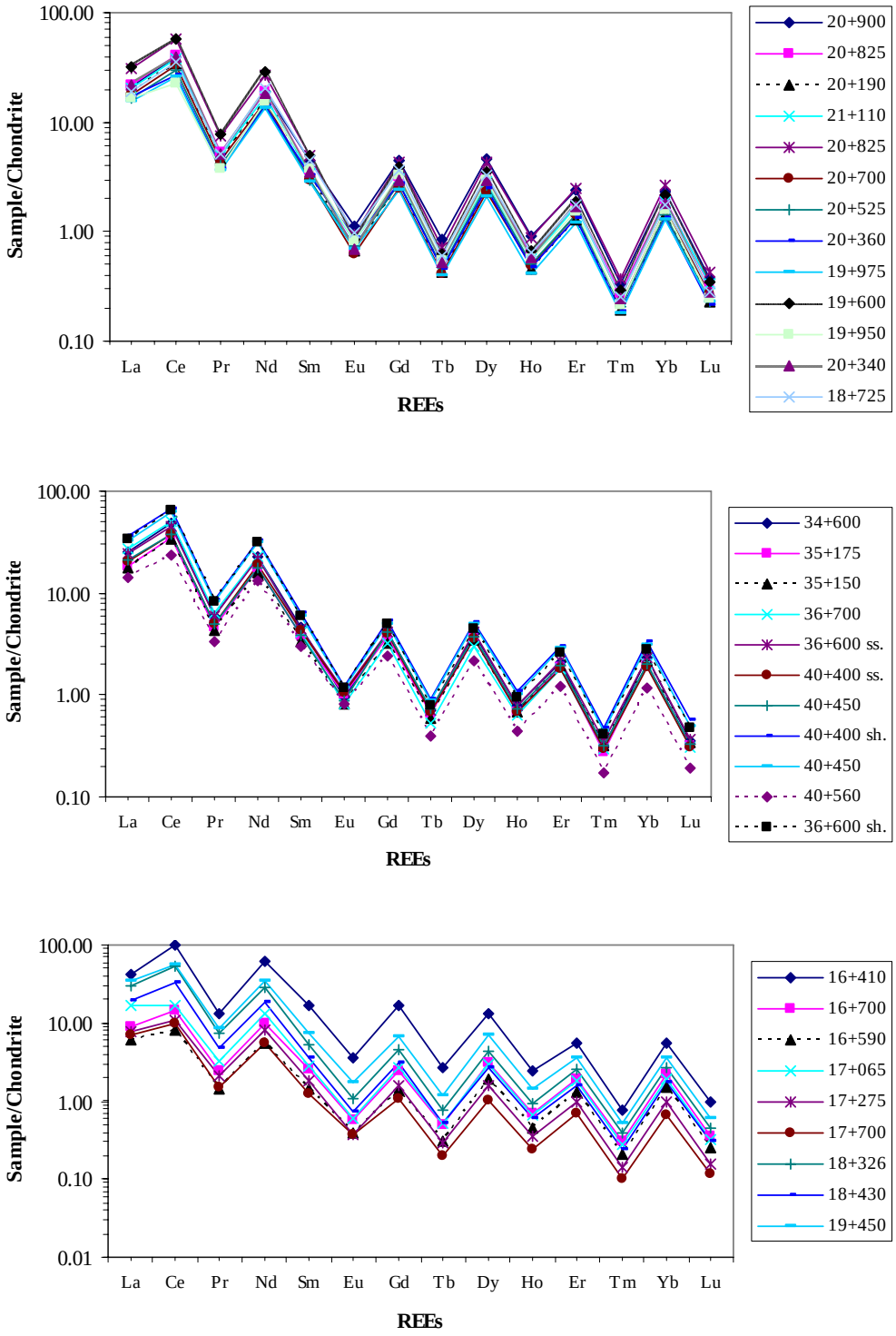


**Figure 4.10** Chondrite normalized rare earth element distributions in pelagic, flysch, and molasse samples display similar characteristic especially for flysch and molasse.

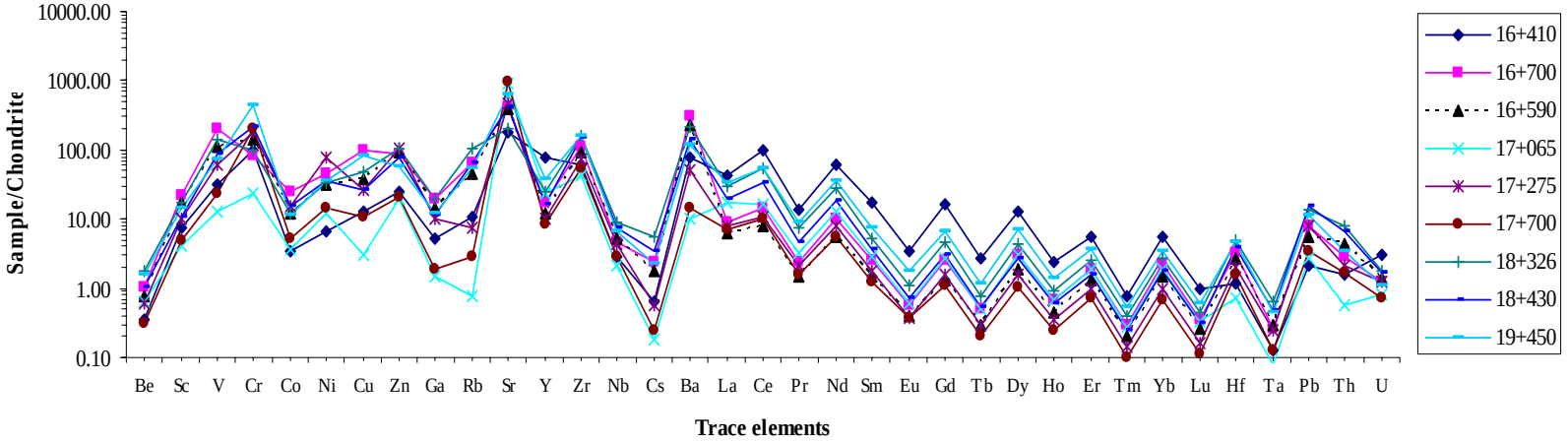


**Figure 4.11** Chondrite normalized trace elements and rare earth elements distribution in pelagic sample, Nam Duk Formation.

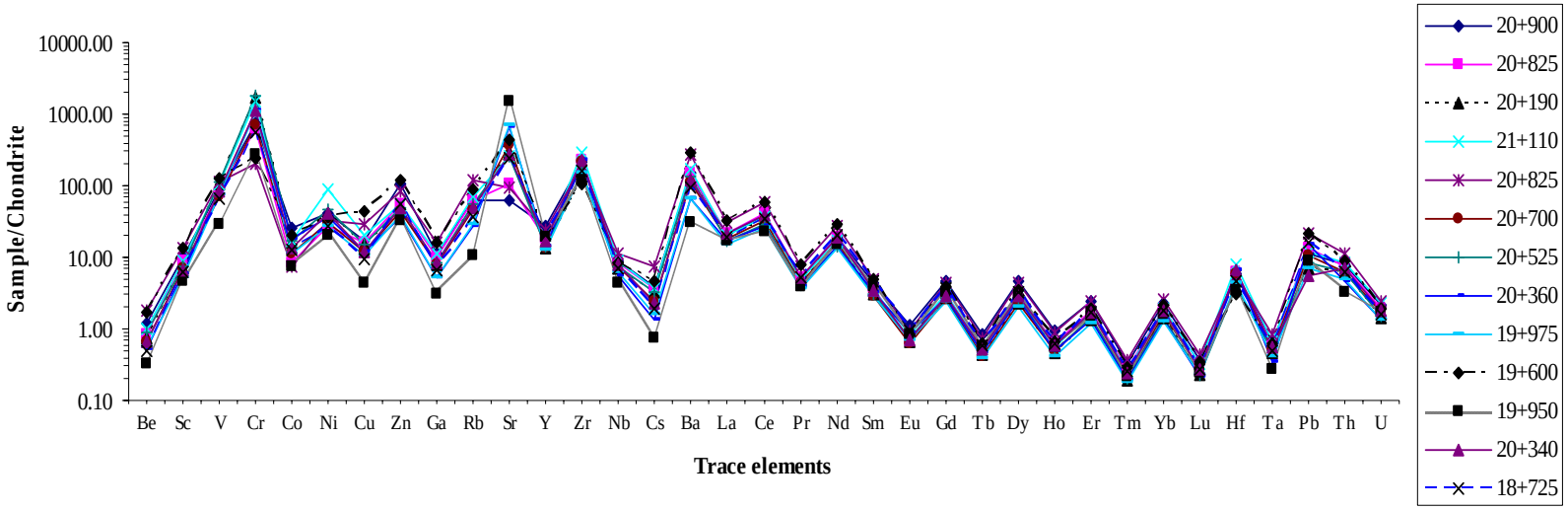


**Figure 4.12** Chondrite normalized trace elements and rare earth elements distribution in flysch sample, Nam Duk Formation.

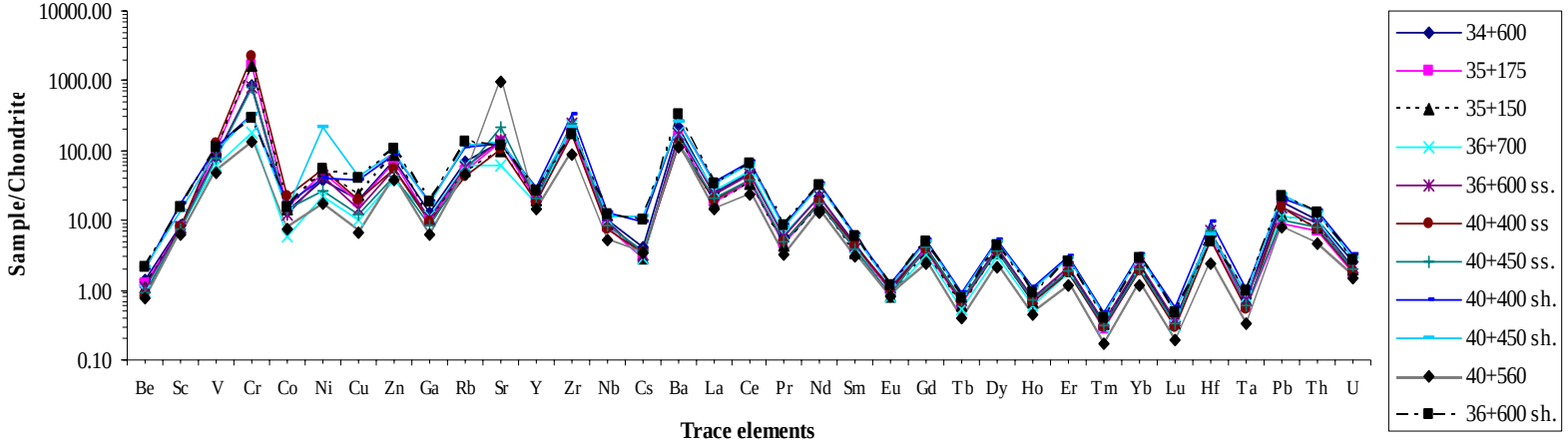


**Figure 4.13** Chondrite normalized trace elements and rare earth elements distribution in molasse sample, Nam Duk Formation.

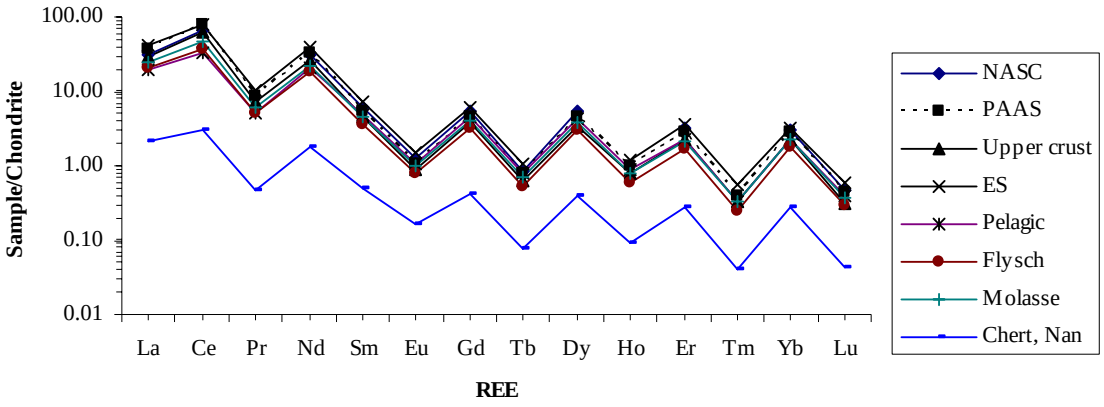


**Figure 4.14** Chondrite normalized rare earth elements of average pelagic, flysch, molasse, and chert from Nan Suture in comparison with the standard sedimentary rocks (data from Table 4.1).

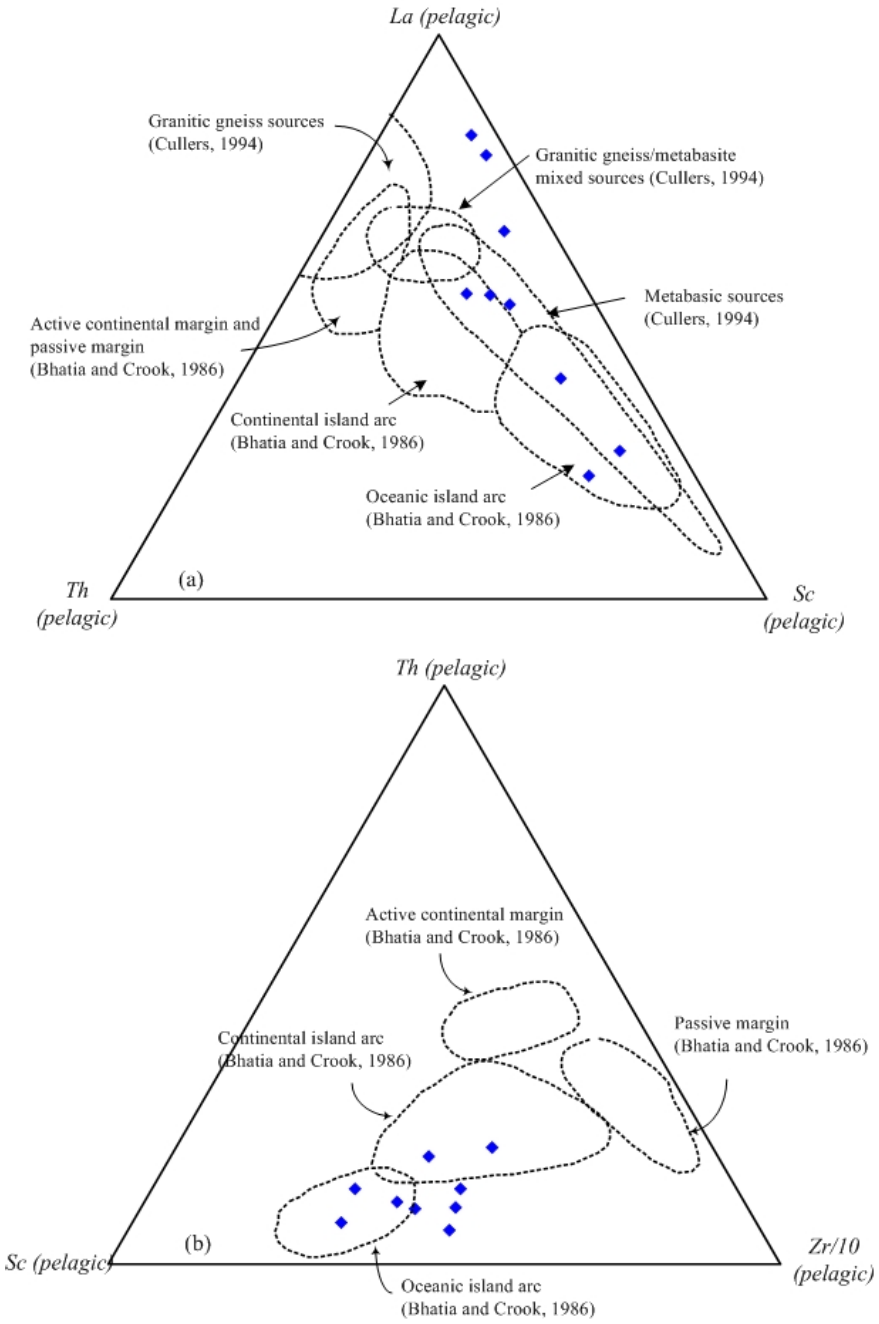


**Figure 4.15** (a) La-Th-Sc ternary diagram for pelagic samples of the Nam Duk Formation (after Bhatia and Crook, 1986; Cullers, 1994). (b) Th-Sc-Zr/10 ternary diagram for pelagic samples of the Nam Duk Formation (after Bhatia and Crook, 1986). Explanation of tectonic setting and provenance are shown in each figure.

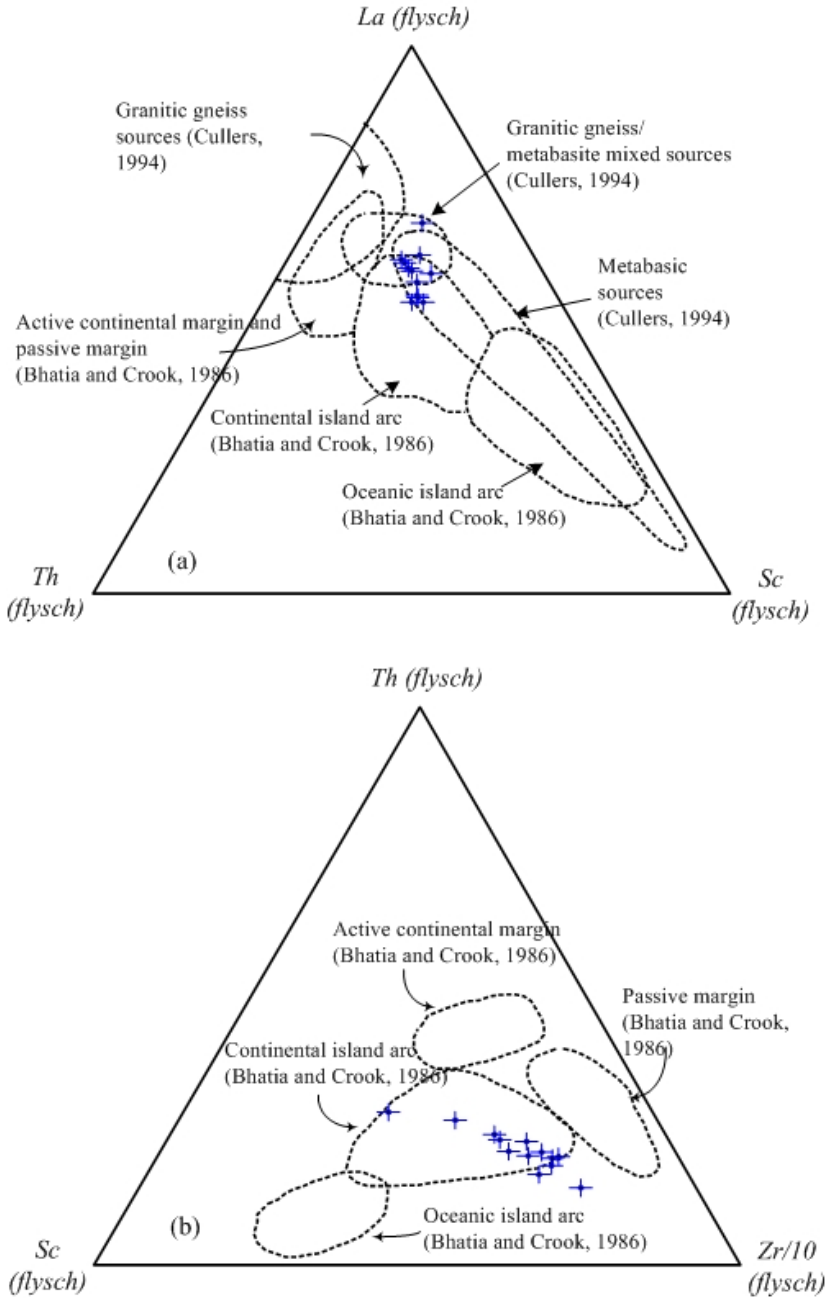


**Figure 4.16** La-Th-Sc ternary diagram for flysch samples of the Nam Duk Formation (after Bhatia and Crook, 1986; Cullers, 1994). Th-Sc-Zr/10 ternary diagram for flysch samples of the Nam Duk Formation (after Bhatia and Crook, 1986). Explanation of tectonic setting and provenance are show in each figure.

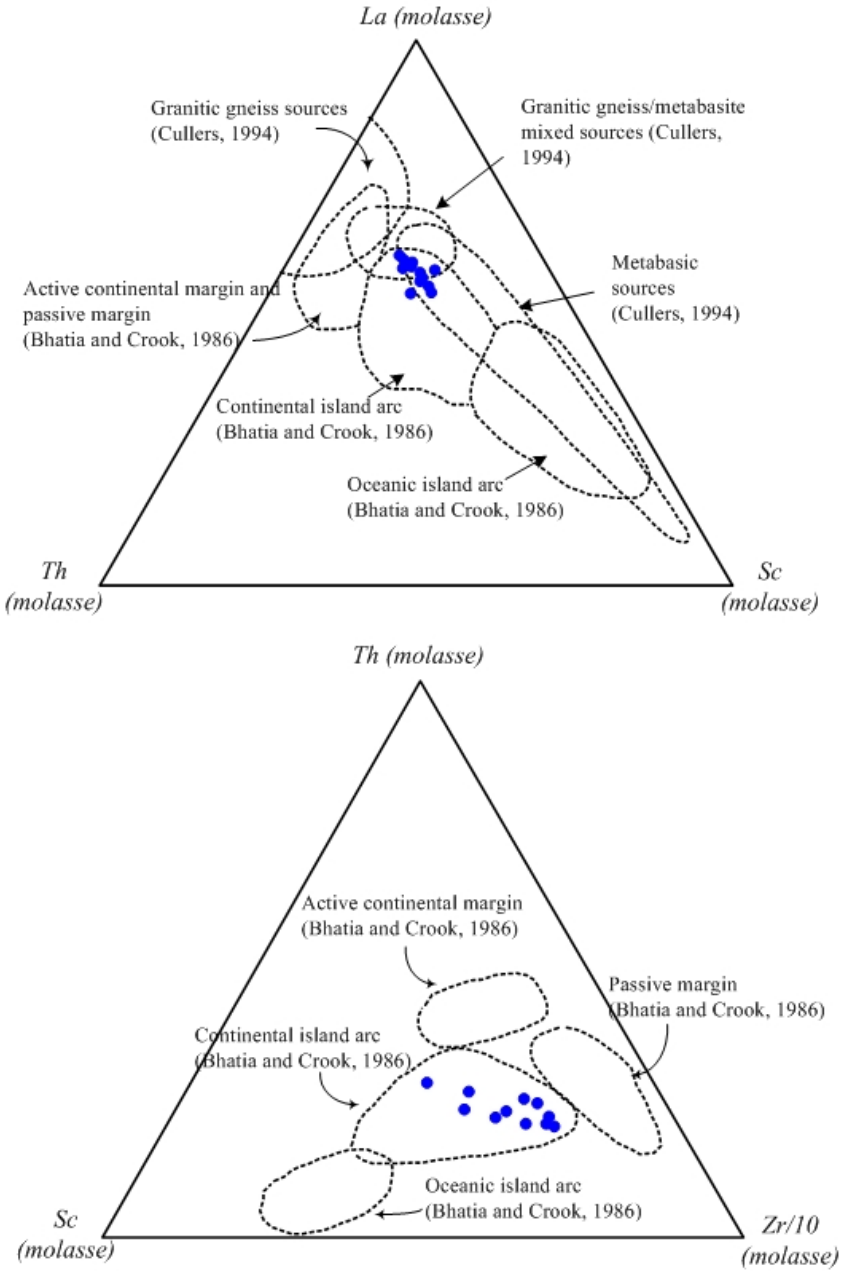


**Figure 4.17** La-Th-Sc ternary diagram for molasse samples of the Nam Duk Formation (after Bhatia and Crook, 1986; Cullers, 1994). Th-Sc-Zr/10 ternary diagram for molasse samples of the Nam Duk Formation (after Bhatia and Crook, 1986). Explanation of tectonic setting and provenance are shown in each figure.

### 4.1.2 Nam Duk Formation at Tha Li

On highway No. 201 at approximately 50 kilometer west of Chiang Khan, at junction 3 kilometer east of Ban Nong Phu, there are two open pits exposing well bedded sandstones interbedded with dark shales (Figure 1.6 in Chapter 1). The samples were taken from 2 open pits east and west of the junction near the small military camp close to Thai-Laos border (sample no. THL 05-09). Altermann (1989) reported this outcrop as Permian (P2) flysch sediments (Nam Duk Formation) which are a northern continuation more than 150 kilometer from the Lom Sak – Chum Phae Highway. The flysch seems to be overthrusted above the P3 Formation (Pha Dua Formation), which crops out to the east. Based on Altermann (1989), sandstones comprise up to 60% texturally immature fine-grained lithic graywackes with mainly sericitic-chloritic and some carbonate matrix.

***Major elements***

The major elements composition is compiled in Appendix A. The $SiO_2$/ $Al_2O_3$ and $Fe_2O_3$/ $K_2O$ plots of the collected samples fall mainly into the field of Fe-sand and wacke (Figure 4.18). The samples contain very high $TiO_2$ (ave. 1.57%) and $Fe_2O_3$ (ave. 19.62%), and low $Al_2O_3$ (ave. 7.57%), and overall values are more than those of type locality from Phetchabun Fold Belt. The $Na_2O$ concentration is lower concentration similar to Phetchabun sample, only a few ppm (three samples) can be detected.

The tectonic-setting discrimination diagram using $K_2O$/ $Na_2O$ ratio and $SiO_2$ content (Roser and Korsch, 1986) is plotted. Due to less $Na_2O$ content, only one sample (THL 07) is plotted and it shows indication of an oceanic island arc setting (Figure 4.19). The discrimination of these samples, based upon a bivariation plot of

$TiO_2$ and ($Fe_2O_3$ + MgO), cannot be plotted due to the high $TiO_2$ content. The provenance signature of siliciclastic sediments are plotted following discrimination diagram of Roser and Korsch (1988). The plots are scattered and show dominantly mafic igneous provenance (Figure 4.20) with one sample falling into the field of felsic igneous provenance. The best-fit line of the $TiO_2$ versus $Al_2O_3$ passes through the estimated peridotite end member which indicates an ultramafic-mafic provenance (Figure 4.21).

***Trace elements***

The trace elements composition is compiled in Appendix A. Correlation trends of bivariate plots in sediments demonstrate that the detritus was well mixed. The Y/Ni and Cr/V elemental ratios which are used to identify mafic-ultramafic sources are plotted in Figure 4.22 (Hiscott, 1984). Cr/V ratios of Tha Li samples are higher than 1 which indicates the presence of chromite among the heavy minerals during deposition. Y/Ni ratios are low and confirm that abundant mafic and ultramafic rocks must have been exposed in the source area of the Tha Li siliciclastic sediments. Cr/V versus Y/Ni ratios are analyzed and mainly indicate ultramafic sources, except for a sample THL 08 which is close to the filed of PAAS.

Chondrite normalized REE and trace elements characteristics of Tha Li samples are plotted in Figure 4.23. The samples have higher concentration of Cr, Sr, Zr, Ba, and light rare earth elements (LREE, La through Eu) similar to flysch type section of Phetchabun area. Summation of REE of the samples is higher than flysch and molasse but still lower than the average values of NASC, PAAS, Upper Crust and European Shale (Table 4.1). The result indicates that the Tha Li siliciclastic sediments

were not derived from the Upper Crust and have a geochemical character similar to flysch and molasse sequences of the Nam Duk Basin.

According to the comparison data in Table 4.3, Tha Li samples show similarity of continental island arc setting (Bhatia and Crook, 1986) and indicate low-silica metamorphic sources (Culler, 1994). A La-Th-Sc and Th-Sc-Zr/10 ternary diagrams, which are plotted to discriminate tectonic setting and composition of source rocks, are shown in Figure 4.25 (Bhatia and Crook, 1986: Cullers, 1994). The result of a La-Th-Sc ternary diagram shows that the samples fall into the field of continental island arc setting and were derived from metabasic and mixed granitic gneiss sources. The samples show a scattering Th-Sc-Zr/10 plot and mainly fall into the field of continental island arc setting.

## 4.2 Pha Dua Formation

The sandstone sample THL-01 was collected from three kilometer west of Chiang Khan, on highway 2195 running along the border between Thai-Laos (Figure 1.6 in Chapter 1). The outcrop consists of fine-grained sandstone, siltstones, and mudstones in beds ranging from a few centimeters up to two meters thickness. The beds show gradded bedding and plant fragments and are highly micaceous. THL-04 sample was collected from highway 203 at milestone 8+300 from Loei to Dan Sai (UTM: 47Q 0782182N, 1934720E). The outcrop consists of silty, fine-grained sandstonse, and shales with one or two centimeter to over fifty centimeter thick. THL-14 sample was collected from a small quarry at approximately 10 kilometer from Loei to Tha Li on the eastern side of highway 2115. The outcrop consists of thick sequence of thin-bedded siliceous shale containing Agathiceras ammonoid (Middle Permian).

***Major elements***

The $SiO_2/Al_2O_3$ and $Fe_2O_3/K_2O$ plots, THL-01, THL-04, and THL-14 samples fall into the field of Fe-sand, Wacke to Askose, and Litharenite respectively (Figure 4.18). The THL-01 and THL-04 samples display very high $TiO_2$ but the THL-14 sample is low in $TiO_2$ (0.74%) content. THL-04 sample contains low $Fe_2O_3$ (3.9%) which is the lowermost value of the siliciclastic samples from Loei area. The tectonic-setting discrimination diagram using $K_2O/Na_2O$ ratio and $SiO_2$ content (Roser and Korsch, 1986) is plotted. Due to undetected $Na_2O$ content of THL-04 and THL-14, only THL-01 is plotted and it shows indication of an oceanic island arc setting (Figure 4.19). However, it seems to be inconsistency with the sedimentological evidence and the low $SiO_2$ (41.41%) of the sample. The discrimination, based upon a bivariation plot of $TiO_2$ and ($Fe_2O_3$ + MgO), can not be plotted due to the high $TiO_2$ content. The provenance signature of siliciclastic sediments is plotted by using discrimination diagram of Roser and Korsch (1988) (Figure 4.20). The THL-01 samples fall into the field of intermediate igneous provenance. The THL-04 samples fall into the field of felsic igneous provenance. The THL-14 samples are in the field of quartzose sedimentary provenance. In contrast to the plotted of the $TiO_2$ versus $Al_2O_3$ diagram, all samples pass through the estimated peridotite end member which indicates an ultramafic-mafic provenance (Figure 4.21).

***Trace elements***

The Y/Ni and Cr/V elemental ratios which are used to identify mafic-ultramafic sources are plotted in Figure 4.22 (Hiscott, 1984). Y/Ni versus Cr/V diagram displays a field of PAAS for THL-04 and THL-14 and is close to a field of ultramafic end member for THL-01 sample. Chondrite normalized REE and trace

elements characteristics of Chiang Khan and north of Loei samples are plotted in Figure 4.24.

According to the comparison data in Table 4.3, THL-01, THL-04, and THL-14 samples are not clearly defined between continental to oceanic island arc setting (Bhatia and Crook, 1986) but indicate low-silica metamorphic sources (Culler, 1994). A La-Th-Sc and Th-Sc-Zr/10 ternary diagram are plotted to discriminate tectonic setting and composition of source rocks in Figure 4.25 (Bhatia and Crook, 1986: Cullers, 1994). The result of the plotted La-Th-Sc ternary diagram falls into the field of continental island arc setting with mainly metabasic source for the THL-01 sample. A plotted ternary diagram of THL-04 falls into the field of continental island arc setting with overlapping of metabasic and granitic gneiss mixed sources. THL-14 sample can not be plotted into a defined tectonic setting but is close to a continental island arc field. In the Th-Sc-Zr/10 diagram, the THL-01 sample falls into the field of continental island arc setting and displays an oceanic island arc setting for THL-14 sample. THL-04 sample can not be plotted into a defined tectonic setting but is close to a continental island arc and passive margin.

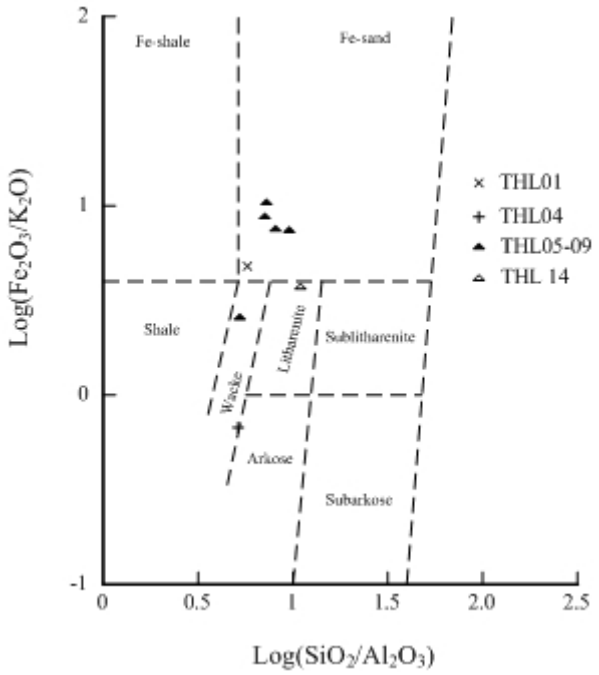


**Figure 4.18** Classification of terrigeneous sandstones and shales of Late Paleozoic samples from Loei area (after Herron, 1988).

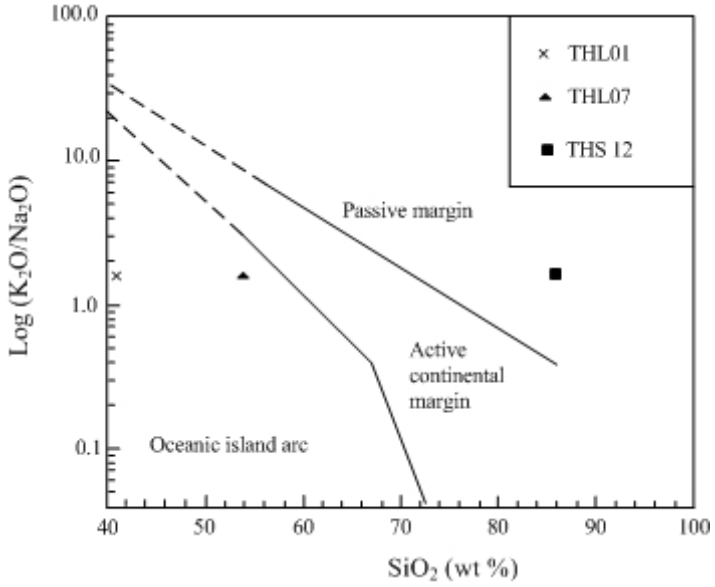


**Figure 4.19** Discrimination diagrams of Roser and Korsch (1986) for Loei and Saraburi sandstones showing the field of oceanic island arc to active continental margin.

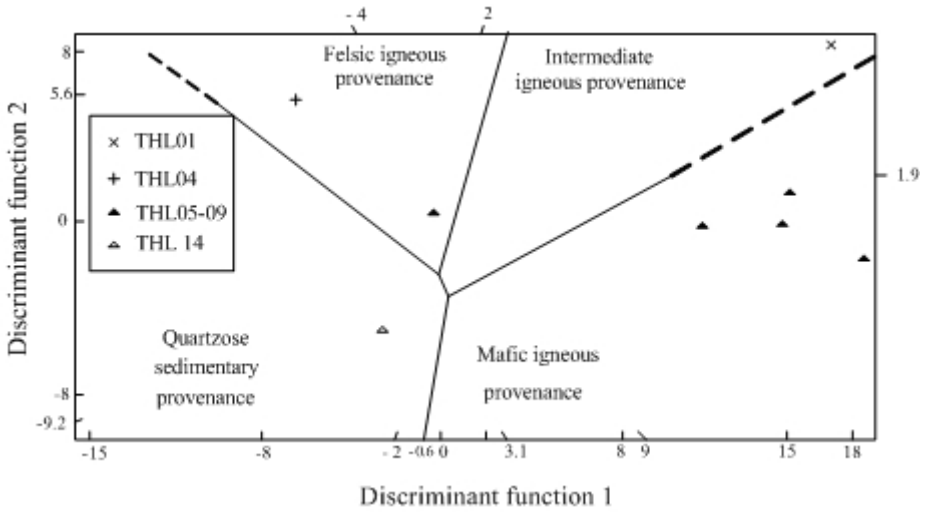


**Figure 4.20** Provenance signature of Loei siliciclastic sediments using major elements indicates mafic igneous to quartzose sources (modified from Roser and Korsch, 1988).

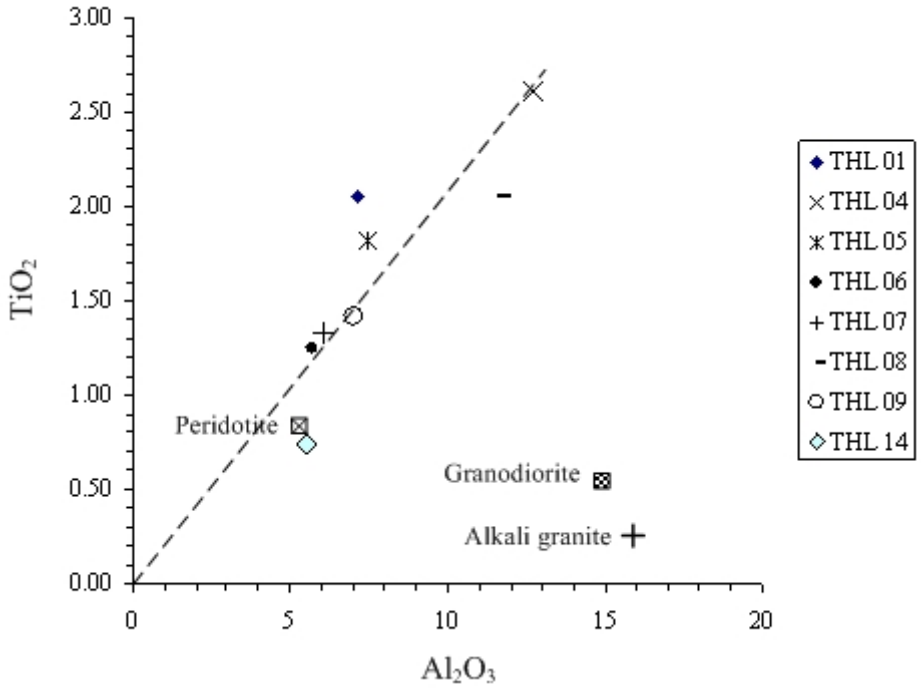


**Figure 4.21** $TiO_2$ versus $Al_2O_3$ plot for Loei samples shows a positive correlation trend with peridotite end member (Young and Nesbitt, 1998).

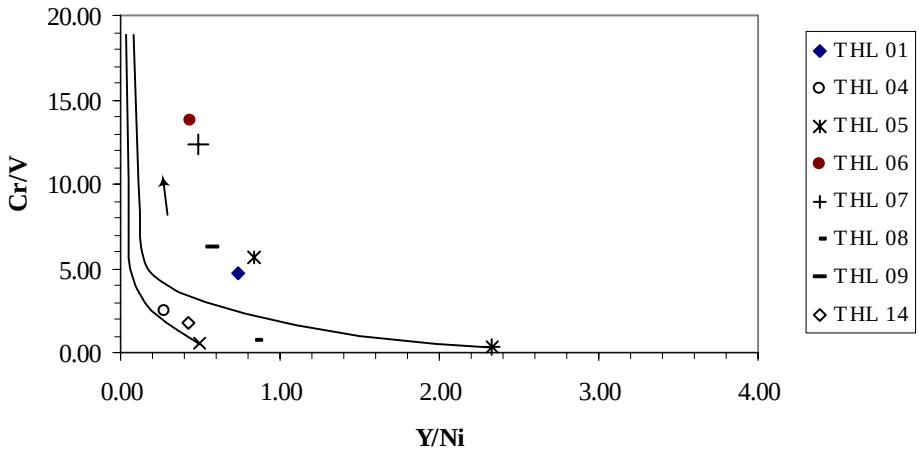


**Figure 4.22** Cr/V vs. Y/Ni diagram showing ultramafic, PAAS, and Granite member of Loei samples (Hiscott, 1984).

**Table 4.3** Trace element discriminators of tectonic settings and source composition, comparison with Loei and Saraburi areas.

| | Graywackes, Bhatia and Crook (1986) | | | | Culler (1994) | | this study | | | | | | |
|---|---|---|---|---|---|---|---|---|---|---|---|---|---|
| Trace ele. | Passive margin | Active continental margin | Continental island arc | Oceanic island arc | high-silica metamorphic sources | low-silica metamorphic sources | Tha Li (P2) | Chiang Khan (P2) | Loei-Dan Sai (P3) | Loei-Tha Li (P3) | Pang Asok Fm. | Khao Khad Fm. | Hua Na Kham Fm. |
| Discriminators decreasing toward oceanic island or low silica sources | | | | | | | | | | | | | |
| Pb | 16.00 | 24.00 | 15.10 | 6.90 | | | 10.50 | 8.55 | 17.21 | 16.06 | 17.52 | 19.45 | 10.29 |
| Th | 16.70 | 8.80 | 11.10 | 2.27 | 17.00 | 8.00 | 9.95 | 6.78 | 12.97 | 2.62 | 11.91 | 6.51 | 11.15 |
| Zr | 298.00 | 179.00 | 229.00 | 96.00 | | | 278.00 | 166.80 | 520.23 | 54.84 | 225.07 | 176.05 | 217.72 |
| Hf | 10.10 | 6.80 | 6.30 | 2.10 | 12.20 | 6.90 | 7.90 | 4.88 | 13.88 | 1.56 | 6.65 | 5.48 | 6.47 |
| Nb | 7.90 | 10.70 | 8.50 | 2.00 | | | 9.71 | 8.19 | 11.22 | 4.16 | 11.00 | 6.40 | 8.05 |
| La | 33.50 | 33.00 | 24.40 | 8.72 | 57.00 | 45.50 | 27.10 | 20.93 | 33.99 | 21.28 | 31.11 | 67.73 | 27.78 |
| Ce | 71.90 | 72.70 | 50.50 | 22.53 | 127.00 | 87.00 | 50.80 | 37.66 | 65.71 | 17.18 | 60.71 | 34.54 | 27.78 |
| Nd | 29.00 | 25.40 | 20.80 | 11.36 | | | 23.80 | 18.87 | 30.46 | 19.25 | 29.29 | 89.48 | 23.02 |
| Rb/Sr | 1.19 | 0.89 | 0.65 | 0.05 | | | 0.577 | 0.366 | 1.490 | 1.212 | 0.896 | 0.094 | 0.592 |
| La/Y | 1.31 | 1.33 | 1.02 | 0.48 | | | 1.173 | 0.889 | 1.504 | 1.275 | 1.176 | 1.639 | 1.495 |
| La/Sc | 6.25 | 4.55 | 1.82 | 0.55 | 20.00 | 1.80 | 2.533 | 2.069 | 3.301 | 2.281 | 2.841 | 2.943 | 2.138 |
| Th/Sc | 3.06 | 2.59 | 0.85 | 0.15 | 7.00 | 0.33 | 0.930 | 0.671 | 1.262 | 0.281 | 1.088 | 0.283 | 0.862 |
| Th/U | 5.60 | 4.80 | 4.60 | 2.10 | | | 4.061 | 3.809 | 4.262 | 2.426 | 4.093 | 3.519 | 4.706 |
| Ba/Sc | | | | | 268.00 | 29.50 | 18.598 | 17.129 | 25.437 | 10.707 | 24.438 | 31.043 | 16.308 |
| La/Cr | | | | | 3.70 | 0.98 | 0.038 | 0.058 | 0.197 | 0.112 | 0.107 | 1.663 | 0.070 |
| Th/Cr | | | | | 1.10 | 0.11 | 0.014 | 0.019 | 0.075 | 0.014 | 0.041 | 0.160 | 0.028 |
| Discriminators increasing toward oceanic island or low silica sources | | | | | | | | | | | | | |
| Ti | 0.22 | 0.26 | 0.39 | 0.48 | | | | | | | | | |
| Sc | 6.00 | 8.00 | 14.80 | 19.50 | 4.50 | 31.00 | 10.70 | 10.07 | 10.34 | 9.34 | 10.95 | 22.97 | 13.03 |
| Co | 5.00 | 10.00 | 12.00 | 18.00 | | | 12.30 | 9.12 | 2.78 | 4.85 | 12.33 | 7.69 | 13.19 |
| Zn | 26.00 | 52.00 | 74.00 | 89.00 | | | 58.30 | 55.23 | 24.71 | 23.68 | 68.40 | 83.40 | 72.12 |
| Cr | | | | | 18.50 | 113.00 | 719.00 | 359.97 | 173.21 | 191.15 | 290.66 | 40.68 | 396.25 |
| Ti/Zr | 6.74 | 15.30 | 19.60 | 59.80 | | | | | | | | | |
| Zr/Hf | 29.50 | 26.30 | 36.30 | 45.70 | | | 35.190 | 34.221 | 37.410 | 35.128 | 33.845 | 32.117 | 33.694 |
| Zr/Th | 19.10 | 9.50 | 21.50 | 48.00 | | | 27.940 | 24.631 | 40.000 | 20.916 | 18.898 | 27.035 | 19.464 |
| La/Th | 2.20 | 1.77 | 2.36 | 4.26 | | | 2.724 | 3.083 | 2.615 | 8.130 | 2.612 | 10.399 | 2.482 |
| Sc/Cr | 0.16 | 0.30 | 0.32 | 0.57 | | | 0.015 | 0.028 | 0.060 | 0.049 | 0.038 | 0.565 | 0.033 |

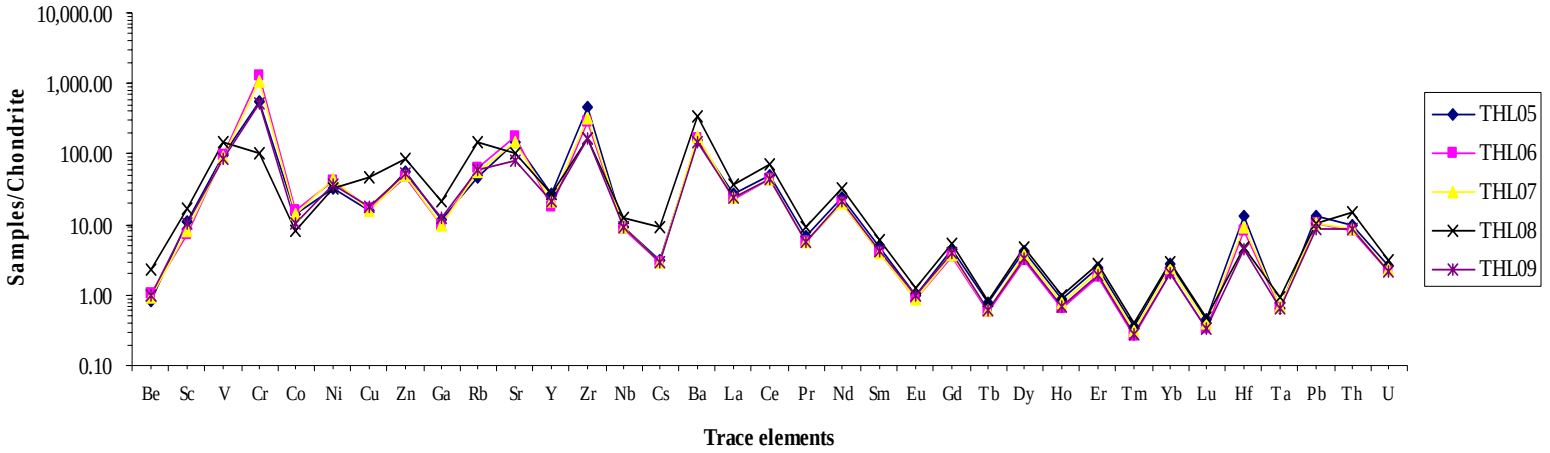


**Figure 4.23** Chondrite normalized trace elements and rare earth elements distribution in Tha Li samples, north of Loei.

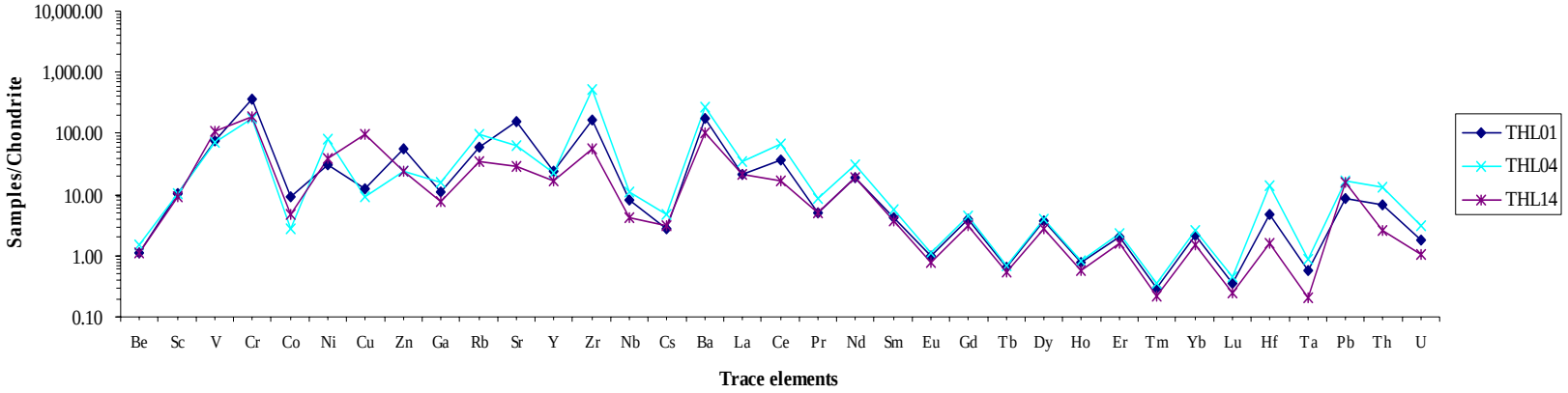


**Figure 4.24** Chondrite normalized trace elements and rare earth elements distribution of the Pha Dua Formation.

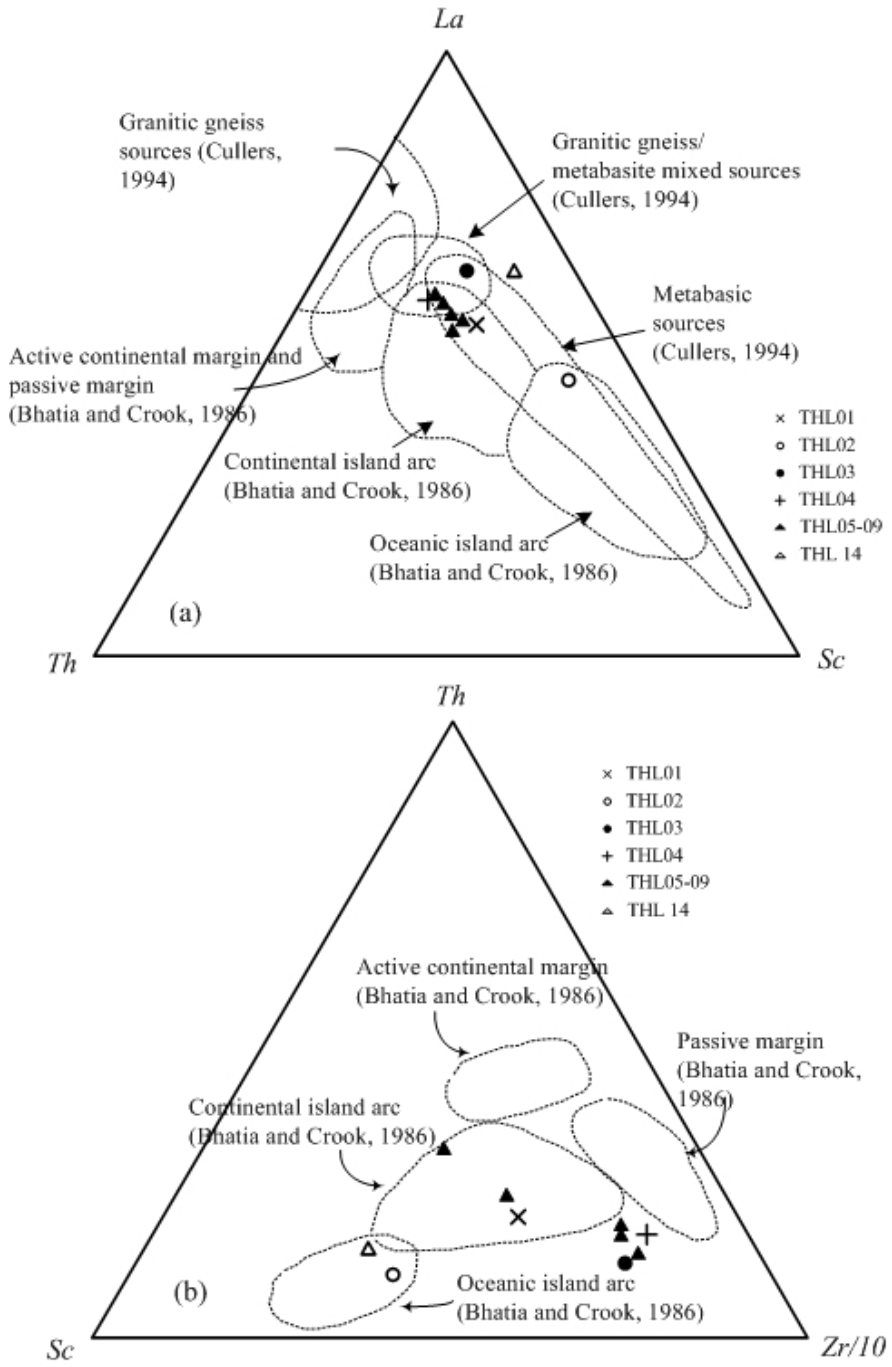


**Figure 4.25** (a) La-Th-Sc ternary diagram for Late Paleozoic samples of Loei area (after Bhatia and Crook, 1986; Cullers, 1994). (b) Th-Sc-Zr/10 ternary diagram for Late Paleozoic samples of Loei area (after Bhatia and Crook, 1986). Explanations of tectonic setting, provenance and sample locality are shows in each figure.

## 4.3 Pang Asok Formation

The sandstone sample THS-10 was collected from a road cut, three kilometer from Muak Lek to Pak Chong of Friendship Highway (no.2) (Figure 1.7 in Chapter 1). The outcrop is exposed approximately 500 meter on left hand side and opposite to a limestone mountain. This outcrop consists of thin-bedded fine-grained sandstone and tuffaceous sandstone intruded by younger volcanic dike. Hinthong et al. (1976) reported this outcrop belonging to the Pang Asok Formation (P2). The shale sample THS-15 was collected from a large quarry for dimension stone in Pak Chong area. The outcrop is located at the left hand side of Friendship Highway from Muak Lek to Pak Chong opposite to animal check point station (Khao Bandai Ma). Thin to thick shale and slate and interbedded fine-grained sandstone is prominent in the quarry. They belong to the Pang Asok Formation (P2).

***Major elements***

The $SiO_2/Al_2O_3$ and $Fe_2O_3/ K_2O$ plots of THL-10 and THL-15 samples fall into the field of Fe-sand and Fe-shale respectively (Figure 4.26). The samples contain very high $TiO_2$ (THL-10, 1.52% and THL-15, 1.70%). The tectonic-setting discrimination diagram using $K_2O/ Na_2O$ ratio and $SiO_2$ content (Roser and Korsch, 1986) can not be plotted due to undetected $Na_2O$ content. The provenance signature of siliciclastic sediments are plotted following discrimination diagram of Roser and Korsch (1988) (Figure 4.27). The plots show a mafic igneous provenance. The best-fit line of the $TiO_2$ versus $Al_2O_3$ passes through the estimated peridotite end member which indicates an ultramafic-mafic provenance (Young and Nesbitt, 1998; Figure 4.28).

***Trace elements***

The trace elements composition is compiled in Appendix A. The Y/Ni and Cr/V elemental ratios which are used to identify mafic-ultramafic sources are plotted in Figure 4.29 (Hiscott, 1984). Y/Ni versus Cr/V diagram displays between a field of PAAS and ultramafic. Chondrite normalized REE and trace elements characteristics of the Pang Asok samples are plotted in Figure 4.30.

According to the comparison data in Table 4.3, the samples clearly defined as a continental island arc setting of low silica metamorphic sources. A La-Th-Sc and Th-Sc-Zr/10 ternary diagram are plotted to discriminate tectonic setting and composition of source rocks in Figure 4.31 (Bhatia and Crook, 1986: Cullers, 1994). The result of the plotted La-Th-Sc ternary diagram falls into the field of continental island arc setting with mainly overlapping of metabasic source and granitic gneiss mixed sources. In the Th-Sc-Zr/10 diagram, the sample falls into the field of continental island arc setting.

## 4.4 Hua Na Kham Formation

The sandstone sample THP-13 was collected at kilometer 84+530 on Highway No. 12 from Lom Sak to Chum Phae of the Khon San area (Figure 1.5 in Chapter 1). This outcrop belongs to the Hua Na Kham Formation (P2) or Upper Clastic sequence of Loei-Phetchabun area.

***Major elements***

The $SiO_2/Al_2O_3$ and $Fe_2O_3/ K_2O$ plots of THP-13 sample fall into the field between Fe-sand and Fe-shale (Figure 4.26). The samples contain very high $TiO_2$ (1.54 %). The tectonic-setting discrimination diagram using $K_2O/Na_2O$ ratio and $SiO_2$

content (Roser and Korsch, 1986) cannot be plotted due to undetected $Na_2O$ content. The provenance signature of siliciclastic sediments are plotted following discrimination diagram of Roser and Korsch (1988) (Figure 4.27). The plots show a mafic igneous provenance. The best-fit line of the $TiO_2$ versus $Al_2O_3$ passes through the estimated peridotite end member which indicates an ultramafic-mafic provenance (Young and Nesbitt, 1998; Figure 4.28).

***Trace elements***

The trace elements composition is compiled in Appendix A. The Y/Ni and Cr/V elemental ratios which are used to identify mafic-ultramafic sources are plotted in Figure 4.29 (Hiscott, 1984). Y/Ni versus Cr/V diagram displays between a field of PAAS and ultramafic. Chondrite normalized REE and trace elements characteristics of the Hua Na Kham sample are plotted in Figure 4.30.

According to the comparison data in Table 4.3, the plotted sample between oceanic island arc and continental island arc setting and indicates low silica metamorphic sources. A La-Th-Sc and Th-Sc-Zr/10 ternary diagram are plotted to discriminate tectonic setting and composition of source rocks in Figure 4.31 (Bhatia and Crook, 1986: Cullers, 1994). The result of the plotted La-Th-Sc ternary diagram falls into the field of continental island arc setting and it was derived from a metabasic source. In the Th-Sc-Zr/10 diagram, the sample falls into the field of continental island arc setting.

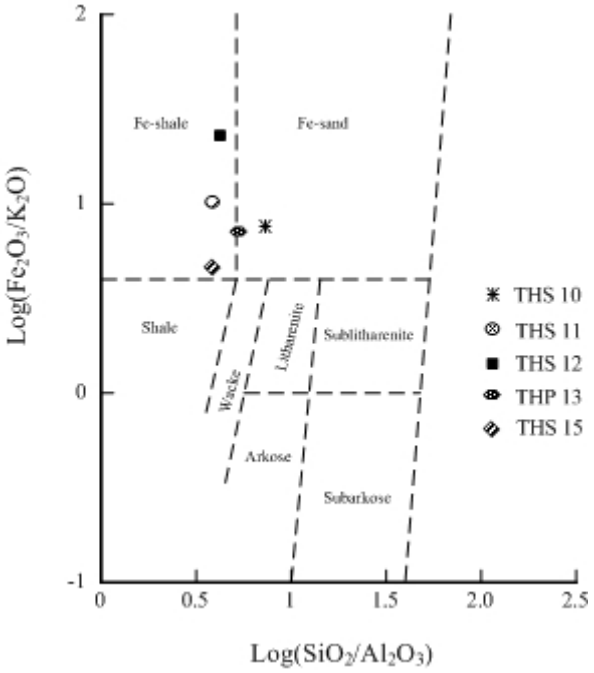


**Figure 4.26** Classification of terrigeneous sandstones and shales of Late Paleozoic samples from Saraburi and Chaiyaphum areas (after Herron, 1988).

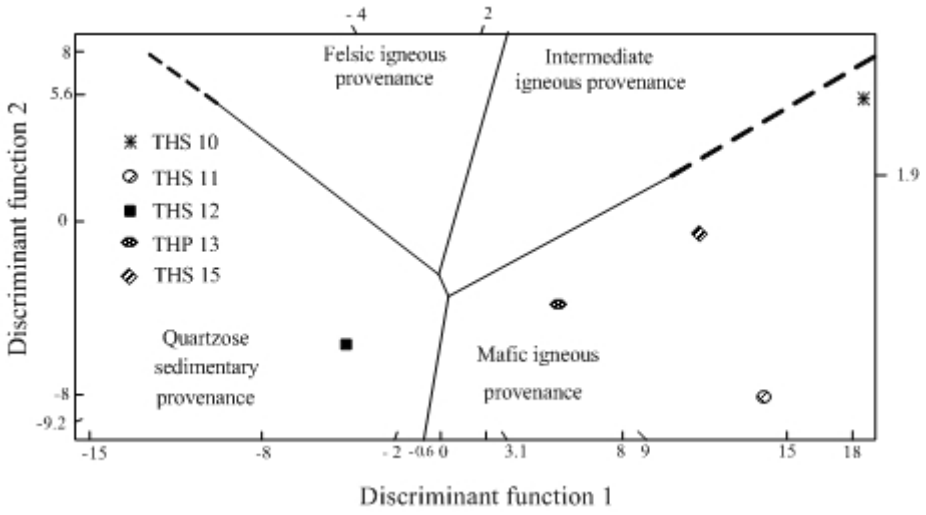


**Figure 4.27** Provenance signature of Saraburi and Chaiyaphum siliciclastic sediments using major elements indicates mafic igneous sources (modified from Roser and Korsch, 1988).

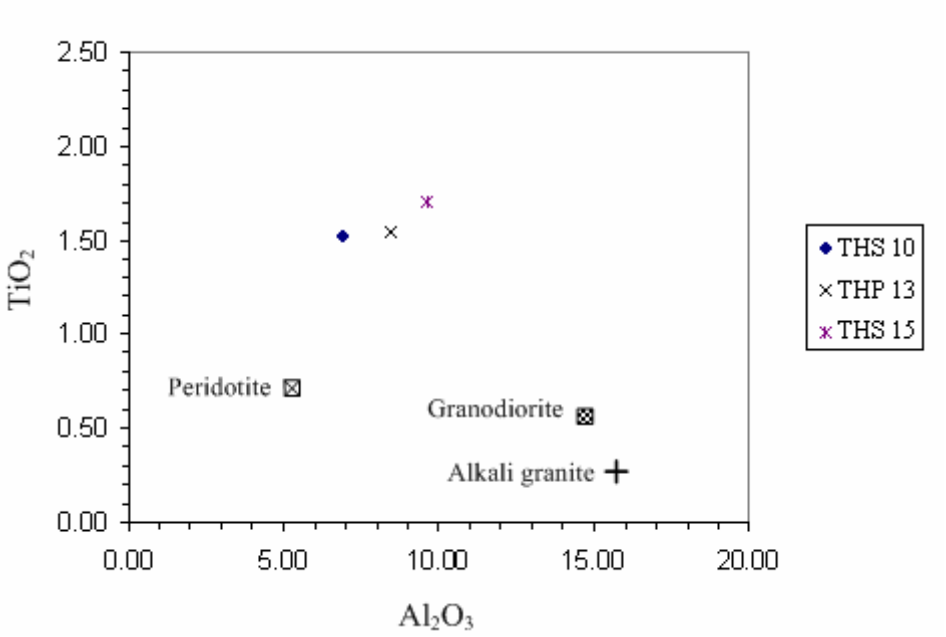


**Figure 4.28** $TiO_2$ versus $Al_2O_3$ plot for the sandstone from Saraburi and Chaiyaphum shows a positive correlation trend with peridotite end member (Young and Nesbitt, 1998).

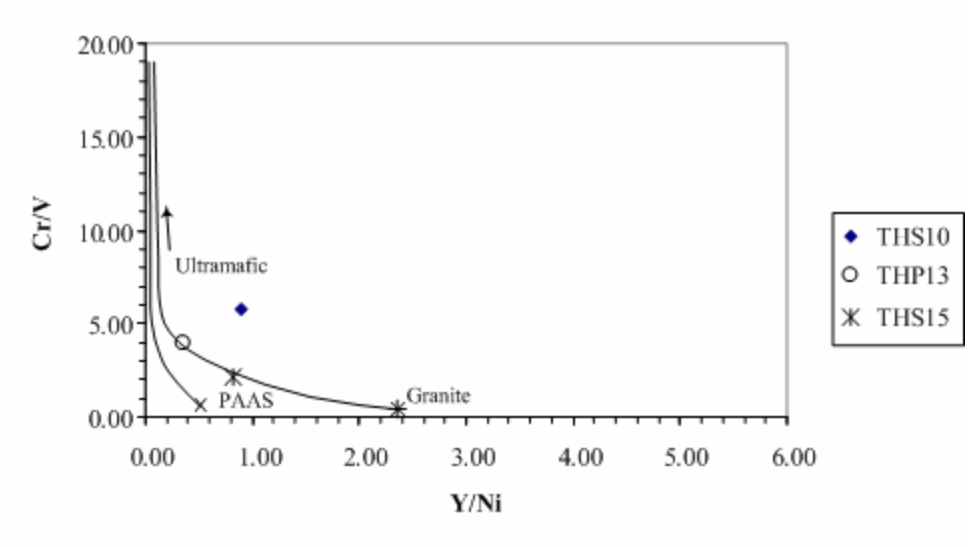


**Figure 4.29** Cr/V vs. Y/Ni diagram showing ultramafic and PAAS end member of Saraburi and Chaiyaphum samples (Hiscott, 1984).

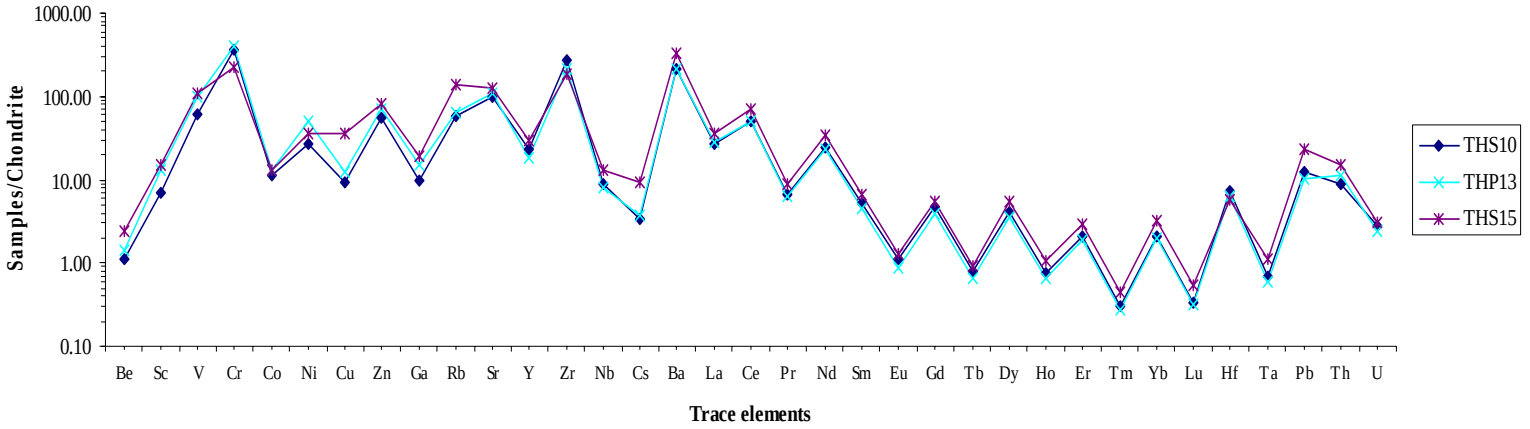


**Figure 4.30** Chondrite normalized trace elements including rare earth elements distribution in Saraburi and Chaiyaphum samples.

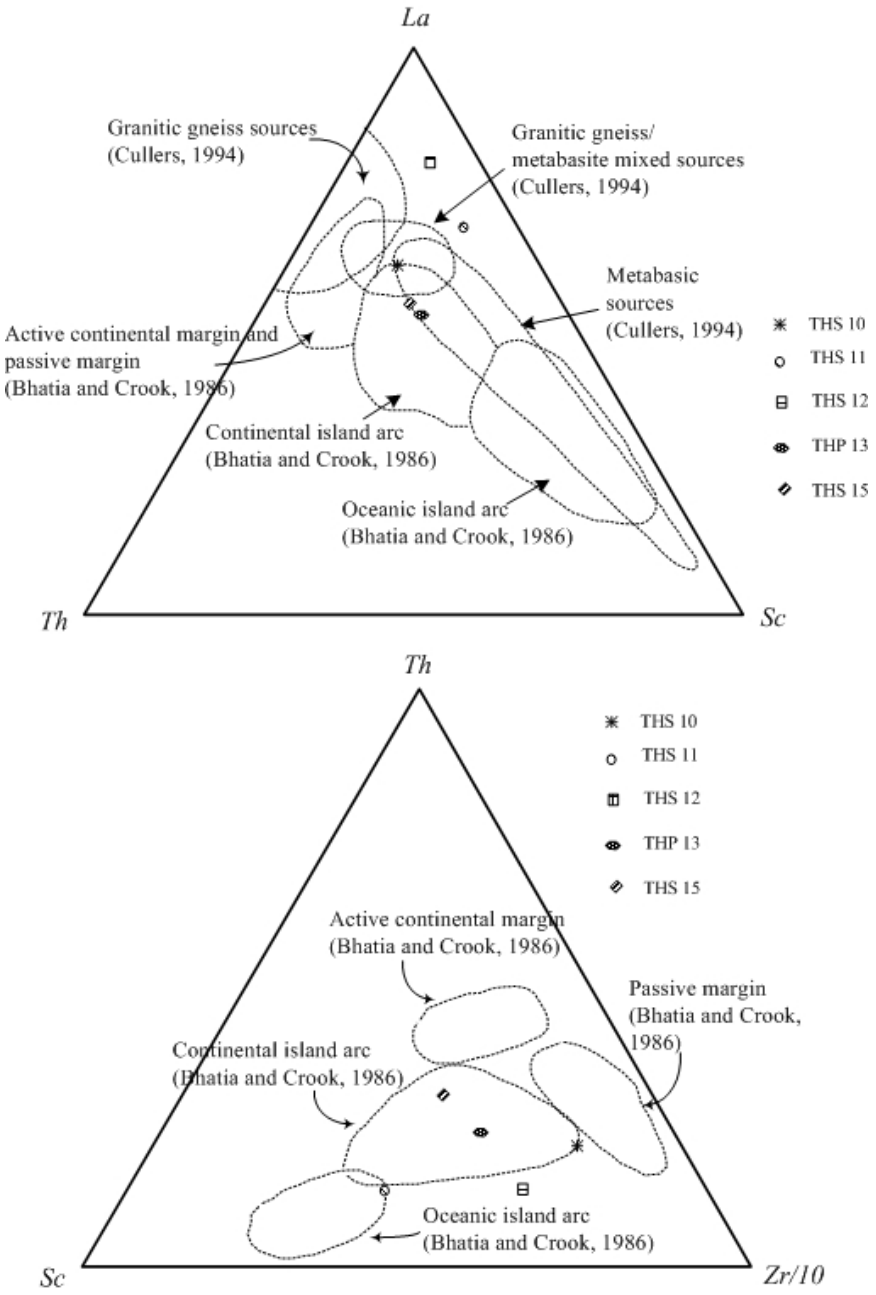


**Figure 4.31** La-Th-Sc ternary diagram for Late Paleozoic samples of Saraburi and Chaiyaphum areas (after Bhatia and Crook, 1986; Cullers, 1994) and Th-Sc-Zr/10 ternary diagram for the same area (after Bhatia and Crook, 1986). Explanations of tectonic setting, provenance and sample locality are shown in each figure.

# CHAPTER V

# CATHODOLUMINESCENCE RESULT AND INTERPRETATION

The cathodoluminescence characteristics of quartz grains in several units of sandstones and allodapic limestone can be observed. These data are essential for interpretation of the provenance of the detrital quartz grains in the investigated stratigraphic units. The result can contribute to a better understanding of the plate tectonic evolution of the study area during the Late Paleozoic.

## 5.1 Nam Duk Formation

The allodapic limestone samples were collected from pelagic sequence at milestone 17+100, 17+120 and 17+227 (Figure 1.5 in Chapter 1). Sample numbers indicate milestone at the sampling locality along highway No. 12. Thin sections under ordinary light and cathodoluminescence for each sample are given in Figures 5.1, 5.2, 5.3, 5.4, 5.5 and 5.6. In general, photomicrographs of all samples are crystalline packstones comprising skeletal fragments. Some foraminifera (fusulinid), deformed quartz and feldspar grains can be observed. Thin-section under CL shows syn-sedimentary elements of clastic and biogenic components. The alteration rim of calcite and quartz grains with overgrowth of authigenic quartz is well observed. Micro-vein, which is invisible from ordinary light, and younger calcite vein (growth zonation) with associated opaque mineral are well developed. Most of the quartz

grains show typical blue color and some grains were deformed before deposition. A zoned structure of blue luminescence quartz with an authigenic vein is clearly shown in Figure 5.6. In addition, fine-grained crystalline quartz texture is represented by dark brown luminescence. A more detail explanation is given in Figure 5.1, 5.2, 5.3, 5.4, 5.5 and 5.6.

From the result of CL analysis, the detrital quartz grains from the allodapic limestone of the pelagic facies display the blue CL which indicates the volcanic and plutonic sources. The presence of brown crystalline quartz indicates its derivation from Low-T hydrothermal influence associated with acidic volcanics.

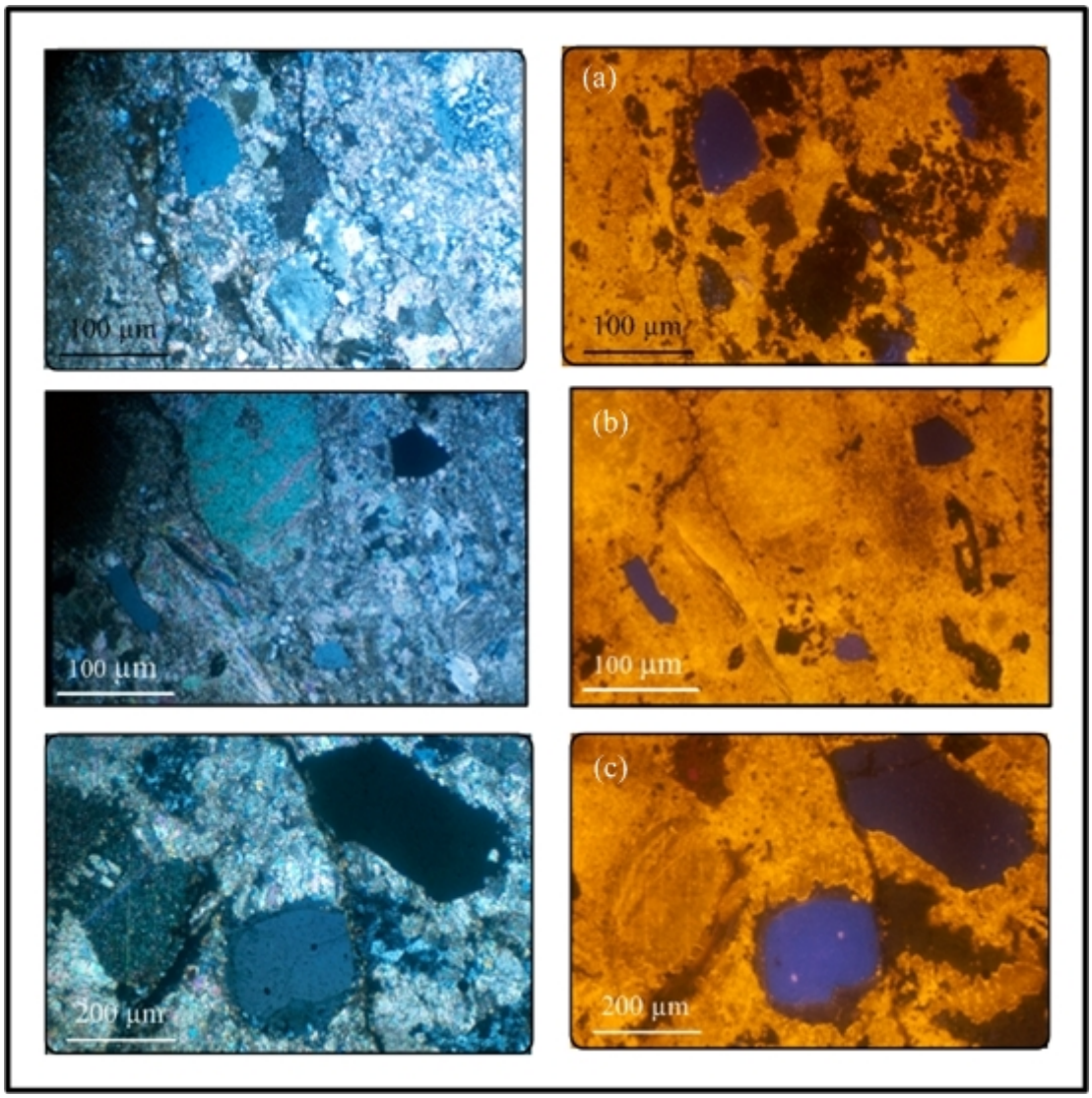


**Figure 5.1** Thin section under CL of pelagic sample no. 17+100, comparing between ordinary light (left) and cathodoluminescence (right), (a) volcanic detrital grains are represented by dark blue luminescence in the allodapic limestone (dark yellow to orange), (b) tabular shape of detrital volcanic quartz grains (left position on CL image) and metamorphic detrital quartz grains are represented by dark brown CL (right position on CL image), (c) detrital quartz luminescence showing violet and blue color indicates its derivation from plutonic and volcanic sources.

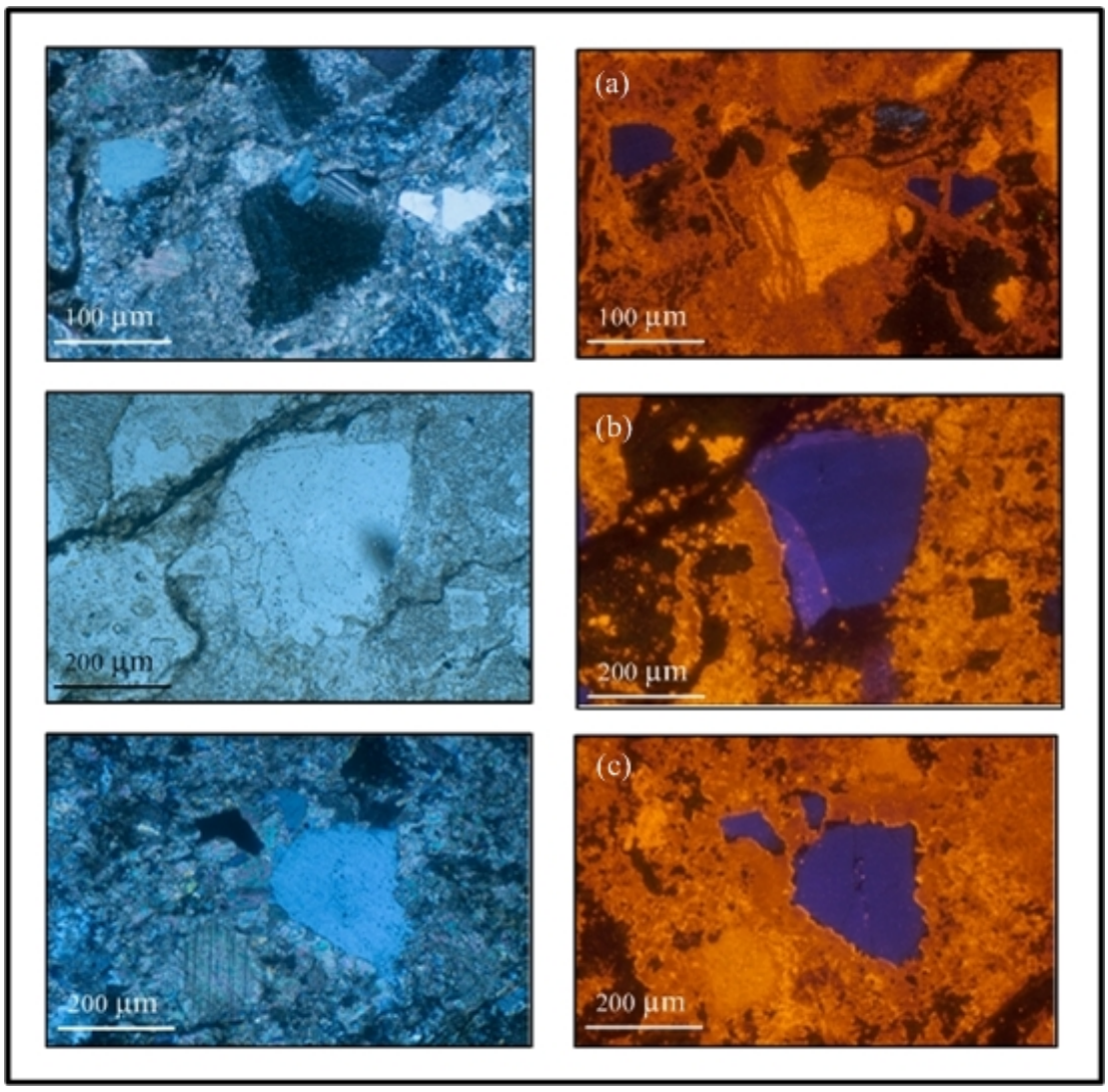


**Figure 5.2** Thin section under CL of pelagic sample no. 17+100, comparing between ordinary light (left) and cathodoluminescence (right), (a) fine-grained, blue (left and right position) and crystalline dark brown (lower right corner) CL quartzes indicate its derivation from two component sources, (b) this figure clearly shows alteration rim of violet CL quartz from original dark blue detrital quartz with zoned feature, (c) authigenic (dark CL) overgrowth in original dark blue CL quartz indicates low temperature of crystallization.

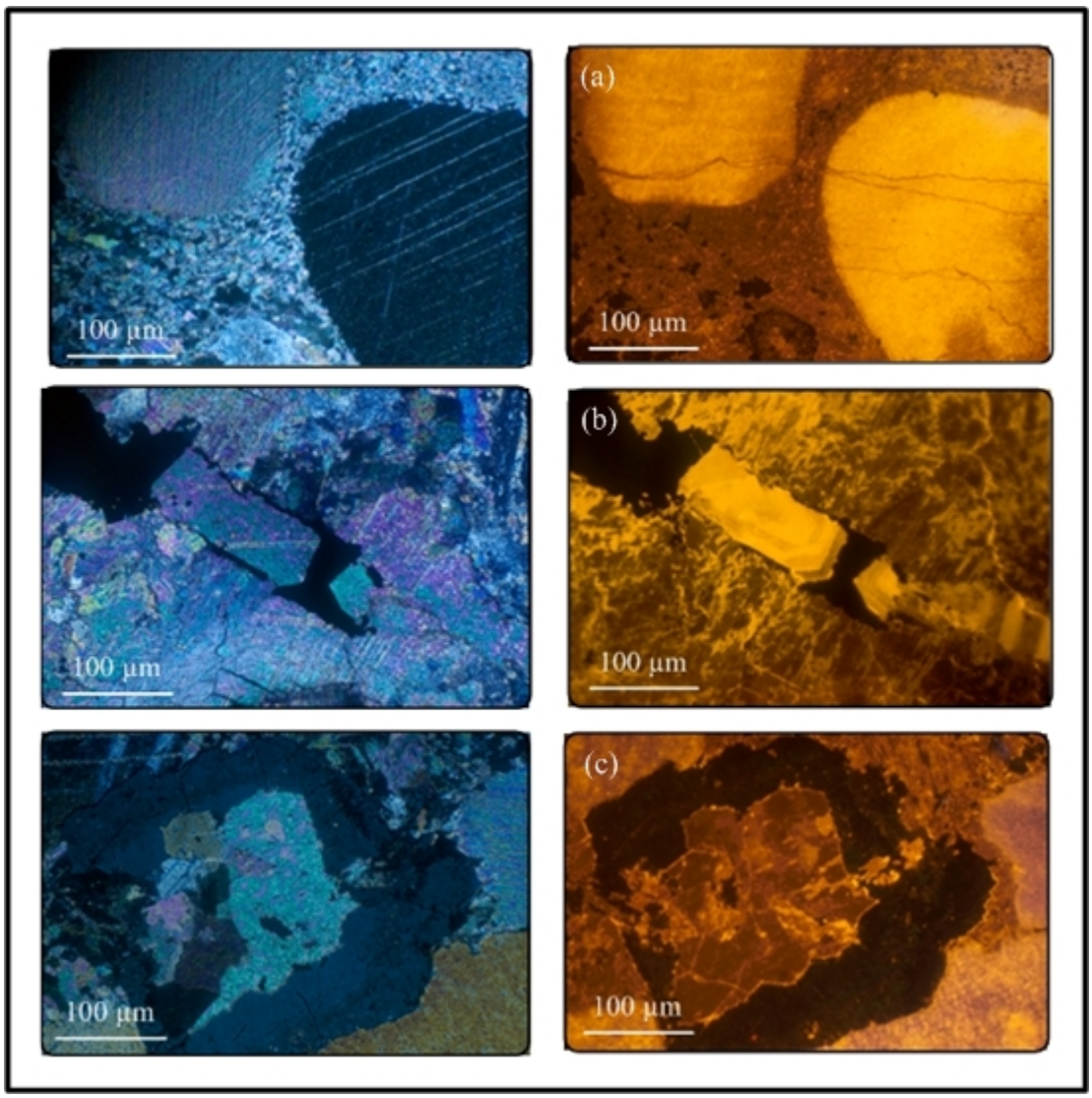


**Figure 5.3** Thin section under CL of pelagic sample no. 17+120, comparing between ordinary light (left) and cathodoluminescence (right), (a) the figure displays two calcite grains (bright yellowish CL) with micro-veins pass through from left to right which can be observed by CL image, (b) the figure displays an opaque mineral in a younger dark CL vein (free of $Mn^{2+}$ and $Fe^{2+}$), (c) the figure displays a bright zone containing $Mn^{2+}$ activator and a dark zone more or less free of $Mn^{2+}$ and $Fe^{2+}$ indicating a second phase of diagenesis.

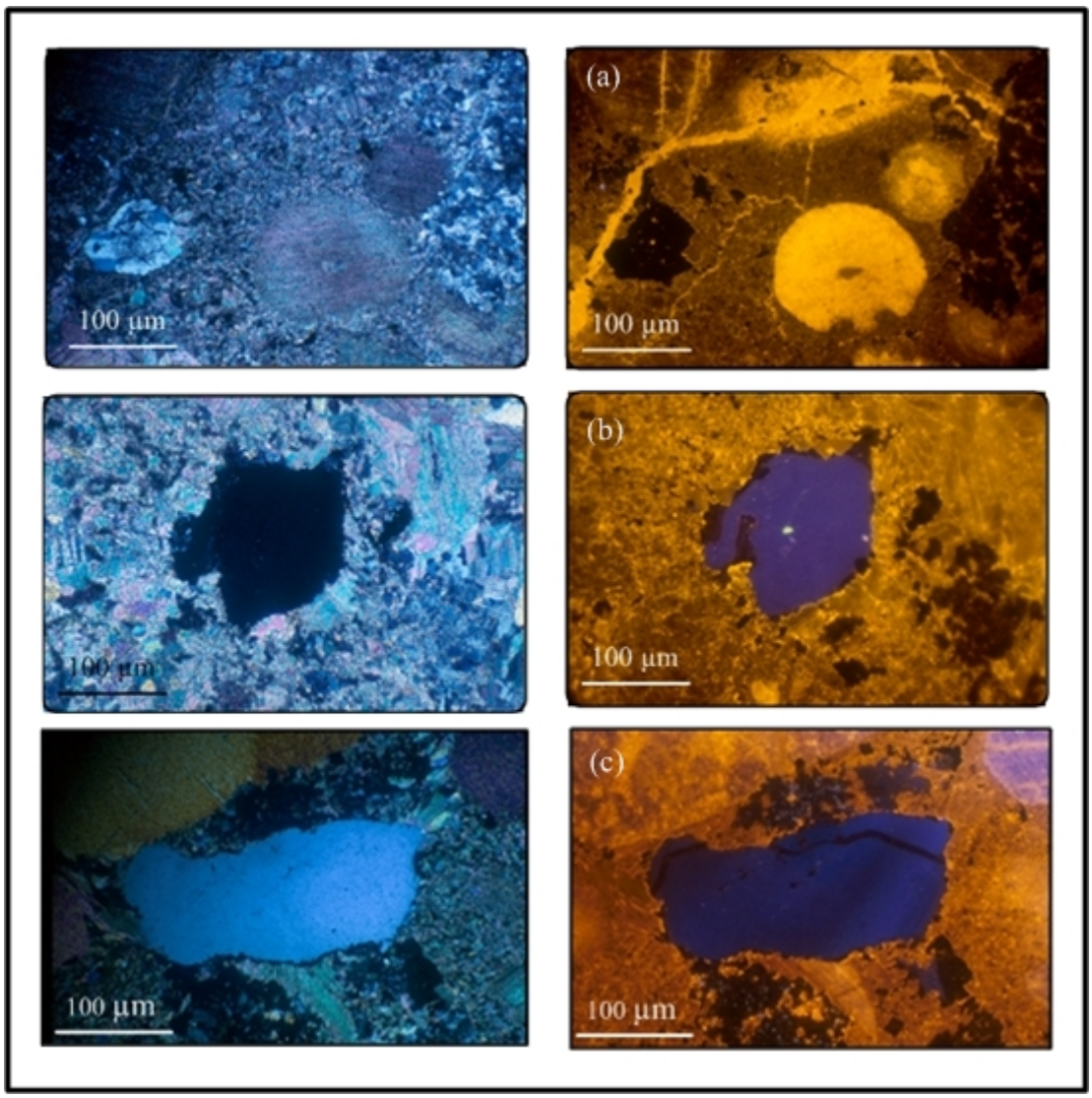


**Figure 5.4** Thin section under CL of pelagic sample no. 17+120, comparing between ordinary light (left) and cathodoluminescence (right), (a) the figure shows bright yellowish CL and calcite vein. (b) authigenic quartz is well developed around original dark blue to violet detrital CL quartz grain, (c) deformed detrital quartz with replacement of authigenic quartz vein.

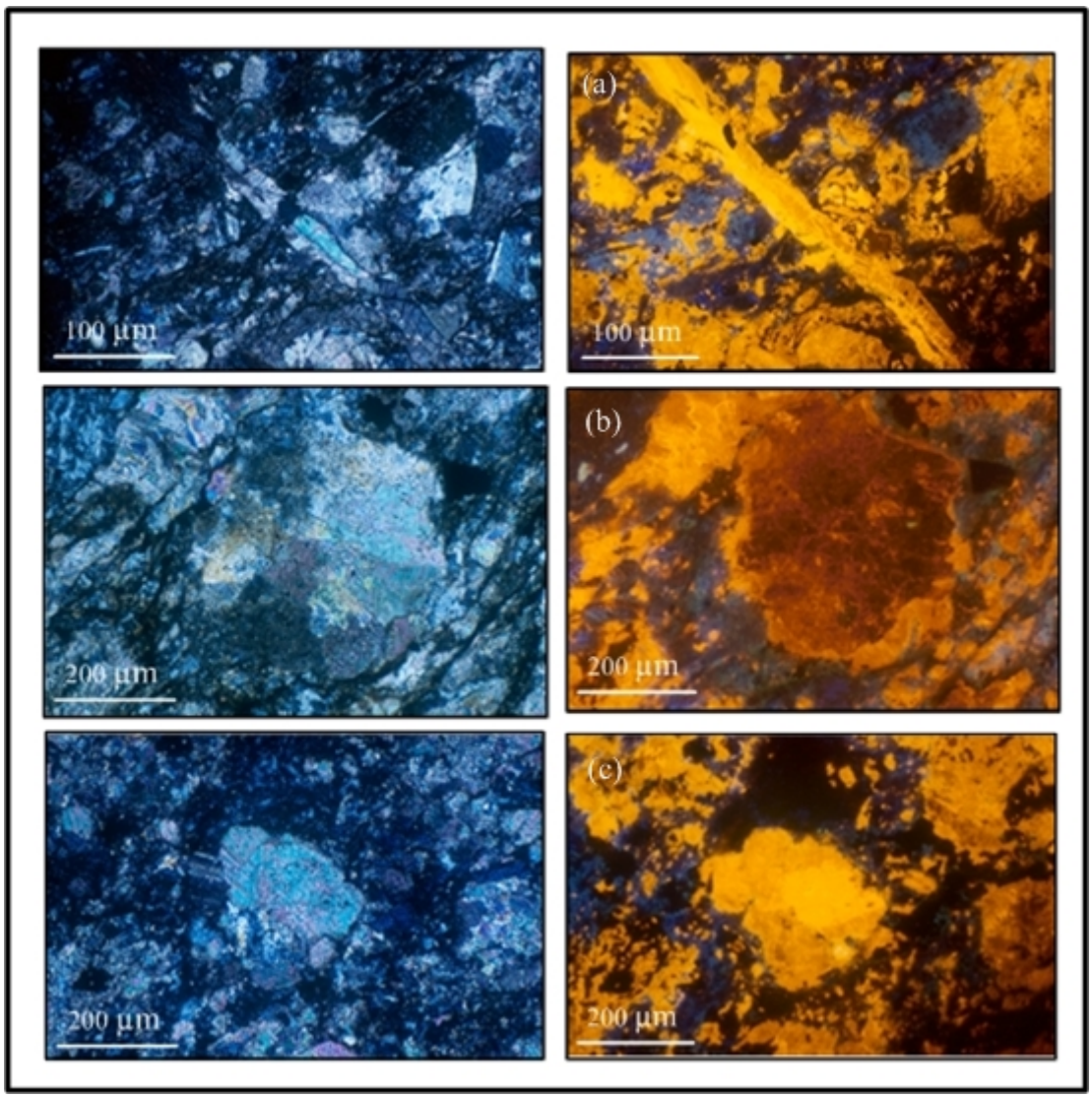


**Figure 5.5** Thin section under CL of deformed pelagic sample no. 17+227 comparing between ordinary light (left) and cathodoluminescence (right), (a) the figure shows dark yellowish and yellow luminescence with scatter of feldspar (dark blue), (b) sparitic texture displays the second phase of diagenesis (dark yellowish to bright yellow, round shape at the center), (c) calcite grain displays bright yellow luminescence while the cement shows dark luminescence.

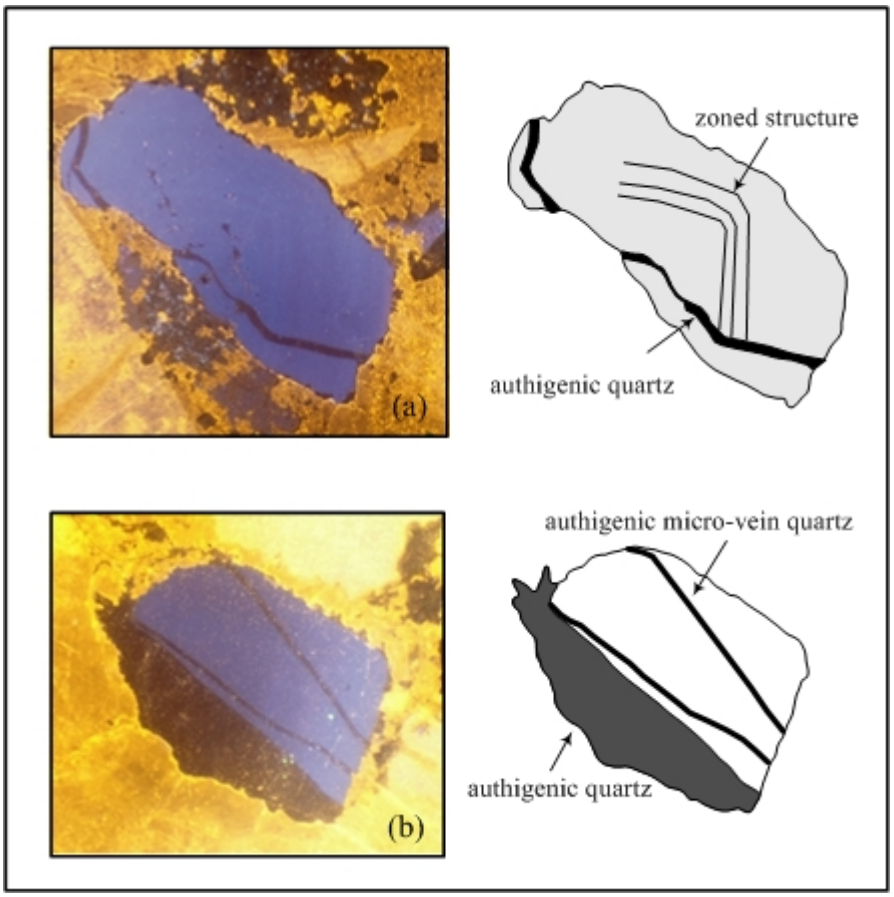


**Figure 5.6** Thin section under cathodoluminescence of quartz properties; (a) deformed detrital volcanic quartz in allodapic limestone of sample no.17+120 displays blue CL with zoned feature and healed authigenic quartz, (b) overgrowth of authigenic quartz in an original volcanic quartz grain of sample no. 17+120.

The sandstone samples of flysch facies were collected from milestone 18+720, 20+375, 20+550, and 21+050 (Figure 1.5 in Chapter 1). The sandstones are identified under normal thin section as immature lithic greywacke. They are very fine- to medium-grained, angular to sub-rounded sandstones. From percentage point counting, thin-section under CL shows approximately typical 55% dark brown and brown, 45% blue and violet CL color of quartz grains and dominant calcareous and siliceous cements. It contains less than 2% of feldspars and zircons. Sample no. 18+720 from the lower part of flysch sequence displays mainly brown luminescence with calcite cement. Sample no. 20+375 displays inhomogeneous mixed CL color of blue and violet in the same grain. Younger calcite vein is well observed in sample no. 21+050. A more detail explanation is given in Figure 5.7 to 5.10.

The result of detrital quartz CL in flysch facies shows brown and blue color. Detrital quartz grains of sample no. 18+720 (lower part of flysch sequence) show mainly brown color and some of them display crystalline texture indicating a regional low-grade metamorphic provenance. Blue CL quartz grains are increasing and more prominent in the upper part of the section and interpreted as derived mainly from high temperature quartz of plutonic/volcanic origin. No internal feature of detrital quartz is found.

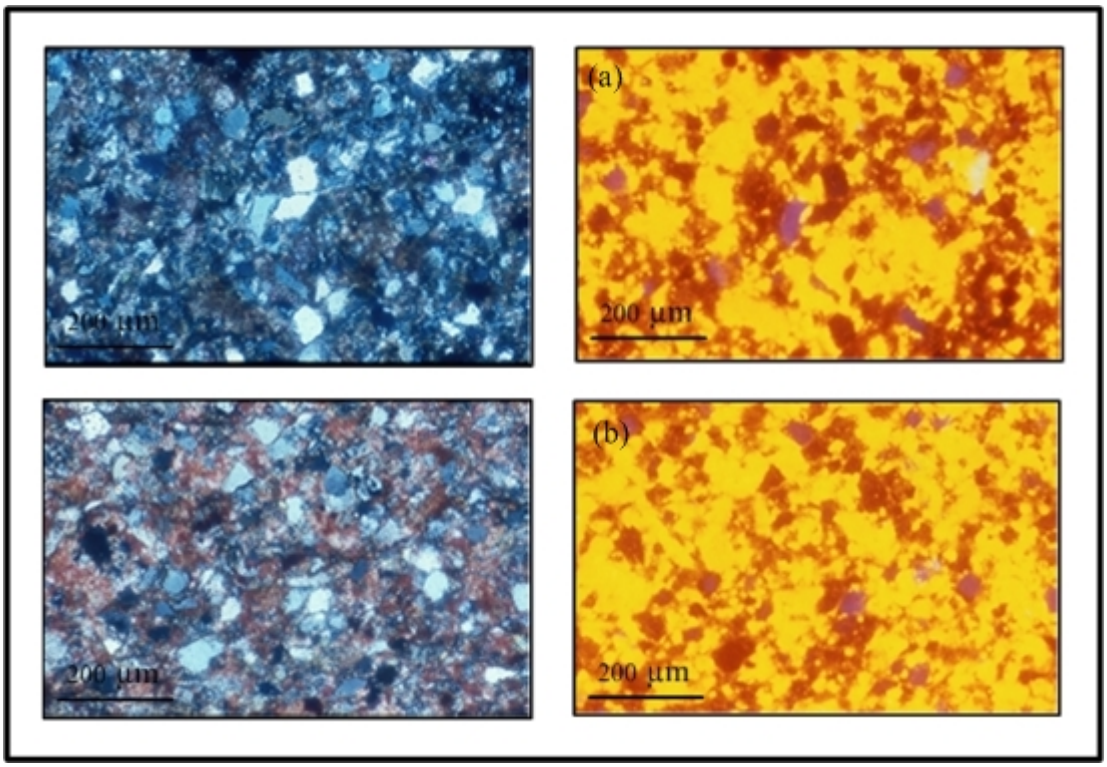


**Figure 5.7** Thin section under CL of flysch sample no. 18+720 comparing between ordinary light (left) and cathodoluminescence (right), a. and b. fine-grained sandstone shows the majority of brown quartz while the minority is blue luminescence. Calcareous cement is dominant.

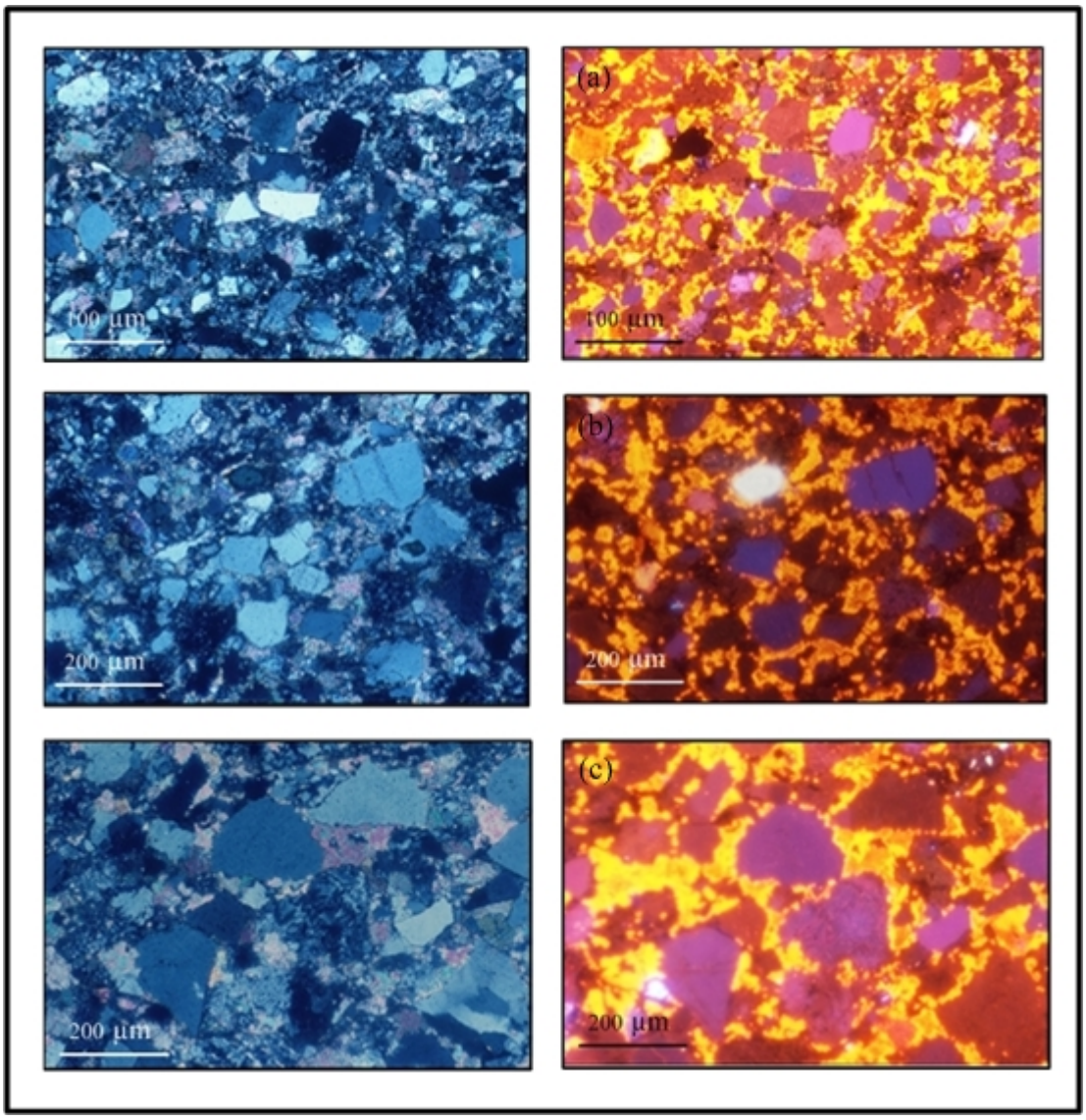


**Figure 5.8** Thin section under CL of flysch sample no. 20+375, comparing between ordinary light (left) and cathodoluminescence (right). Detrital quartz grain shows mixed composition of violet, light purple, blue, and brown luminescence with calcite cement, (a) some quartz grain displays mixed color in the same grain, (b) zircon grain is indicated by bright luminescence, (c) light purple quartz shows irregular shape with pinkish streak color indicating a cooling phase or hydrothermal process.

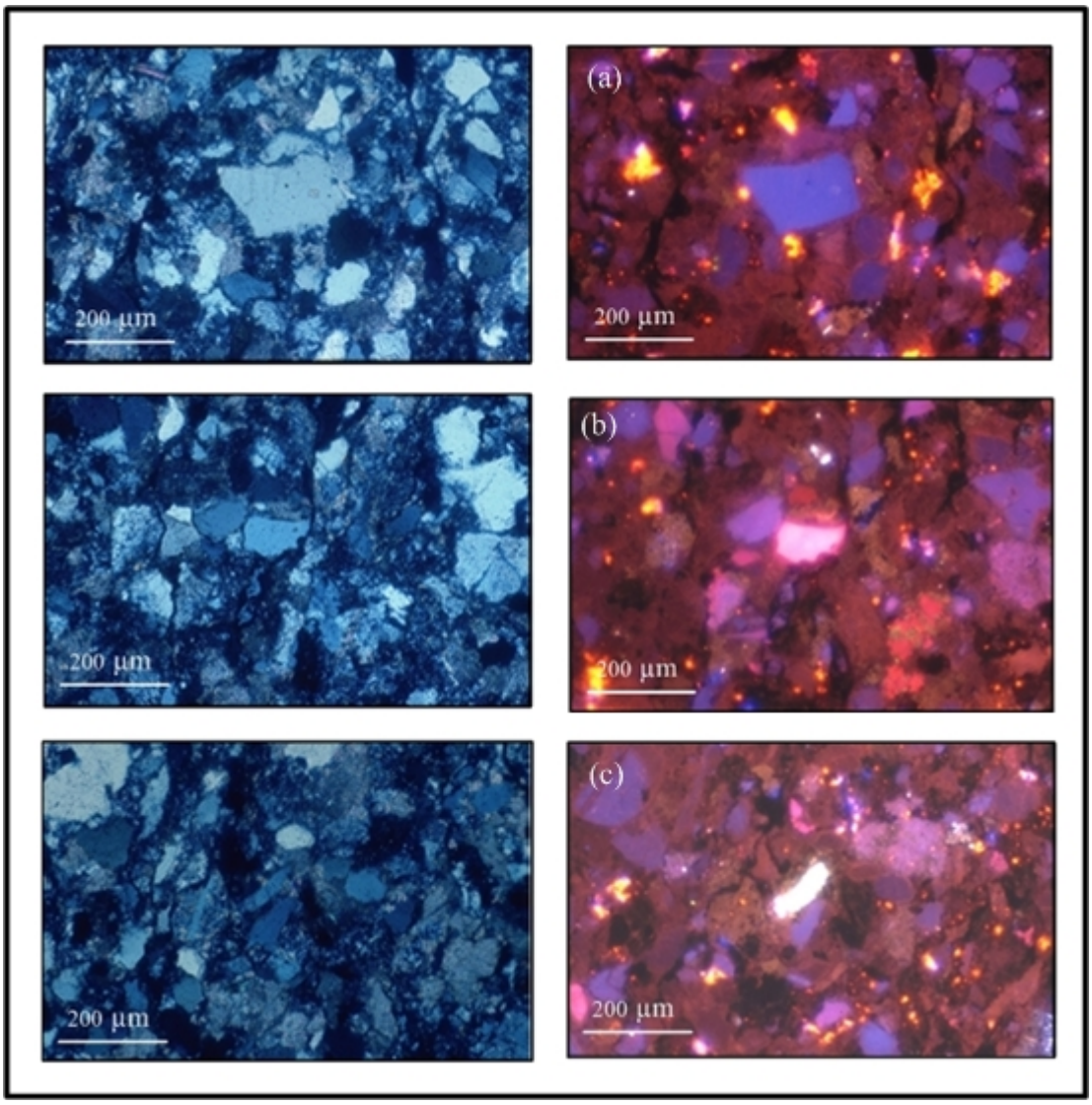


**Figure 5.9** Thin section under CL of flysch sample no. 20+550, comparing between ordinary light (left) and cathodoluminescence (right). The sample is fine- to medium-grained sandstone with quartz cement and carbonate matrix. Quartz crystalline texture in ordinary light displays mainly brown color in CL image. (a) The majority of quartz is brown while the minority is blue and light purple. The matrix is carbonate, (b) bright pinkish luminescence and pinkish purple quartz are well observed, (c)

upper left corner displays deformed quartz with healed brown CL, a few feldspar grains with shined azure are scattered in the section.

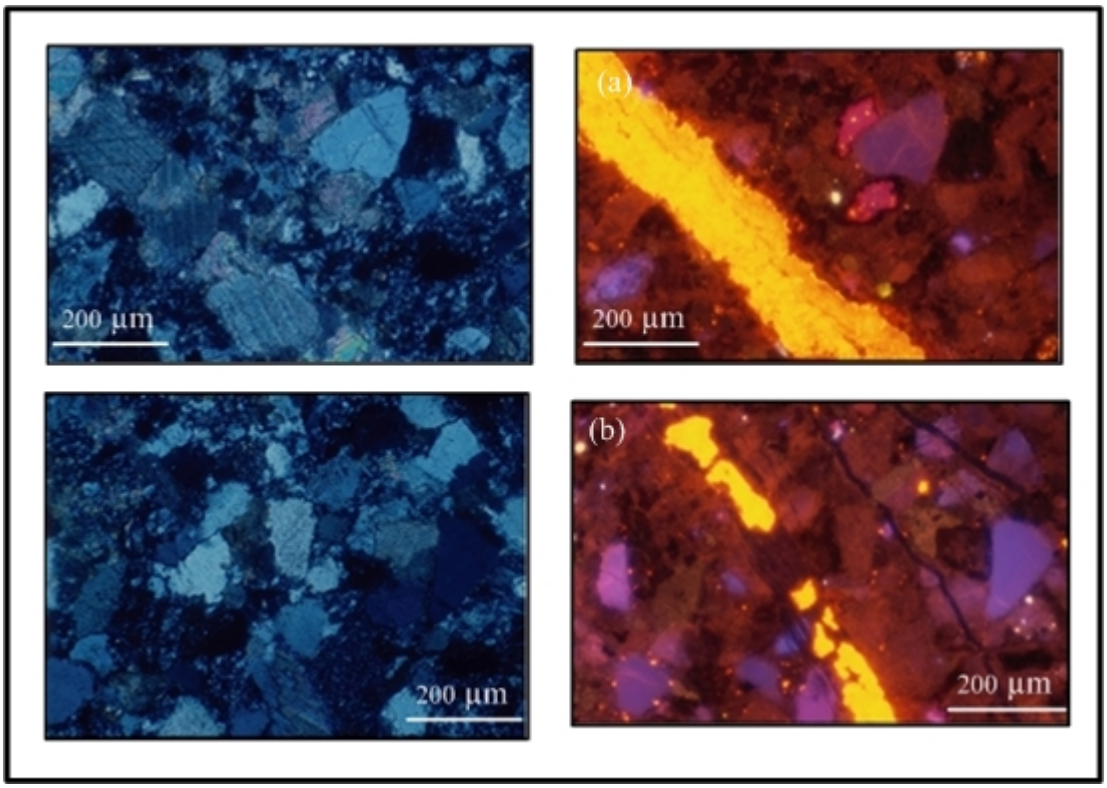


**Figure 5.10** Thin section under CL of flysch sample no. 21+050 comparing between ordinary light (left) and cathodoluminescence (right). The sample shows deformed fine- to medium-grained sandstone with siliceous cement, (a) younger calcite vein is well presented, the majority of quartz is brown while the minority is blue color, (b) authigenic quartz vein together with calcite vein indicates filling of carbonate mineral after authigenic vein generated.

Sandstone samples of molasse facies were collected from milestone 34+600, 34+750, 35+175, 36+650, 37+550, and 40+400 (Figure 1.5 in Chapter 1). The sandstone samples are identified as immature fine- to medium-grained, angular to sub-rounded lithic greywacke and lithic arenite under normal thin section. From percentage point counting, thin-section under CL shows approximately typical 48% dark brown to brown, 52% blue and violet CL color of quartz grains and dominant calcareous and siliceous cements. The CL image displays blue luminescence streak and healed pinkish and non-luminescence fractures. Patchy mottled texture with pinkish violet luminescence is also present. A zoned feature in quartz grain is well shown and the quartz grains display blue, purple and yellowish brown luminescence. A more detail explanation is given in Figure 5.11 to 5.16. Zonation of quartz pattern in molasse samples is given in Figure 5.17.

In molasse sequence, quartz CL population seems to be similar to flysch sequence but represents more variety of quartz provenances. CL characteristic of internal quartz grain such as zoned, mottled, and streak structures is well presented. For example, sample no. 40+400 represents a variety of detrital quartz family and indicates its derivation from volcanic, plutonic, and hydrothermal quartzs.

The percentage of quartz population from flysch and molasse sequences is summarized in Figure 5.18.

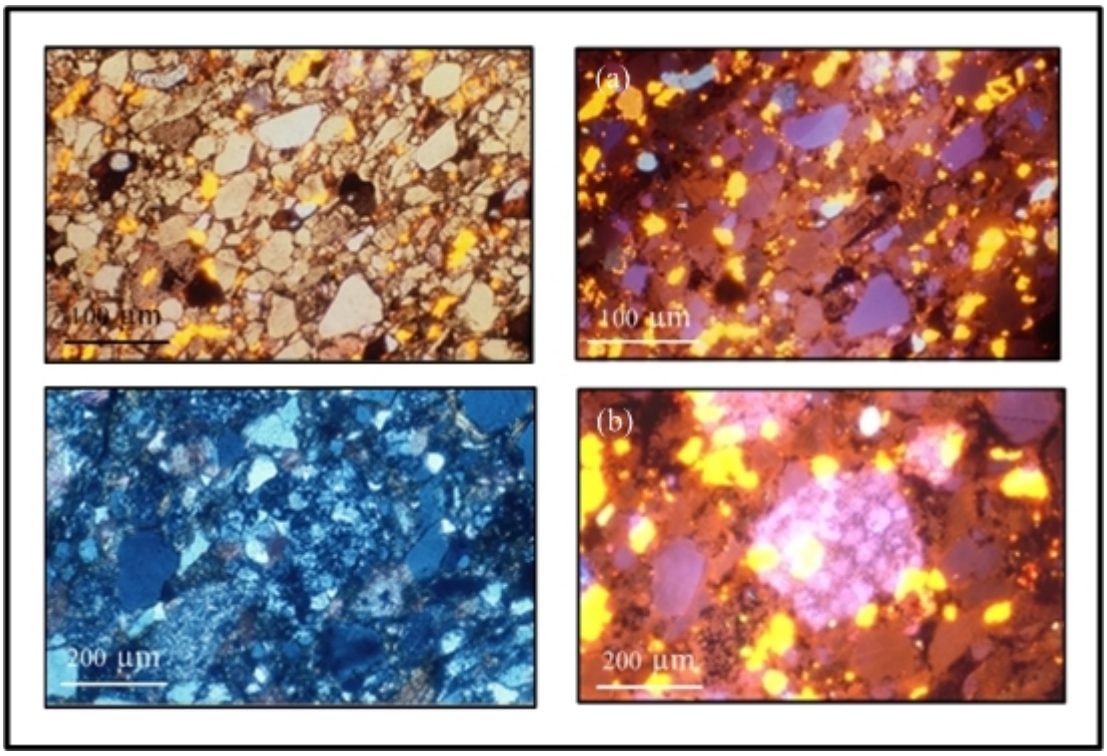


**Figure 5.11** Thin section under CL of molasse sample no. 34+600, comparing between ordinary light (left) and cathodoluminescence (right), (a) the majority of quartz is brown while the minority is blue with carbonate matrix and cement, left figure demonstrates a mixture between ordinary light and CL light, (b) mottled texture in the pinkish coarse grains indicates thermally metamorphosed quartz.

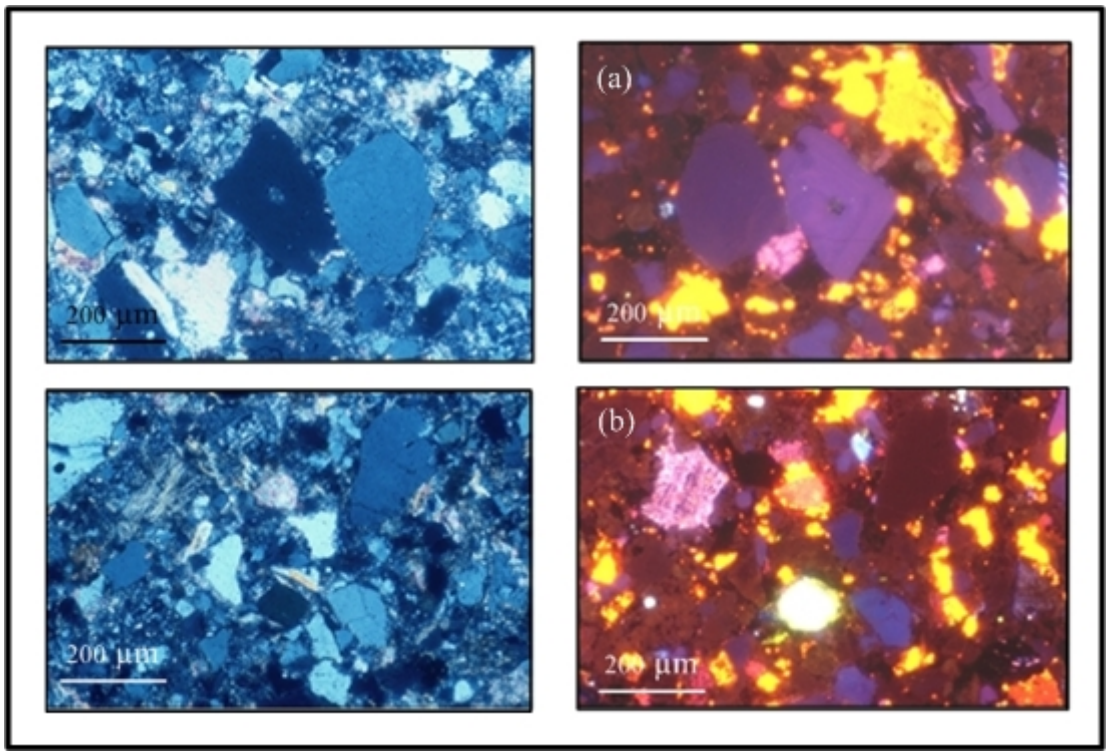


**Figure 5.12** Thin section under CL of molasse sample no. 34+750 comparing between ordinary light (left) and cathodoluminescence (right), (a) the sample displays light purple and dark blue CL in coarse grains and brown CL in fine grains, a few pinkish CL and carbonate matrix are presented, (b) brown quartz grains are dominant in the sample, a few coarse quartz grains are blue and light purple in carbonate matrix.

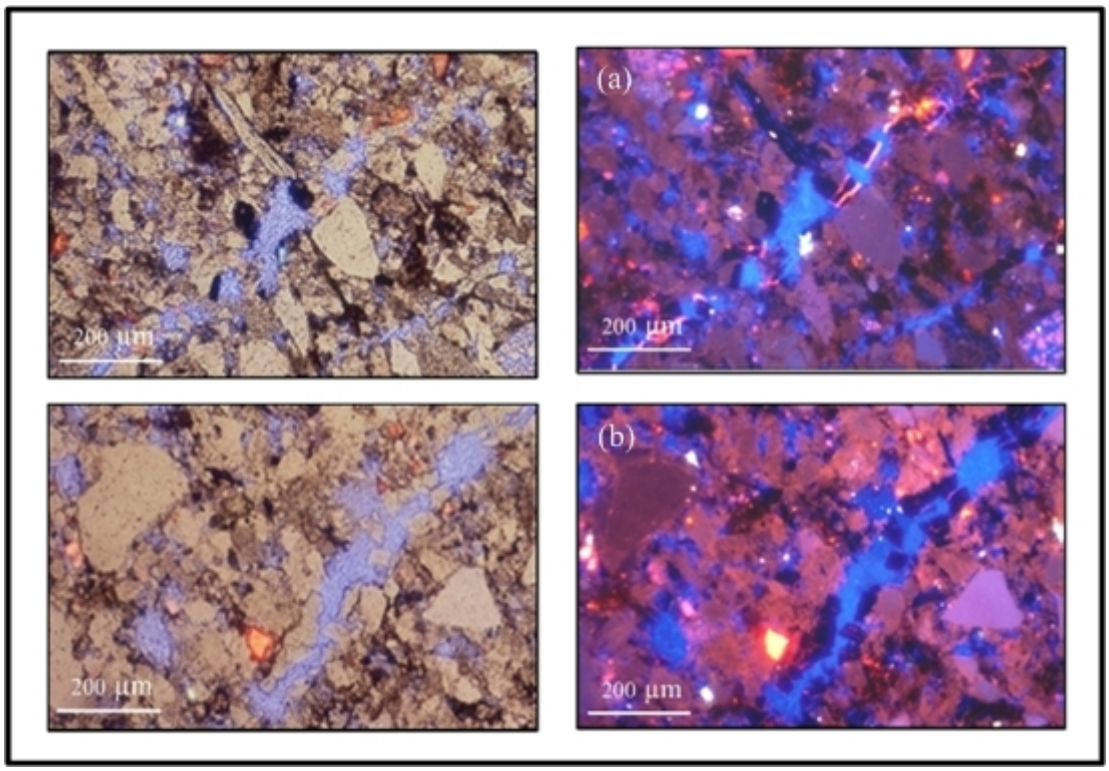


**Figure 5.13** Thin section under CL of molasse sample no. 35+175, comparing between a mixture of ordinary light and CL (left) and cathodoluminescence (right), (a) greywacke sandstone displays mainly brown and light purple CL, feldspar is scattering in matrix and vein, red and reddish orange spots probably indicate dolomitic composition, (b) some authigenic quartz is present in vein with replacement of blue CL material.

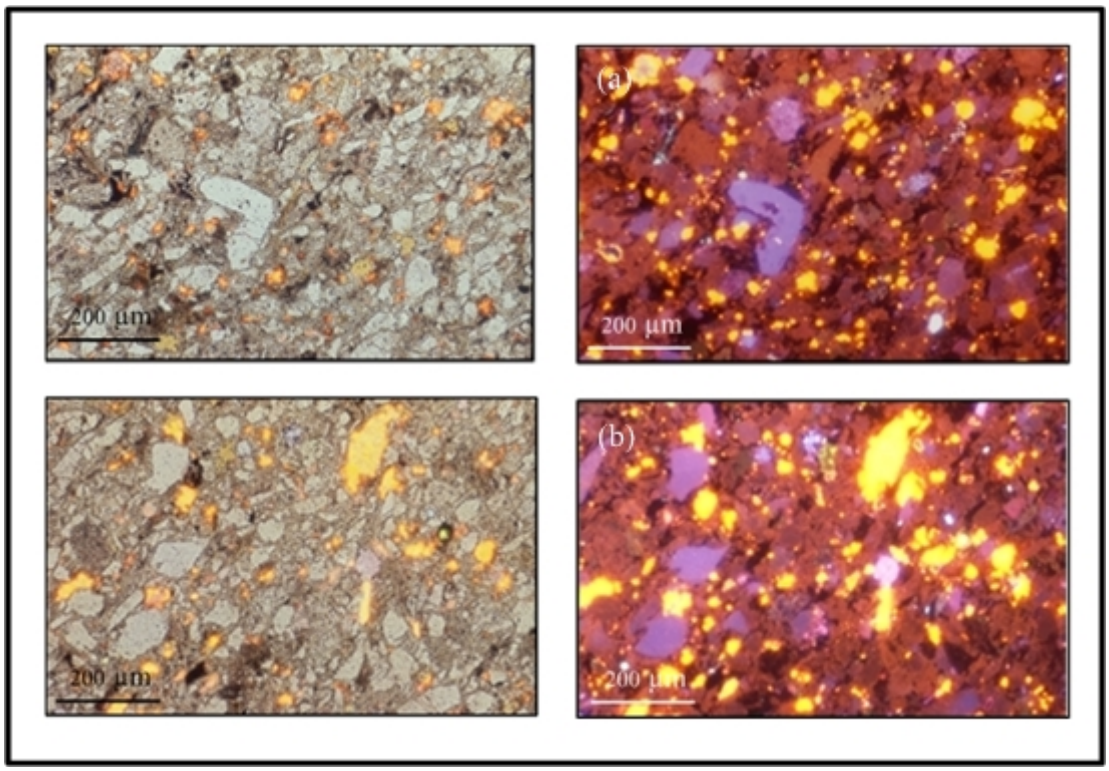


**Figure 5.14** Thin section under CL of molasse sample no. 36+650, comparing between a mixture of ordinary light and CL (left) and cathodoluminescence (right). The sample displays very fine-to fine-grained grewwacke sandstone. (a) The majority of quartz is brown while the minority is light purple and pinkish blue in carbonate matrix. (b) Fine-grained brown quartz is dominant in the rock, a few coarse quartz grains are blue and pinkish blue.

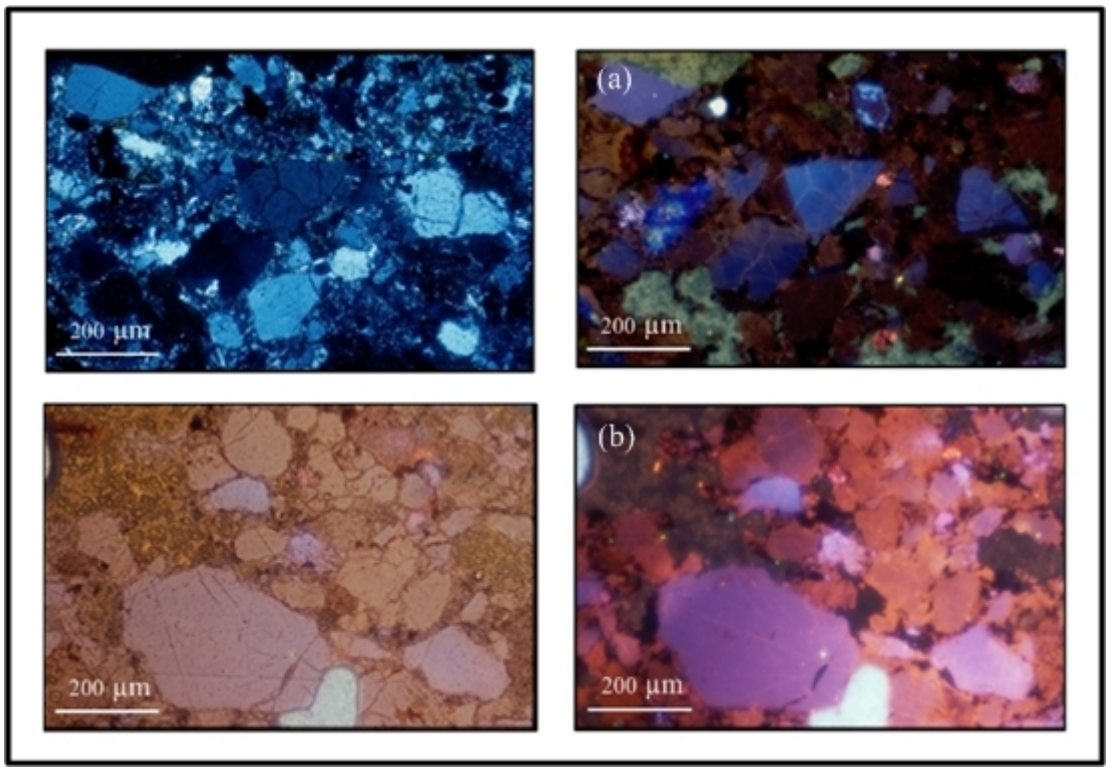


**Figure 5.15** Thin section under CL of molasse sample no. 37+550 comparing between ordinary light and CL (left) and cathodoluminescence (right). (a) The majority of quartz is blue and violet color while the minority is brown. Deformed detrital quartz represented by blue CL. (b) The majority of quartz is brown and brownish blue.

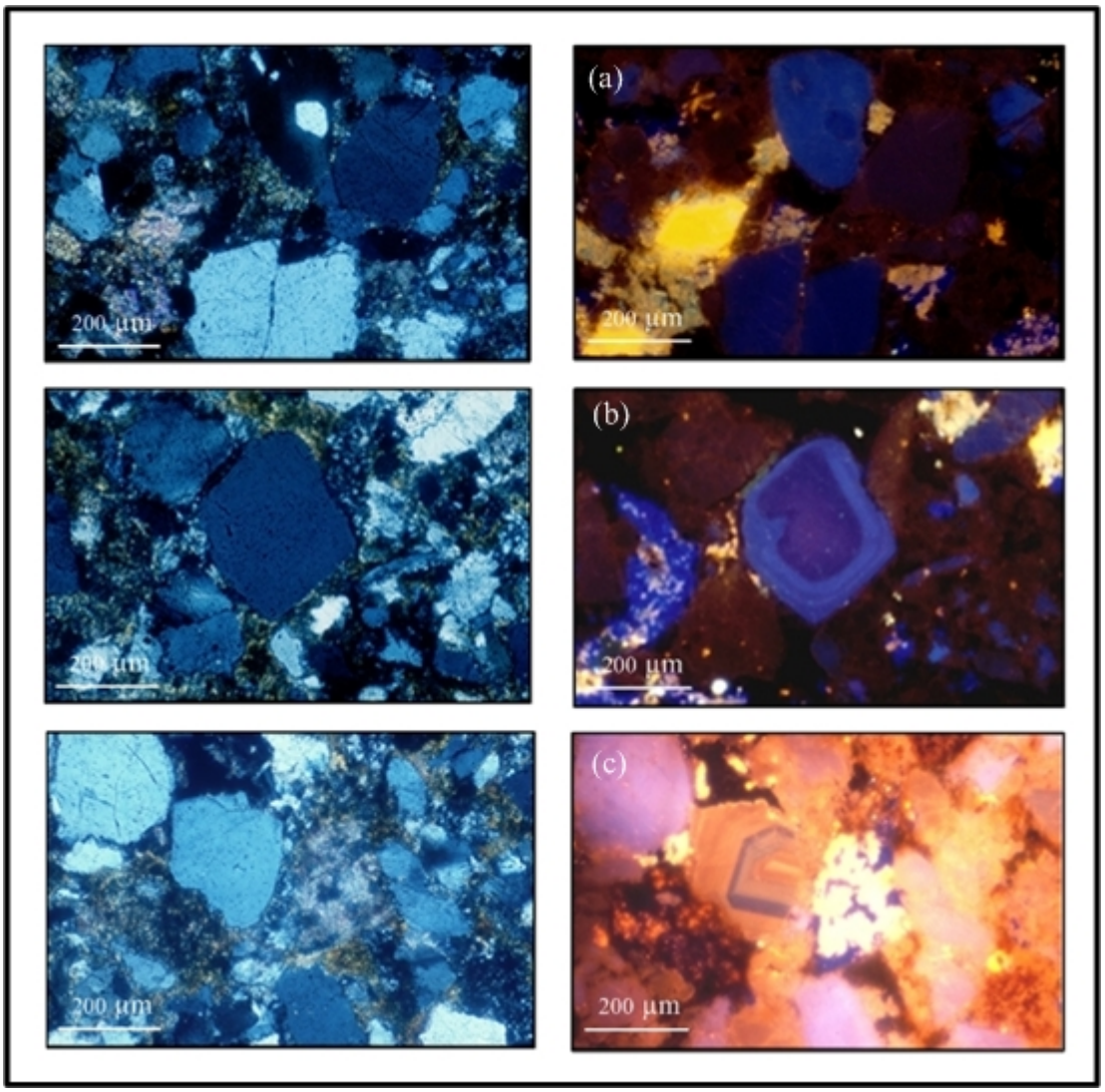


**Figure 5.16** Thin section under CL of molasse sample no. 40+400 comparing between ordinary light (left) and cathodoluminescence (right). (a) The majority of quartz is blue and violet color while the minority is brown. Carbonate grain is well defined by bright yellowish and scattered feldspar is dark blue. (b) The majority of quartz is brown while the minority is blue. K-feldspar (azure color) is at the left between quartz grain and scattering all over. (c) Low temperature hydrothermal quartz displays stepped zoning.

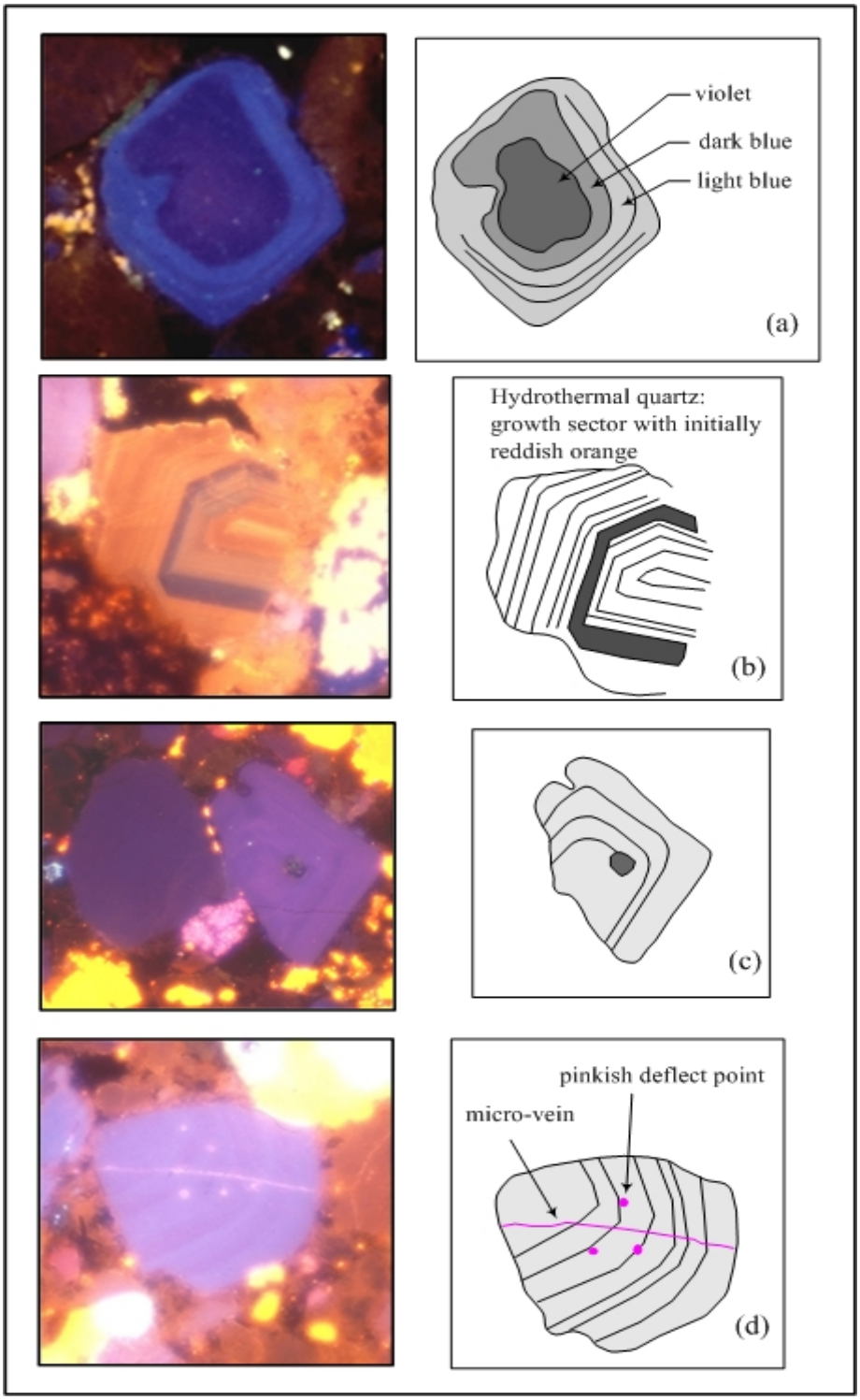


**Figure 5.17** (a) Zoned pattern of quartz grain in molasse sample no. 40+400 displays stepped zoning of violet-light blue-dark blue. (b) Zoned pattern of

quartz grain in molasse sample no. 40+400 displays growth sector with initially light reddish brown, light purple, violet, light reddish brown. (c) Zoned pattern of quartz grain in molasse sample no. 34+750 displays stepped zoning of light purple with non luminescent deflecting near the center. (d) Zoned pattern of quartz grain in molasse sample no. 34+750 displays stepped zoning of light blue with pinkish point and micro-vein.

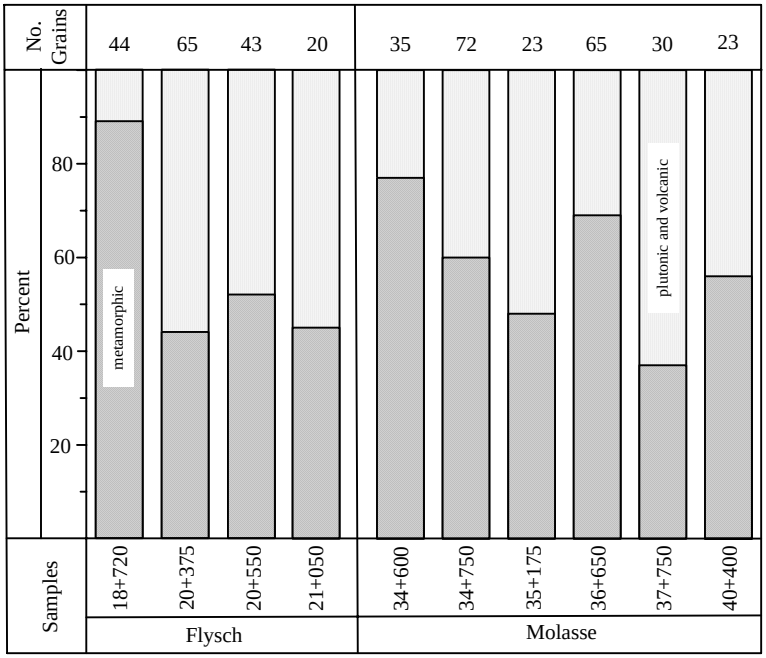


**Figure 5.18** Bar plot showing percentage of metamorphic, plutonic and volcanic quartz grains in sandstone samples from flysch and molasse sequences of the Nam Duk Formation.

## 5.2 Nong Pong and Pang Asok Formations

In Saraburi area, allodapic limestone sample was collected from the Nong Pong Formation (PC-02) and sandstone sample from the Pang Asok Formation (THS-10) (Figure 1.7 in Chapter 1). The PC-02 sample was collected along the road from Muak Lek to Ban Sab Noi Nua (UTM 47P; 0759480N, 1640614E). The outcrop approximately 300 meter wide is on a small hill and composed of thin-bedded allodapic limestones, siliceous shales, and cherts. These rocks belong to the Nong Pong Formation (Hinthong et al., 1976). The THS-10 sample was collected from a road cut three kilometer from Muak Lek to Pak Chong of Friendship Highway (No.2). The outcrop is exposed approximately 500 meter wide on left hand side and opposite a limestone mountain.

In general, PC-02 sample under thin section CL displays bright yellowish luminescence indicating a homogeneous texture (Figure 5.19 a). Detrital quartz grains are scattered and display light purple color. The result indicates a volcanic provenance similar to the pelagic sequence of the Nam Duk Formation. THS-10 sample is a fine-grained sandstone with calcareous cement (Figure 5.19 b). Detrital quartz shows mainly brown with minor blue color. Its source interprets as derived mainly from the low-grade regional metamorphic terrane.

The Nong Pong and the Pang Asok Formations show indication of a southern continuation from the Nam Duk Formation of the Phetchabun Fold Belt based on cathodoluminescence result.

## 5.3 Hua Na Kham Formation

The THP-13 sandstone sample was collected from kilometer 84+530 of Highway No. 12 from Lom Sak to Chum Phae of the Khon San area (Figure 1.5 in Chapter 1). This outcrop belongs to the Hua Na Kham Formation (P2) or Upper Clastic sequence of Loei-Phetchabun area. THP-13 sample shows sub-angular to sub-rounded fine- to medium-grained sandstone. CL image displays very clear brown and light blue quartz luminescence (Figure 5.19 c). A metamorphic quartz grain is indicated by crystalline texture and brown luminescence. Slightly overprinting of deformed texture is well observed by CL.

Sandstone of the Upper Clastic sequence (Hua Na Kham Formation) of the section from Chum Phae-Lom Sak shows CL petrography of different quartz characteristic to the molasse sequence on the west. The quartz grains could be derived from different provenances as they consist mainly of detrital quartz from metamorphic terrane.

## 5.4 Pha Dua Formation

The outcrops of the thin-bedded, fine-grained clastic sequence with a preponderance of dark shale and siltstone in Chiang Khan, Loei area were mapped by Chairangsree et al. (1990) as the Late Permian Pha Dua Formation. The unit comprises predominantly siltstone and claystone, often tuffaceous, with rare thin beds of sandstone, coal, and limestone (Mouret, 1994). It was deposited mainly in upper delta to alluvial plain environments, with minor interruption of lower delta plain and bay facies.

The sandstone samples were collected from western part of Chiang Khan, north of Loei Province along the border between Thai-Laos border (Figure 1.6 in Chapter 1). Three kilometer west of Chiang Khan on Highway 2195, the outcrop of fine-grained sandstone, siltstones, and mudstones in beds ranging from a few centimeters up to two meters thickness was studied and the sandstone sample was collected. The sandstone 03TH01 sample is identified as immature lithic greywacke from thin-section. Photomicrograph shows 50% very fine-grained quartz with sub-angular to sub-rounded grains 10% feldspar and 40% lithic fragments. Thin-section under cathodoluminescence shows dominant calcareous cement and typical 80% dark brown to brown color and 10% blue and light purple color of quartz grains (Figure 5.20). From the CL result, these sediments are interpreted to be derived from a regional metamorphic region and a few from high temperature source such as a volcanic rock. The result clearly indicates a source area of metamorphic terrane.

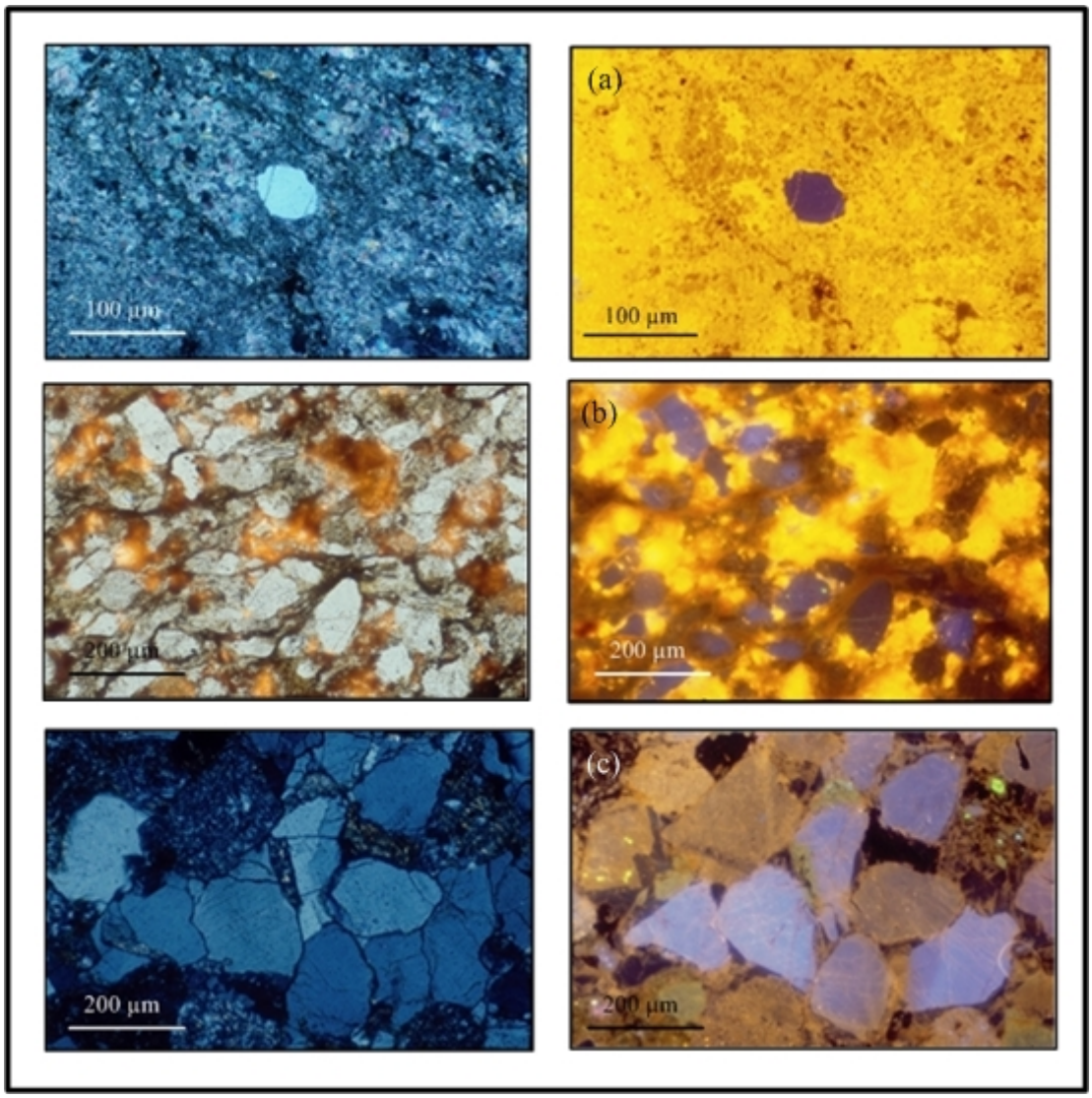


**Figure 5.19** Thin section under CL of the Nong Pong and the Pang Asok Formations in Saraburi-Pak Chong areas and from Upper Clastics “Hua Na Kham Formation” of the Khon San, Chaiyaphum. (a) Sample PC-02 of the Nong Pong Formation shows bright yellowish color and homogeneous texture with volcanic detrital quartz grain represented by light purple color. (b) Sample THS-10 of the Pang Asok Formation shows the majority of quartz is brown while the minority is blue and light purple

luminescence in calcite cement. (c) Sample THP-13 of the Hua Na Kham Formation shows typical brown and blue quartz luminescence color. Crystalline quartz texture from ordinary light is represented by brown color indicating the metamorphic sources.

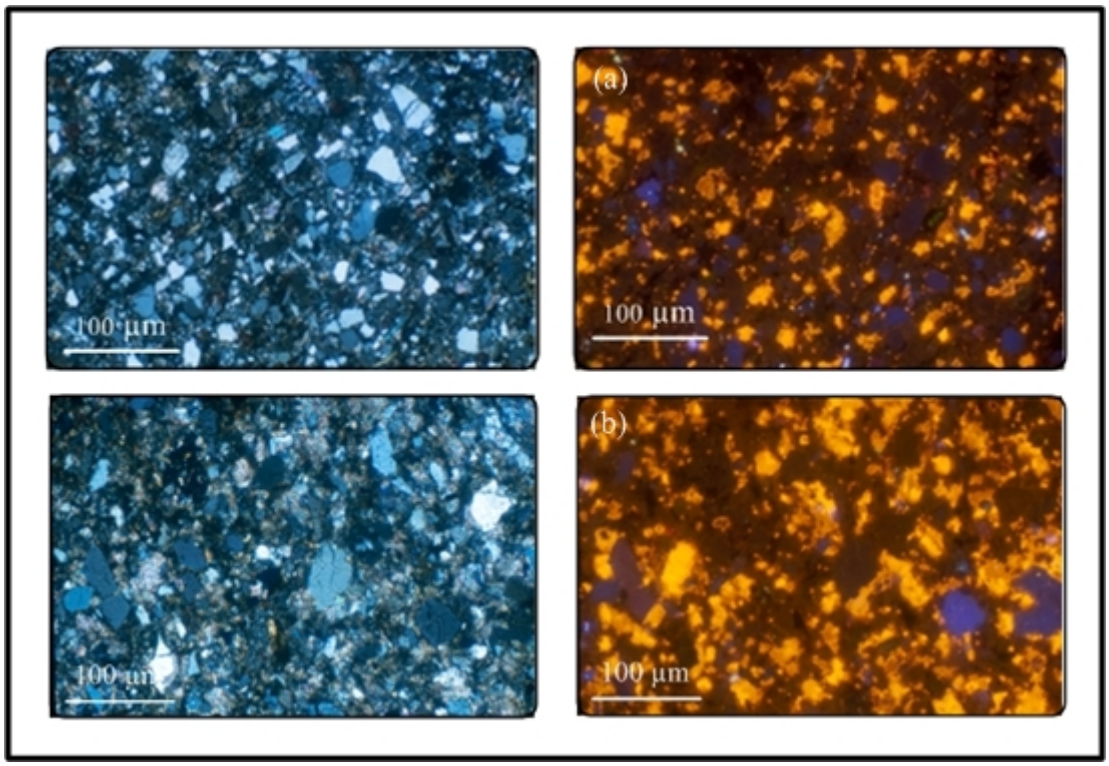


**Figure 5.20** Thin section under CL of Pha Dua Formation, west of Chiang Khan, comparing between ordinary light (left) and cathodoluminescence (right). (a) Thin section shows very fine- to fine-grained sandstone with micaceous fragments. (b) CL micrograph shows the majority of quartz is brown while the minority is blue and light purple luminescence in calcite cement.

# CHAPTER VI

# TECTONIC EVOLUTION OF THE NAM DUK BASIN

In this chapter, the geodynamic evolution of the Nam Duk Basin and Phetchabun Fold Belt based on geochemical analysis, cathodoluminescence and field investigations including data from published literature are proposed and discussed.

## 6.1 Provenance and Tectonic setting of the Nam Duk Formation

The evolution of the Nam Duk Basin started from the pelagic sequence which consists predominantly of pelagic shale and allodapic limestone. This sequence was formed in an oceanic setting between oceanic island and continental island arc environments according to the result of major and trace elements analyses. The source of the quartz detritus in the allodapic limestone was from metabasic and volcanic provenance as indicated by blue luminescence family quartz.

The subsequent deposition of flysch and molasse sequences consists of thick siliciclastic sediments. Tectonic setting discrimination diagrams and trace elements characteristics of flysch and molasse siliciclastic sediments indicate similar geochemical characteristics. The most important sources for both flysch and molasse were mixed mafic igneous, metabasic, granitic gneiss, and low-silica metamorphic sources. Both sequences were deposited in a continental island arc setting. The detrital quartz grains in the flysch sequences show characteristic of regional low-grade metamorphic sources in the lower part and mixed between low-grade

metamorphic and volcanic/plutonic quartzs in the upper part of the section. Quartz luminescence composition of molasse shows similarity to flysch sequences but has more variety of volcanic provenances as indicated by well developed internal zoned structure. Detail of provenance and tectonic setting of the Nam Duk Formation is given in Figure 6.1.

Comparisons of geochemical and cathodoluminescence characteristic of the sections north and south of the Nam Duk Formation at its type section have been done. The result shows that the Tha Li siliciclastic sediments approximately 150 kilometers north of the Lom Sak and the Pang Asok Formation in the Saraburi region to the south can be correlated with the flysch sequence. This indicates that the axis of the Nam Duk Basin is at least 400 kilometers long in a N-S direction along the western margin of the Khorat Plateau.

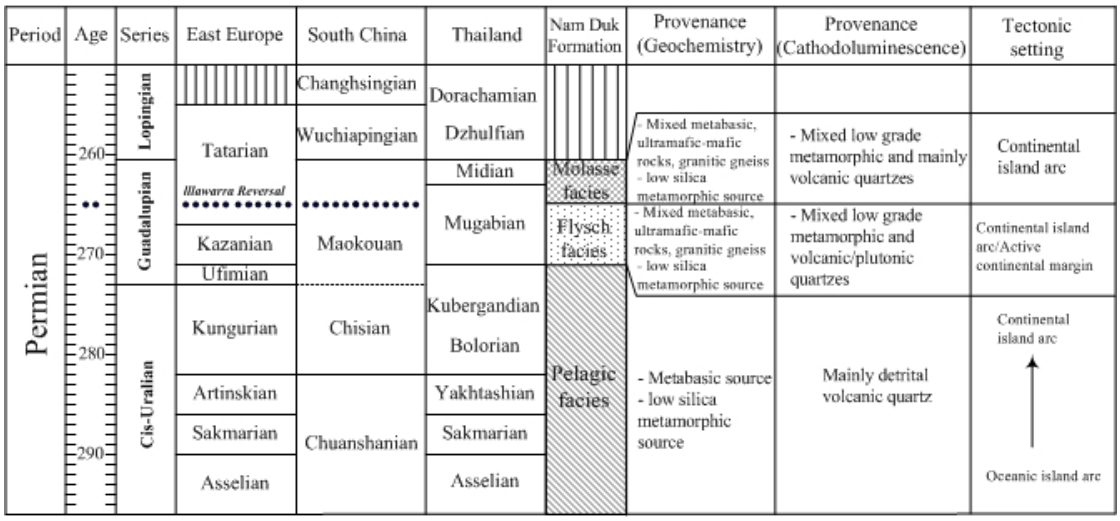


**Figure 6.1** Detailed stratigraphic succession of the Nam Duk Formation including its provenance and tectonic setting based on geochemical and cathodoluminescence data.

## 6.2 Geodynamic model of the Phetchabun Fold Belt

From geochemical and cathodoluminescence results including the published data from various authors, the possible evolution and paleotectonic reconstruction of the Nam Duk Formation is summarized as following.

The Nam Duk Basin was formed as a back arc basin after the closure of small oceanic basin (Loei Ocean) in Indosinia continent during the Devonian-Carboniferous (Intasopa and Dunn, 1994). This basin rifting probably occurred in Middle Carboniferous (Kozar et al., 1992) and subsequently the pelagic sediments were accumulated during Middle – Late Carboniferous to lower Middle Permian in a deep sea basin (Figure 6.2). This deep sea oceanic basin was bordered on both sides by shallow marine sea. The geochemical and cathodoluminescence results indicate that the pelagic facies of a deep sea basin was formed close to an oceanic island and on an oceanic crust.

The Pha Nok Khao and the Khao Khwang Platforms (or probably one coherent unit) were located in the eastern side of the Nam Duk Basin or the western margin of the Indochina plate. The subduction of Indochina beneath the Shan-Thai cratons (on the west) towards west was started in the upper Middle Permian. During subduction the accretionary complex comprising mixture of pelagic sediments including radiolarian chert and mafic-ultramafic rocks was formed at the eastern margin of the Shan-Thai block. This ophiolite belt has been known as the Nan-Uttaradit Suture Zone. Erosion of the accretionary complex produced the influx of siliciclastic or flysch sediments to the Nam Duk Basin. The provenance signature of the flysch sequence shows the mafic igneous source which is interpreted as being derived from the accretionary complex.

The result of geochemical analysis of flysch sequence as discussed in the previous chapter indicates that it was deposited in a continental island arc setting. It could be interpreted that it was in an outer or a fore-arc environment. Upon the oceanic crust was completely consumed the Indochina collided with the Shan-Thai terranes causing the Variscan Orogeny (Helmcke and Lindenberg, 1983). The basin was shallowing, the siliciclastic sediments were continuously supplied from the same sources representing the molasse sediments. The geochemical and cathodoluminescence results confirm that both flysch and molasse sequences show similar characteristics representing the same provenance and tectonic setting. However, the molasse contains more volcanic quartz grains than flysch and more recycled sediments.

A geodynamic model based on geochemical and cathodoluminescence analysis is shown in Figure 6.2.

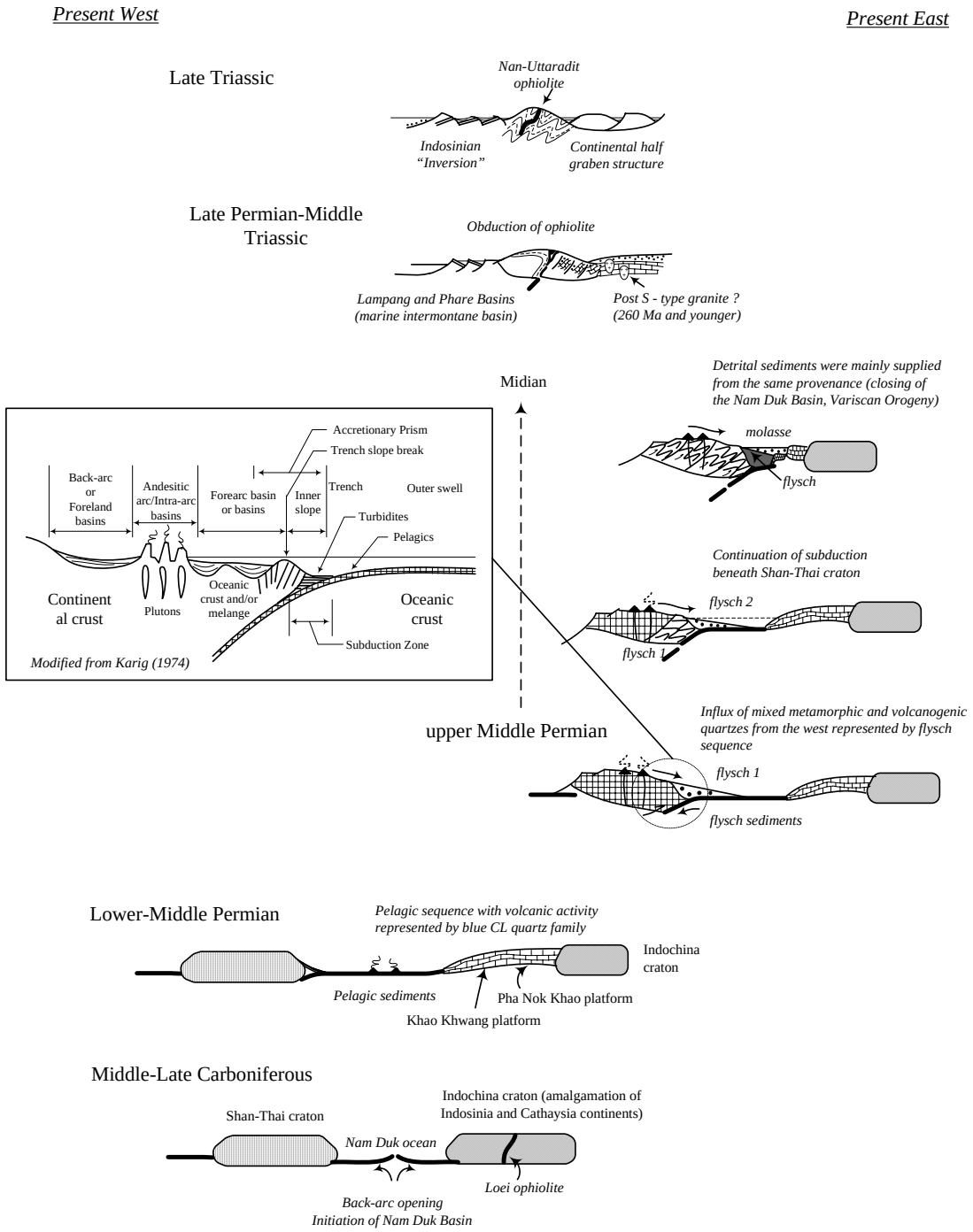


**Figure 6.2** Tectonic model and evolution of the Nam Duk Basin and adjacent region during Late Paleozoic - Triassic based on geochemical and cathodoluminescence analysis including data from various publications.

## 6.3 Discussion

The discovery of detrital chromain spinels in the flysch and molasse sequences of the Nam Duk Formation was reported by Chutakositkanon et al. (1999). However, interpretation of the provenance of the chromain spinels from the Loei ultramafic located in eastern edge of Nam Duk Basin is unlikely and inconsistent with the geologic evolution of the region (Chonglakmani and Helmcke, 2001; Chonglakmani et al., 2001). The present study confirms that the sources of the chromian spinels is likely to be derived from the ultramafic accreted to the subduction complex in the west. This provenance contributed the siliciclastic sediments of flysch and molasse sequences including detrital chromian spinels.

The sandstone sample from Chiang Khan (Middle-Late Permian Pha Dua Formation) displays mainly detrital quartz grains derived from metamorphic sources. This could be related to the denudation of metamorphic terrane on the east of the Nam Duk Basin. The metamorphic sources could be the older orogen deformed during Late Devonian-Early Carboniferous (Intasopa and Dunn, 1994).

Correlation of the Late Paleozoic strata in the Nan-Uttaradit suture zone and the Phetchabun Fold Belt reveals a continuous sedimentary sequence which can be used for the paleotectonic reconstruction. Figure 6.3 displays an idealized vertical sequence from oceanic igneous rocks and chert (ophiolite sequence) passing upward through pelagic, greywacke turbidite (flysch) to shallow marine clastic (molasse) deposits. Interpretation of vertical sequence are the result of seafloor spreading to form an oceanic crust (pillow basalt, gabbro, and peridotile) followed by chert sequence in Nan and part of the pelagic facies in the Nam Duk Formation. These were subsequently followed by terbidite limestone and flysch sedimentation in a

remnant ocean basin. After the remnant ocean was closed, a peripheral foreland basin was formed with molasse sedimentation. The changing of flysch to molasse sediments as the result of the termination of the oceanic basin indicates the maximum deformation or disturbance which is known as the Variscan orogeny (Helmcke and Lindenberg, 1983).

From an economic point of view, volcanic and plutonic activities during Permo-Triassic in the Phetchabun Fold Belt may contribute significantly for mineral exploration targets. However, from the basin evolution and tectonic interpretation, this region is considered as a peripheral foreland basin with typical late and uplift stage of plutonic (post orogeny S-type granite) and intermediate to acidic volcanic rocks. It seems to be contradictory with the result of 260 Ma calcalkaline I-type granites dated by Beckinsale et al. (1986). Therefore, mineralization in this belt is considered to be not prospective. Even though the epithermal gold and silver deposits have been found in Phichit-Phetchabun area but they cannot be correlated with the Permo-Triassic igneous rocks along the western margin of the Khorat Plateau. Thick column of siliciclastic sediments of the peripheral foreland basin in the Phetchabun Fold Belt especially the Permian upper clastic sequences (molasse) can be considered as reservoir, source, and even seal rocks for hydrocarbon exploration.

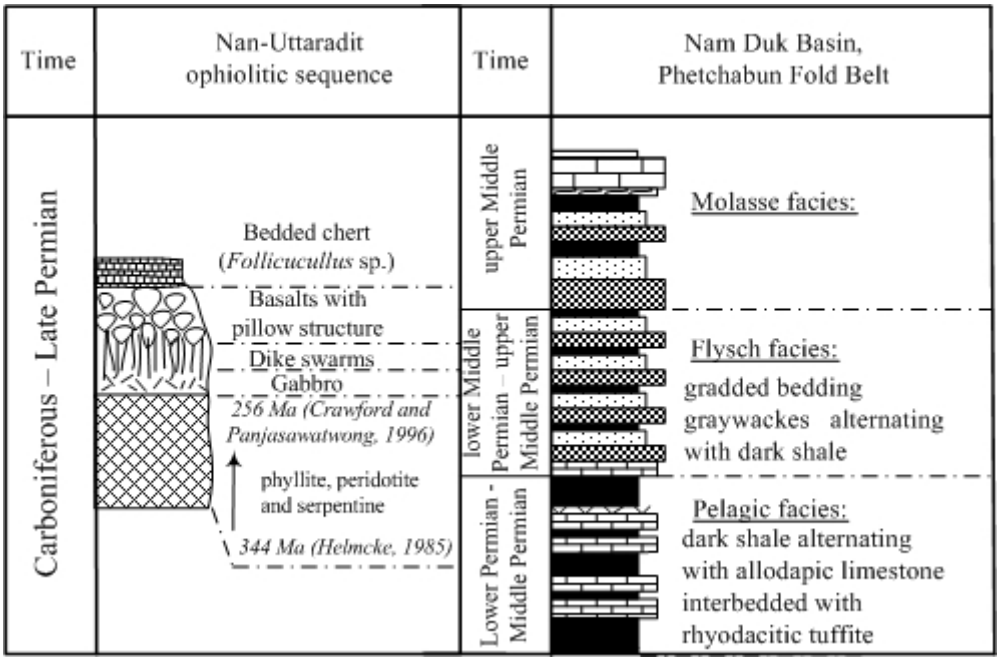


**Figure 6.3** Idealized vertical sequence from ophiolite suite of Nan-Uttaradit Suture Zone and the Nam Duk Basin during Late Paleozoic.

# CHAPTER VII

# CONCLUSIONS

The result of this study of major and trace element compositions and cathodoluminescence analysis of the siliciclastic sediments in the Nam Duk Formation and Permian sequences in Loei and Saraburi areas have implications for tectonic interpretations in Thailand. Based on geochemical and cathodoluminescence analyses the result can be summarized as follows;

1. The pelagic sequence of the Nam Duk Formation was formed in an oceanic setting between oceanic island and continental island arc environments. The source of the quartz detritus in the allodapic limestone was from metabasic and volcanic provenance.

2. The flysch and molasse sequences show similar geochemical characteristics (very high $TiO_2$ and $Fe_2O_3$, low $Al_2O_3$) and indicate mixed mafic igneous, metabasic, granitic gneiss, and low-silica metamorphic sources. Both sequences were deposited in a continental island arc setting.

3. The Nam Duk Formation at Tha Li in Loei and the equivalent Pang Asok Formation in Saraburi-Pak Chong area can be correlated with the flysch sequence at its type section in the Phetchabun Fold Belt.

4. The sandstone sample from Chiang Khan (Middle-Late Permian Pha Dua Formation) displays mainly detrital quartz grains derived from metamorphic sources

and could be related to the denudation of metamorphic terrane from older orogen of Late Devonian-Early Carboniferous age (Intasopa and Dunn, 1994).

5. Tectonically, subduction of the Indochina beneath the Shan-Thai cratons (on the west) towards west was started in the upper Middle Permian resulting in the formation of an accretionary complex. The provenance signature of the flysch sequence shows the mafic igneous source which is interpreted as being derived from the accretionary complex and it was in an outer or a fore-arc environment. The maximum orogenic movement occurred during the completion of suturing process. The molasse sequence was accumulated after mountain building process consisting predominantly of the siliciclastic sediments.

6. This study supports an idea of Nan-Uttaradit suture as being one branch of the main Paleo-Tethys represented by the Nam Duk remnant ocean Basin in the Phetchabun Fold Belt. This ocean was already closed during the short period of Middle Permian.

Finally, the following works are recommended to be carried out for some geological clarification:

- Tracing of the continuation of Permian Nam Duk Basin across Thai-Laos border to Pak Lay - Luang Phrabang in Laos, and SW-Yunnan.

- U-Pb dating of a small set of zircon population from Nam Duk Formation and correlatives with the equivalent rock units in order to determine the age of its components and the provenance of the components.

- More detail structural analysis in order to recognize phase of deformation during Mesozoic to Tertiary.

- Micro-paleontology study of a pelagic sequence of the Nam Duk Formation and the equivalent section in Saraburi (Nong Pong and Khao Phaeng Ma Formations) in order to study the paleogeography during Permian time.

# REFERENCES


Ahrendt, H., Chonglakmani, C., Hansen, B.T. and Helmcke, D. (1993). Geochronological cross section through northern Thailand. **Journal of Southeast Asian Earth Sciences** 8 (1-4), pp. 207-214.

Akermann, T.E. (1986). The geology of the Lower Paleozoic Talutao Formation. **Unpublished B.Sc. Hon. thesis**, University of Tasmania, Australia.

Altermann, W. (1989). Facies development in the Permian Petchabun basin central Thailand. **Verlag fur Wissenschaft und Bildung**, Berlin, 236 p.

Altermann, W., Grammel, S., Ingavat, R., Nakornsri, N. and Helmcke, D. (1983). On the evolution of the Paleozoic terrains bordering the Northwestern Khorat Plateau. **Conference on Geology and Mineral Resources of Thailand**. DMR, Bangkok, November. preprint 5 p.

Andre, L., Deutsch, S. and Hertogen, J. (1986). Trace-element and Nd isotopes in shales as indexes of provenance and crustal growth: The early Paleozoic from the Brabantmassif (Belgium). **Chemical Geology**. 57: 101-115.

Asama, K., Iwaii, J., Veeraburas, M. and Hongnusonthi, A. (1968). Permian plants from Loei. **Geology and Paleontology of Southeast Asia**. 4(82-99): 14-18.

Barr, S.M. and Macdonald, A. S. (1987). Nan-River suture zone, northern Thailand. **Geology** 15: 907-910.

Barr, S. M. and Macdonald,A. S. (1991). Toward a late Paleozoic-early Mesozoic tectonic model for Thailand. **Journal of Thai Geosciences**, 1: 11-22.

Barr, S.M., Macdonald, A.S., Yaowanoiyothin, V. and Panjasawatwong, Y. (1985). Occurrence of blueschists in the Nan River mafic-ultramafic belt, northern Thailand. **Warta Geologi**, 11:47-50.

Barr, S.M., Tantisukrit, C., Yaowanoiyothin, W. and Macdonald, A.S. (1990). Petrology and tectonic implications of Upper Paleozoic volcanic rocks of the Chiang Mai belt, northern Thailand. **J. Southeast Asian Earth Sci**. 4:37-47.

Baum, F., Braun, E., Hahn, L., Hess, A., Koch, K.E., Kruse, G., Quarch, H. and Siebenhüner, M. (1970). On the Geology of Northern Thailand. Beih. Geol. Jahrb. 102:3-24.

Beckinsale, R.D., Suensilpong, S., Nakapadungrat, S., Walsh, J.N., Cobbing, E.J. and Ridd, M.F. (1979). Geochronologz and geochemistry of granite magmatism in Thailand in relation to a plate tectonic model. **Jour. Geol. Soc. Lond**., V. 136 (pt.5), pp. 529-540.

Bhatia, M.R. (1983). Plate tectonics and geochemical composition of sandstones. **Journal of Geology**, 91, 611-627.

Bhatia, M.R. (1985). Rare earth element geochemistry of Australian Paleozoic graywackes and mudrocks: Provenance and tectonic control. **Sedimentary Geology**, 45, 97-113.

Bhatia, M.R. and Crook, K.A.W. (1986). Trace element characteristics of graywackes and tectonic discrimination of sedimentary basins. **Contrib. Mineral. Petrol**., 92, 181-193.

Bunopas, S. (1981). **Paleogeographic history of western Thailand and adjacent parts of Southeast Asia: A plate tectonics interpretation**. Ph.D. Dissertation, Victoria University of Wellington, New zealand. Reprinted 1982 as Geological Survey Paper 5, Department of Mineral Resources, Bangkok, Thailand.

Bunopas, S. (1991). The pre-Late Triassic collision and stratigraphic belts of Shan-Thai and Indochina Microcontinents in Thailand. **Proc. of papers presented at the 1st intern. Symp. of the IGCP Project 321, Gondwana:Dispersal and Accretion of Asia**. Kunming, China

Bunopas, S. (1992). Regional stratigraphic correlation in Thailand. In: Piancharoen, C. (ed.). **Proceeding of the National Conference on the Geologic Resources of Thailand: Potential for Future Development** (pp. 2-24). DMR. Bangkok, Thailand.

Bunopas, S. and Vella, P. (1978). Late Paleozoic and Mesozoic structural evolution of Northern Thailand: A plate tectonic model. In: Nutalaya, P. (ed.). **Proc. GEOSEA III** (pp. 133-140). Bangkok, Thailand.

Bunopas, S. and Vella, P. (1983). Tectonic and geologic evolution of Thailand. In: Nutalaya, P. (ed.). **Proceeding of the Workshop on Stratigraphic correlation of Thailand and Malaysia** (pp. 307-323). Haad Yai, Thailand.

Burrett, C. F. and Stait, B. A. (1985). Southeast Asia as part of an Ordovician Gondwanaland; a palaeobiogeographic test of the tectonic hypothesis. **Earth and Planetary Science Letters**. 75: 184-190.

Caridroit, M., Bohlke, D., Lamchuan, A., Helmcke, D. and De Wever, P. (1993). A mixed Radiolarian fauna (Permian/Triassic) from clastics of the Mae Sariang area, northwestern Thailand. In:Thanasuthipitak, T. (ed.), **Proceedings of the International Symposium on Biostratigraphy of Mainland Southeast Asia: Facies and Paleontology** ( pp.401-413). Chiang Mai, Thailand.

Carnarvan Petroluem Report (2002). Geology Report. Available on http://www.carnarvon.com.au/

Chairangsee, C., Hinze, C., Machareonsap, S., Nakornsri, N., Silpalit., M. and Ainpool-Anunt, S. (1990). **Geological map of Thailand 1:50,000 explanation for the sheets: Amphoe Pak Chom, Ban Huai Khop, Ban Na Kho and King Amphoe Nam Som**. Geologisches Jahrbuch Reihe B, Heft 73, Hannover. 109 p.

Chaodumrong, P., Ukakimapan, Y., Snansieng, S., Janmaha, S., Pradittan, S. and Leow, N.S. (1983). A review of the Tertiary sedimentary rocks of Thailand. Proc. In: Nutalaya, P. (ed.). **Proceeding of the Workshop on Stratigraphic correlation of Thailand and Malaysia** (pp. 105-126). Haad Yai, Thailand.

Charoentitirat, T. (1999). Latest Carboniferous-Early Permian fusulinacean faunas from Loei, Northeast Thailand. **Master Thesis**, University of Tsukuba, Japan (unpublished).

Charoentitirat, T. (2002). Permian Fusulinodean Biostratigraphy and Carbonate Development in the Indochina Block of Thailand with Their Paleogeographic Implication. **Doctoral thesis**. University of Tsukuba, Japan

Charusiri, P., Kosuwan, S. and Imsamut, S. (1997). Tectonic evolution of Thailand : From Bunopas (1981)'s to a new secnario. In: Dheeradilok, P., (eds.). **Proceedings of the Conference on Stratigraphy and Tectonic Evolution of Southeast Asia and the South Pacific**, DMR Bangkok, Thailand, pp. 414-420.

Chonglakmani, C. (2001). The Saraburi Group of North-Central Thailand: Implication for Geotectonic Evolution. **Gondwana Research**. 4: 597-598.

Chonglakmani, C. (2002). Current Status of Triassic Stratigraphy of Thailand and Its Implication for Geotectonic Evolution. In: Mantajit, N., (eds). **Proceeding of the Symposium on Geology of Thailand 2002** (pp.1-3). DMR Bangkok, Thailand.

Chonglakmani, C. (2005). **Assessment of Limestone Resources of Pak Chong Area, Changwat Nakhon Ratchasima**. Research Project No. SUT 7-719-43-24-49. Suranaree University of Technology. 40 p (in Thai with English abstract).

Chonglakmani, C. and Fontaine, H. (1992). The Lam Narai-Phetchabun region: A platform of Early Carboniferous to Late Permian age. In: Charusiri, P., et al (eds.). **Proceedings of the Technical Conferences on Development Geology for Thailand into the Year 2000**. Chulalongkorn University, Thailand. pp. 39-98.

Chonglakmani, C., Fontaine, H. and Vachard, D. (1983). A Carboniferous-Lower Permian(?) Section in Chon Dan Area, Central Thailand. In **Conference on Geology and Mineral Resources of Thailand** (preprint 5 p). DMR Bangkok, Thailand.

Chonglakmani, C. and Helmcke, D. (2001). Geodynamic evolution of Loei and Phetchabun regions; Does the discovery of detrital chromain spinels from the Nam Duk Formation (Permian, north-central Thailand) provide new constraint?. **Gondwana Research**. 4(3): 437-442.

Chonglakmani, C., Qinglai, F., Meischner, D., Ingavat-Helmcke, R. and Helmcke, D. (2001). Correlation of Tectono-Stratigraphic Units in Northern Thailand with Those of Western Yunnan (China). **Journal of China University of Geosciences**: 12(3): 207-213.

Chonglakmani, C. and Sattayarak, N. (1978). Stratigraphy of the Huai Hin Lat Formation (Upper Triassic) in northeastern Thailand. In: Nutalaya, P. (Ed.), **Proc. GEOSEA III**, Bangkok, 14-18 Nov., pp. 739-762.

Chutakositkanon, V., Charusiri, P. and Sashida, K. (2000). Lithostratigraphy of Permian marine sequences, Khao Pun area, central Thailand: Paleoenvironments and tectonic history. **The Island Arc**: 9: 173-187.

Chutakositkanon, V., Hisada, K., Charusiri, P., Arai, S. and Charoentitirat, T. (1999). Characteritics of Detrital Chromian Spinels from the Nam Duk Formation: Implication for the Occurrence of Mysterious Ultramafic and Volcanic Rocks in Central Thailand. In: Khantaprab, C. et al. (eds.). **Symposium on Mineral, Energy, and Water Resources of Thailand: Towards the year 2000** (pp. 604-606). Chulalongkorn University, Thailand.

Chutakositkanon, V., Hisada, K., Uneo, K. and Charusiri, P. (1997). New suture and terrane deduced from detrital chromian spinel in sandstone of the Nam Duk Formation, north-central Thailand: preliminary report. In: Dheeradilok, P., et

al (Eds), **Proceedings of the International Conference on Stratigraphy and Tectonic Evolution of Southeast Asia and the South Pacific**. 19-24 August, DMR Bangkok, Thailand. pp 368.

Cobbing, E.J., Mallick, D.I.J., Pitfield, P.E.J. and Teoh, L.H. (1986). The granites of the Southeast Asian Tin Belt. **Jour. Geol. Soc. Lond.** 143: 537-550.

Cooper, M.A., Herbert, R. and Hill, G.S. (1989). The structural evolution of Triassic intramontane basins in northeastern Thailand. In:Thanasuthipitak, T., Ounchanum, P. (Eds), **Proceedings of the International Symposium on Intermontane Basins: Geology and Resources, Chieng Mai**, (pp. 231-242). Chiang Mai University.

Crawford, A.J. and Panjsawatwong, Y. (1996). Ophiolites ocean crust, and the Nan Suture in NE Thailand. **Intern. Symp. On lithosphere dynamics of East Asia**, Extended Abstract, Taipei, pp.84-89.

Cullers, R.L. (1994). The chemical signature of source rock in size fractions of Holocene stream sediment derived from metamorphic rocks in the Wet Mountains region, Colorado, U.S.A. **Chemical Geology**. 113: 327-343.

Cullers, R.L., Basu, A. and Suttner, L. (1988). Geochemical signature of provenance in sand-size material in soils and stream sediments near the Tobacco Root Batholith, Montana, U.S.A. **Chemical Geology**: 70: 335-348.

Dawson, O. and Racey, A. (1993). Fusuline-calcareous algal biofacies of the Permian ratburi Limestone, Saraburi, central Thailand. **Journal of Southeastern Asian Earth Sciences**. 8: 49-65.

Dheeradilok, P. (1975). **Precambrian rocks of Thailand in general**. Department of Geological Sciences, Chiang Mai University, Special Publication, 1(2):3-4.

Dheeradilok, P., Wongwanich, T., Tansathien, W. and Chaodumrong, P. (1992). An introduction to Geology of Thailand. In: Piancharoen, C. (ed.). **Proceeding of the National Conference on the Geologic Resources of Thailand: Potential for Future Development** (pp. 641-652). DMR. Bangkok, Thailand.

Dickinson, W.R. (1982). Compositions and sandstones in circumpacific subduction complexes and fore-arc basins. **AAPG Bull**. 66: 121-137.

Dickinson, W.R. (1985). Interpreting provenance relations from detrital modes of sandstones. In Zuffa G.G. (ed.) **Provenance of Arenites**, pp. 333-361. Dordrecht:D.Reidel.

Dott, R.H. and Batten, R.L. (1988). **Evolution of the Earth (4$^{th}$)**. McGrew-Hill, New York, 643 p.

Dunning, G.R., Macdonald, A.S. and Barr, S.M. (1995). Zircon and monazite U-Pb dating of the Doi Inthanon core complex, northern Thailand: implications for extension within the Indosinian Orogen. **Tectonophysics**. 251: 197-213.

Folk, R.L. (1974). **Petrology of Sedimentary Rocks**. Hemphill Publishing, New York.

Fontaine, H. (2002). Permian of Southeast Asia: an overview. **Journal of Asian Earth Sciences**. 20: 567-588.

Fontaine, H., Salyapongse, S. and Vachard, D. (1999). New Carboniferous Fossils found in Ban Bo Nam Area, Central Thailand. In: Khantaprab, C. et al. (eds.).

**Symposium on Mineral, Energy, and Water Resources of Thailand: Towards the year 2000** (pp. 201-211). Chulalongkorn University, Thailand.

Fontain, H. and Suteethorn, V. (1988). Late Paleozoic and Mesozoic fossils of west Thailand and their environments. **CCOP Technical Bulletin**. 20:1-217, 46 p.

Fontaine, H. and Suteethorn, V. (1992). Permian corals of Southeast Asia and the bearing of a recent discovery of Lower Permian corals in Northeast Thailand. In: Charusiri, P., et al (eds.). **Proceedings of the Technical Conferences on Development Geology for Thailand into the Year 2000**. Chulalongkorn University, Thailand. pp. 346-354.

Götze, J. and Simmerle, W. (2000). Quartz and silica as guide to provenance in sediments and sedimentary rocks. **Contrib. Sediment. Geol**. 12: 91 pp.

Hahn, L. and Siebenhuner, M. (1982). **Explanatory notes on the Geological Maps of Northern and Western Thailand 1:250,000**. B.G.R., Hannover, 76 pp.

Heggemann, H. (1994). Sedimentäre Entwicklung der Khorat-Gruppe (Ober-trias bis Paläogen) in NE-und N-Thailand. **Ph.D. thesis**, University of Göttingen, F.R.Germany.

Helmcke, D. (1985). The Permo-Triassic “Paleotethys” in Mainland Southeast-Asia and adjacent parts of China. **Geol. Rundschau**, 74/2, 215-228.

Helmcke, D. (1994). Distribution of Permian and Triassic syn-orogenic sediments in central mainland SE-Asia. In: Angsuwathana, P., (eds). **Proceedings of the Internation Symposium on Straigraphic Correlation of Southeast Asia**, Bangkok, Thailand, pp. 123-128.

Helmcke, D. and Kraikhong, C. (1982). On the geocynclinal and orogenic evolution of central and northeastern Thailand. **Jour. Geol. Soc. Thailand**. 5: 52-47.

Helmcke, D. and Lindenberg, H.G. (1983). New data on the Indosinian orogeny from Central Thailand. **Geologische Rundschau** 72: 317-328.

Herron, M.M. (1988). Geochemical classification of terrigenous sands and shales from core or log data. **Journal of Sedimentary Petrology**. 58: 820-829.

Hills, J. (1989). The geology of the Phuket District of Thailand. **B.Sc. Honours Dissertation**, University Tasmania (unpublished).

Hiscott, R.N., (1984). Ophiolitic source rocks for Taconic-age flysch: trace element evidence. **Geological Society of America Bulletin**. 95: 1261-1267.

Hinthong, C. (1981). Geology and mineral resources of the Changwat Phrakorn Sri Ayutthaya, Map ND 47-8. **Geological Survey report no. 4**, Department of Mineral Resources, Bangkok, Thailand (in thai).

Hinthong, C., Chuaviroj, Waewyana, W., Srisukh, S., Pholprasit, C. and Pholchan, S. (1976). **Geological map of Changwat Pranakhon Si Ayutthaya (ND 47-8)**, 1:250,000. Department of Mineral Resources, Bangkok Thailand.

Huang, J. (1984). New research on the tectonic characteristics of China. In: Yanshin et al. (eds.), **Tectonics of Asia**: Colloq., 05. Int. Geol. Congr. 27$^{th}$, Moskeow, Rep., 5:13-28.

Hutchison, C.S. (1975). Opliolite in SE Asia. **Bull. Geol. Soc. Am**. 86: 797-806.

Hutchison, C.S. (1989). **Geological Evolution of Southeast Asia**. London Press, Oxford, 368 pp.

Igo, H. (1972). Fusulinaceous fossils from North Thailand. **Geology and Palaeontology of Southeast Asia**. 10: 63-116 pl. 9-19.

Igo, H. (1974). Lower Permian Conodonts from Northern Thailand. **Geology and Palaeontology of Southeast Asia**. 14: 1-6 pl. 1.

Ingavat-Helmcke, R. and Helmcke, D. (1986). Permian Fusulinacean Faunas of Thailand – Event Controlled Evolution. **Lecture Notes in Earth Sciences**. 8: 241-248.

Intasopa, S. and Dunn, T. (1994). Petrology and Sr-Nd isotopic systems of the basalts and rhyolites, Loei, Thailand. **Journal of Southeast Asian Earth Sciences**. 9: 167-180.

Kamata, Y., Sashida, K. and Uneo, K. (2002). Triassic radiolarian faunas from the Mae Sariang area, northern Thailand and their paleogeographic significance. **Journal of Asian Earth Sciences**. 20 (5): 494-506.

Kobayashi, T. and Hamada, T. (1979). Permo-Carboniferous trilobites from Thailand and Malaysia. **Geology and Palaeontology of Southeast Asia**. 20: 1-21 pl. 1-3.

Kon'no, E. and Asama, K. (1973). Mesozoic Plaints from Khorat, Thailand. **Geol. Palaeont. SE Asia**. 12: 149-171.

Kozar, M.G., Crandall, G.F. and Hall, S.E. (1992). Integrated Structural and Stratigraphic Study of the Khorat Basin, Ratburi Limestone (Permian), Thailand. In: Piancharoen, C. (ed.). **Proceeding of the National Conference on the Geologic Resources of Thailand: Potential for Future Development** (pp. 692-736). DMR. Bangkok, Thailand.

Kwon, Y. I. and Boggs, Jr. S. (2002). Provenance interpretation of Tertiary sandstones from the Cheju Basin (NE East Chian Sea): a comparison of

conventional petrographic and scanning cathodoluminescence techniques. **Sedimentary Geology**. 152: 29-43.

Liu, B., Feng, Q. and Fang, N. (1996). Tectonic evolution of the Palaeo-Tethys in Changning-Menglian belt and adjacent regions, Western Yunnan**. Jour. China Univ. Geos**. 2(1): 18-27.

Macdonald, A.S. and Barr, S.M. (1978). Tectonic significance of a Late Carboniferous Volcanic Arc in Northern Thailand. In: Nutalaya, P. (ed.). **Proc. GEOSEA III** (pp. 151-156). Bangkok, Thailand.

Malila, K., Chonglakmani, C., Helmcke, D. and Qinglai, F. (2005). Provenance of the Nam Duk Formation as an Indication for a Late Paleozoic Orogenic Event in Mainland Thailand. **Geophisical Research Abstract**. 7:02123.

Mantajit, N. (1975). Some aspects of the petrology and chemistry of the granitic rocks in Ban Mong area, south of Amphor Mae Chaem,Chiang Mai, Thailand. **Unpublished M.Sc. thesis**, Manchester University, U.K.

Mantajit, N. (1997). Stratigraphy and Tectonic Evolution of Thailand. In: Dheeradilok, P., (eds.). **Proceedings of the International Conference on Stratigraphy and Tectonic Evolution of Southeast Asia and the South Pacific**. DMR Bangkok, Thailand. pp. 1-26.

Matter, A. and Ramseyer, K. (1985). Cathodoluminescence microscopy as a tool for provenance studies of sandstones. In: Zuffa, G. G. (Ed.), **Provenance of Arenite**. Reidel, Dordrecht, pp. 191-211.

Maynard, J.B. (1992). Chemistry of modern soils as a guide to interpreting Precambrian paleosols. **Journal of Geology**, 100, 279-289.

McLennan, S.M., Hemming, S., McDaniel, D.K. and Hanson, G.N. (1993). Geochemical approaches to sedimentation, provenance, and tectonics, **Geological Society of America Special paper**. 284: 21-41.

Meesook, A. and Grant-Mackie, J.A. (1997). Fauna associations, paleoecology nand paleoenvironments of the Thai marine Jurassic: A preliminary study. In: Dheeradilok, P., (eds.). **Proceedings of the International Conference on Stratigraphy and Tectonic Evolution of Southeast Asia and the South Pacific**. DMR Bangkok, Thailand. pp. 177-187.

Metcalfe, I. (1988). Origin and assembly of south-east Asian continental terranes. In: Audley-Charles, M. G., and Hallam, A. (eds.). **Gondwana and Tethys. Geological Society of London Special Publication.** 37: 101-118.

Metcalfe, I. (1997). The Paleo-Tethys and Paleozoic-Mesozoic tectonic evolution of Southeast Asia. In: Dheeradilok, P., et al., (eds.). **Proceedings of the International Conference on Stratigraphy and Tectonic Evolution of Southeast Asia and the South Pacific** (pp. 260-272). DMR Bangkok, Thailand.

Metcalfe, I. (2002). Permian tectonic framework and palaeogeography of SE Asia. **Journal of Asian Earth Sciences**. 20: 551-566.

Mickein, A. (1992). Alter und Intensitat der Schwachmetamorphen Uberpragung des Nam Pat-Fachers E Sirikit Dam (N-Thailand) (K/Ar-Datierung-Lllitkristallinitat). **Unpubl. Ph.D. Thesis**, Univ. Göttingen, 80 p.

Min, M., Lin, K., Qinglai, F., Chonglakmani, C., Meischner, D., Ingavat-Helmcke, R. and Helmcke, D. (2001). Tracing the disrupted outer margin of the

Paleoeurasian continent through the Unian of Myanmar. **Jour. China Univ. Geos**. 12(3): 201-206.

Mouret, C. (1994). Geological history of northeastern Thailand since the Carboniferous: Relations with Indochina and Carboniferous to early Cenozoic evolution model. In: Angsuwathana, P., et al (Eds). **Proceedings of the International Symposium on Straigraphic Correlation of Southeast Asia**. Bangkok, Thailand, pp. 132-158.

Müller, A. (2000). Cathodoluminescence and Characterisation of defect structures in quartz with application to the study of granitic rocks. **Unpubl. Ph.D. Thesis**, Univ. Göttingen, 229 p.

Neuser, R. D., Bruhn, F., Götze, J., Habermann, D. and Ricgter, D. K. (1995). Kathodolumineszenz: Methodik und Auwendung. **Zbl. Geol. Paläont. Teil 1,** 1/2: 287-306.

Pettijohn, F.J., Potter, P.E. and Siever, R. (1987). **Sand and sandstone**. Springer Verlag. New York, 553 pp.

Pitcher, W. S. (1982). **Granite type and tectonic environment**, in Hsu, KJ (Editor): Mountain. building processes, Academic Press, London, pp. 19-40

Pittman, E.D. (1970). Plagioclase as an indicator for provenance in sedimentary rocks. **Journal of Sedimentary Petrology**: 40, 591-598.

Pisutha-Arnond, V., Kusakabe., M., Khantaprab, C. and Vedchakanchana, S. (1997). Sulfur and oxcygen study of the Phichit-Nakhon Sawan gypsum/anhydrite deposit: An implication on the age of ist formation. In: Dheeradilok, P., (eds.). **Proceedings of the International Conference on Stratigraphy and**

**Tectonic Evolution of Southeast Asia and the South Pacific**. DMR Bangkok, Thailand. pp. 188-199.

Piyasin, S. (1975). **Geology of Changwat Uttaradit, Sheet NE47-11.** Report of Investigation no. 15, Department of Mineral Resources, Bangkok. 68 p.

Piyasin, S. (1991). Tectonic events and radiometric dating of the basement rocks of Phitsanulok Basin. **Journal of Thai Geosciences**. 1: 41-48.

Polachan, S., Pradidtan, S., Tongtaow, C., Janmaha, S., Intarawijit, K. and Sangsuwan, C. (1991). Development of Cenozoic basins in Thailand. **Journal of Marine and Petroleum Geology**. 8:85-97.

Potter, P.E. (1978). Petrology and chemistry of modern big river sands. **Journal of Geology**. 86: 423-449.

Putthapiban, P. (2002). Geology and Geochronology of the Igneous Rocks of Thailand. In: Mantajit, N., (eds). **Proceeding of the Symposium on Geology of Thailand 2002,** DMR Bangkok, Thailand, pp.261-283.

Owen, M. R. (1991). Application of Cathodoluminescence to Sandstone Provenance. In Barker, C.E., and Kopp, O.C. (eds.). **SEPM Short Course 25** (pp.67-75).

Qinglai, F. and Helmcke, D. (2001). Late Paleozoic compressional deformation in the Simao region Southern Yunnan, P.R. of China. **Newsl. Stratigr**. 39(1): 21-31.

Qinglai, F., Helmcke, D., Chonglakmani, C., Ingavat-Helmcke, R. and Liu, B. (2004). Early Carboniferous radiolarians from north-west Thailand: palaeogeographical implications. **Paleontology**. 47(2): 377-393.

Raksaskulwong, L. and Wongwanich, T. (1993). **Stratigraphy of the Kaeng Krachan Group, penisular and western Thailand**. Geological Survey Division, Department of Mineral Resources, Thailand. 66 p. (in Thai).

Remus, D., Webster, M. and Keawkan, K. (1993). Rift architecture and sedimentology of the Phetchabun Intermontain Basin, central Thailand. **Journal of Southeast Asian Earth Sciences.** 8 (1-4): 421-432.

Richter, D. K., Götte, Th., Götze, J. and Neuser, R. D. (2003). Progress in application of Cathodoluminescence (CL) in sedimentary petrography. **Mineralogy and Petrography** 79: 127-166.

Ridd, M.F. (1980). Possible Paleozoic drift of SE Asia and Triassic collision with China. **Geol.Soc.London J**. 137:635-640.

Rollinson, H.R. (1993). **Using geochemical data: evaluation, presentation, interpretation**. Longman, Essex, 352 pp.

Roser, B.P. and Korsch, R.J. (1986). Determination of tectonic setting of sandstone-mudstone suites using SiO2 content and K2O/Na2O ratio. **Journal of Geology**. 94: 635-690.

Roser, B.P. and Korsch, R.J. (1988). Provenance signature of sandstone-mudstone suites determined using discriminate function analysis of major element data. **Chemistry Geology**. 67: 119-139.

Sattayarak, N., Srilulwong, S. and Pum-Im, S. (1989). Petroleum Potential of the Triassic pre-Khorat Intermontane Basin in Northeastern Thailand. In: Thanasuthipitak, T., Ounchanum, P. (eds.). **Proceedings of the International Symposium on Intermontane Basins: Geology and Resources** (pp. 43-57). Chieng Mai University.

Sengör, C.A.M. (1979). Mid-Mesozoic closure of Permo-Triassic Tethys and its implication. **Nature**, 279:590-593.

Sengör, C.A.M. (1985). Die Alpiden und die Kimmeriden: Die verdoppelte Geschichte der Tethys. **Geol. Rdsch**. 74(2): 181-213.

Seyedolali, A., Krinsley, D. H., Boggs, S., Ohara, P. F., Dypvik, H. and Goles, G. G. (1997). Provenance interpretation of quartz by scanning electron microscope-cathodoluminescence fabric analysis. **Geology** 25: 787-790.

Shi, G.R. and Waterhouse, J.B. (1991). Early Permainbraciopods from Perak, west Malaysia. **Journal of Southeast Asian Earth Sciences**. 6: 25-39.

Singharajwarapan, S. and Berry, R. (1993). Structural analysis of the accretionary complex in Sirikit Dam area, Uttaradit, Northern Thailand. **Journal of Southeastern Asian Earth Sciences**, 8: 233-245.

Singharajwarapan, S. and Berry, R. (2000). Tectonic implications of the Nan Suture Zone and its relationship to the Sukhothai Fold Belt, Northern Thailand. **Journal of Asian Earth Sciences**. 18: 663-673.

Spiller, F.C.P. (2002). Radiolarian biostratigraphy of Peninsular Malaysia and implications for regional palaeotectonics and palaeogeography. **Palaeontolographica Abteilung a-Palaozoologie-Stratigraphie**. 266 (1-3): 1-8.

Tassanasorn, A.O. (1990). Coalification study in Permian rocks of the Petchabun fold and thrust belt, Thailand. **Ph.D. Thesis**. University of Göttingen, F.R.Germany (unpublished).

Taylor, S.R. and Mclennan, S.M. (1985). **The continental crust:Its composition and evolution**, Oxford and Blackwell, 312 pp.

Thanasuthipitak, T. (1978). Geology of the Uttaradit area and its implications on the tectonic history of Thailand. In: Nutalaya, P. (ed.). **Proc. GEOSEA III** (pp. 187-197). Bangkok, Thailand.

Thanomsap, S. (1992). Structural development on the Khorat Plateau and ist western adjacent area. In: Charusiri, P., et al (eds.). **Proceedings of the Technical Conferences on Development Geology for Thailand into the Year 2000**. Chulalongkorn University, Thailand. pp. 29-38.

Wielchowsky, C.C. and Young, J.D. (1985). **Regional facies variations in Permian rocks of the Phetchabun fold and thrust belt, Thailand**. Conference on the Geology and Mineral Resource Development of NE Thailand, Khon Kaen University, pp. 41-55.

Winkel, R., Ingavat, R. and Helmcke, D. (1983). Facies and Stratigraphy of the Lower-Lower Middle Permian strata of the Phetchabun Fold-Belt in Central Thailand. **Workshop on stratigraphic correlation of Thailand and Malasia**. Haad Yai, 8-10 September. Thailand, pp. 293-306.

Wongwanich, T. and Burrett, C.F. (1983). The Lower Paleozoc of Thailand. **Journal of the Geological Society of Thailand**. 6:21-29.

Wongwanich, T., Burrett, C.F., Tansathein, W. and Chaodumrong, P. (1990). Lower to Mid Paleozoic stratigraphy of mainland Satun province, Southern Thailand. **Journal of Southeastern Asian Earth Sciences**, 4: 1-9.

Wongwanich, T., Wyatt, D., Stait, B. and Burrett, C.F. (1983). The Ordovician system in southern Thailand and northern Malaysia. In: Nutalaya, P. (ed.).

**Proceeding of the Workshop on Stratigraphic correlation of Thailand and Malaysia** (pp. 77-95). Haad Yai, Thailand.

Workman, D.R. (1975). Tectonic evolution of Indochina: **Jour. Geol. Soc. Thailand**, 1: 3-19.

Ueno, K., Igo, H. and Sashida, K. (1993). Lower Permian fusulinaceans from Ban Phia, Chiang Wat Loei, Northeast Thailand. **Transactions and Proceedings of the Paleontological Society of Japan**. N.S. 169: 15-43.

Utha-Aroon, C. and Surinkum, A. (1995). Gypsum Exploration in Wang Sapung, Loei. In: Wannakao, L., (ed.). **Proceedings of the International Conference on Geology, Geotechnology and Mineral Resources of Indochina** (pp. 255-266). Khon Kaen, Thailand.

Yanagida, J. (1966). Early Permian braciopods from north central Thailand. **Geology and Palaeontology of Southeast Asia**. 3: 46-97 pl. 1-23.

Yanagida, J. (1976). Paleobiogeographical consideration on the Late Carboniferous and Early Permian braciopods of central north Thailand. **Geology and Palaeontology of Southeast Asia**. 17: 173-189.

Young, G.M. and Nesbitt, H.E. (1999). Paleoclimatology and provenance of the glaciogenic Gowganda Foramtion (Paleoproterozoic), Ontario, Canada: a chemostratigraphic approach. **Geological Society of America**. 111: 264-274

Zinkernagel, U. (1978). **Cathodoluminescence of quartz and its application to sandstone petrology**. Contrib. to Sediment. 8, Stuttgart E. Schweizerb. Verlag, 69 p.

# APPENDIX A
# GEOCHEMICAL DATA

**Table A-1.** Concentration of trace elements (in ppm) for pelagic sequence, Nam Duk Formation.

| Formation | Pelagic sequence/Nam Duk Formation | | | | | | | | |
|---|---|---|---|---|---|---|---|---|---|
| Sample | *16+410* | *16+590* | *16+700* | *17+065* | *17+275* | *17+700* | *18+326* | *18+430* | *19+450* |
| Rock / Trace ele. | shale | shale | shale | cal.shale | cal.shale | cal.shale | shale | shale | chert |
| Be | 0.36 | 0.76 | 1.05 | 0.64 | 0.60 | 0.31 | 1.74 | 1.06 | 1.56 |
| Sc | 7.52 | 17.5 | 21.9 | 4.05 | 9.84 | 4.82 | 17.7 | 10.7 | 14.7 |
| V | 31.7 | 112 | 208 | 12.5 | 60.8 | 24.1 | 141 | 85.3 | 73.1 |
| Cr | 100 | 141 | 83.5 | 23.1 | 182 | 206 | 100 | 213 | 453 |
| Co | 3.41 | 12.0 | 25.0 | 3.58 | 15.1 | 5.28 | 12.1 | 15.4 | 11.3 |
| Ni | 6.74 | 31.5 | 46.2 | 11.8 | 78.9 | 14.4 | 33.8 | 35.5 | 35.3 |
| Cu | 13.0 | 37.2 | 98.4 | 3.12 | 26.1 | 11.0 | 46.9 | 26.1 | 81.0 |
| Zn | 24.8 | 93.6 | 87.4 | 19.9 | 102 | 21.1 | 104 | 77.2 | 57.8 |
| Ga | 5.23 | 14.4 | 19.9 | 1.45 | 10.4 | 1.88 | 19.4 | 11.3 | 11.9 |
| Rb | 11.1 | 44.9 | 65.2 | 0.79 | 7.40 | 2.85 | 102 | 63.6 | 54.8 |
| Sr | 176 | 395 | 413 | 895 | 473 | 941 | 209 | 407 | 628 |
| Y | 79.2 | 12.2 | 17.4 | 24.1 | 10.1 | 8.69 | 24.3 | 16.3 | 37.0 |
| Zr | 62.5 | 93.9 | 111 | 41.9 | 71.4 | 53.9 | 159 | 147 | 159 |
| Nb | 2.89 | 5.16 | 4.72 | 2.13 | 4.41 | 2.82 | 8.76 | 7.31 | 6.47 |
| Cs | 0.64 | 1.82 | 2.37 | 0.18 | 0.57 | 0.25 | 5.40 | 3.48 | 2.21 |
| Ba | 76.0 | 226 | 300 | 10.2 | 50.5 | 14.2 | 215 | 139 | 116 |
| La | 42.3 | 6.15 | 8.95 | 17.1 | 7.77 | 7.12 | 30.6 | 19.6 | 34.0 |
| Ce | 97.8 | 8.13 | 14.4 | 16.4 | 10.8 | 9.99 | 52.7 | 32.7 | 54.9 |
| Pr | 13.4 | 1.47 | 2.43 | 3.31 | 2.11 | 1.53 | 7.38 | 4.69 | 8.73 |
| Nd | 60.4 | 5.63 | 9.85 | 13.2 | 7.96 | 5.63 | 28.1 | 18.1 | 35.4 |
| Sm | 17.1 | 1.45 | 2.57 | 2.82 | 1.81 | 1.24 | 5.32 | 3.67 | 7.30 |
| Eu | 3.53 | 0.40 | 0.57 | 0.61 | 0.36 | 0.38 | 1.10 | 0.73 | 1.74 |
| Gd | 16.7 | 1.35 | 2.49 | 2.63 | 1.56 | 1.09 | 4.55 | 3.05 | 6.58 |
| Tb | 2.66 | 0.30 | 0.50 | 0.51 | 0.30 | 0.20 | 0.78 | 0.53 | 1.19 |
| Dy | 13.2 | 1.94 | 3.04 | 3.03 | 1.60 | 1.05 | 4.38 | 2.72 | 6.98 |
| Ho | 2.45 | 0.45 | 0.69 | 0.67 | 0.36 | 0.24 | 0.95 | 0.60 | 1.44 |
| Er | 5.62 | 1.31 | 1.94 | 1.83 | 0.99 | 0.71 | 2.57 | 1.61 | 3.60 |
| Tm | 0.76 | 0.20 | 0.30 | 0.28 | 0.14 | 0.10 | 0.39 | 0.24 | 0.53 |
| Yb | 5.55 | 1.52 | 2.21 | 1.92 | 0.98 | 0.67 | 2.75 | 1.76 | 3.52 |
| Lu | 1.00 | 0.25 | 0.36 | 0.32 | 0.16 | 0.11 | 0.45 | 0.31 | 0.59 |
| Hf | 1.16 | 2.64 | 3.31 | 0.73 | 2.02 | 1.56 | 4.84 | 3.84 | 4.66 |
| Ta | 0.12 | 0.30 | 0.27 | 0.08 | 0.25 | 0.13 | 0.64 | 0.48 | 0.44 |
| Pb | 2.13 | 5.58 | 7.86 | 2.69 | 7.74 | 3.38 | 13.7 | 15.4 | 11.1 |
| Th | 1.55 | 4.24 | 2.80 | 0.56 | 2.16 | 1.66 | 8.03 | 6.49 | 3.50 |
| U | 3.10 | 1.43 | 1.27 | 0.83 | 1.27 | 0.71 | 1.81 | 1.65 | 1.12 |

Note: sample no. indicate milestone at the sampling locality along highway no.12

**Table A-2.** Concentration of major elements (in wt%) and trace elements (in ppm) for flysch sequence, Nam Duk Formation.

| Formation | Flysch sequence/Nam Duk Formation | | | | | | | | | | | | | | | |
|---|---|---|---|---|---|---|---|---|---|---|---|---|---|---|---|---|
| Sample | *18+725* | *19+950* | *19+975* | *20+190* | *20+340* | *20+360* | *20+500* | *20+525* | *20+700* | *20+750* | *20+825* | *20+825* | *20+900* | *21+100* | *21+110* | *21+120* |
| Rock / Major ele. | sandstone | sandstone | sandstone | sandstone | sandstone | sandstone | sandstone | sandstone | sandstone | sandstone | shale | sandstone | sandstone | agg. ss. | sandstone | sandstone |
| $SiO_2$ | 42.63 | 18.44 | 45.17 | 50.61 | 54.40 | 27.86 | 59.18 | 50.24 | 61.57 | 47.21 | 53.17 | 59.58 | 57.87 | 38.65 | 51.88 | 51.99 |
| $TiO_2$ | 1.16 | 0.52 | 1.01 | 1.12 | 1.28 | 0.91 | 1.14 | 1.05 | 1.06 | 1.18 | 1.38 | 1.74 | 1.04 | 1.12 | 1.31 | 1.00 |
| $Al_2O_3$ | 4.63 | 1.66 | 3.96 | 5.02 | 5.72 | 2.82 | 5.97 | 5.42 | 6.42 | 5.04 | 6.54 | 9.92 | 7.12 | 4.17 | 6.93 | 5.61 |
| $Fe_2O_3$ | 13.48 | 8.74 | 12.26 | 16.47 | 14.78 | 13.23 | 19.11 | 20.61 | 26.45 | 14.45 | 17.76 | 20.71 | 26.91 | 17.87 | 20.22 | 24.10 |
| MnO | 0.25 | 0.20 | 0.30 | 0.30 | 0.21 | 0.39 | 0.27 | 0.38 | 0.30 | 0.29 | 0.13 | 0.09 | 1.20 | 0.47 | 0.37 | 0.55 |
| MgO | 0.31 | 0.19 | 0.23 | 0.33 | 0.37 | 0.22 | 0.47 | 0.48 | 0.34 | 0.30 | 0.37 | 0.56 | 0.52 | 0.39 | 0.58 | 0.75 |
| CaO | 33.45 | 68.35 | 34.21 | 22.47 | 19.77 | 51.81 | 10.17 | 17.85 | 0.67 | 28.11 | 16.98 | 1.20 | 1.62 | 34.26 | 14.29 | 12.78 |
| $Na_2O$ | 0.00 | 0.00 | *29.43 ppm* | 0.00 | 0.02 | 0.00 | 0.05 | 0.00 | 0.00 | 0.00 | 0.00 | 0.01 | 0.00 | 0.02 | 0.10 | 0.02 |
| $K_2O$ | 1.56 | 0.46 | 1.29 | 2.21 | 2.25 | 1.08 | 2.24 | 2.33 | 2.18 | 1.93 | 2.73 | 5.03 | 2.58 | 1.45 | 2.85 | 1.87 |
| $P_2O_5$ | 0.00 | 0.00 | 0.00 | 0.02 | 0.00 | 0.00 | 0.04 | *17.48 ppm* | 0.10 | 0.00 | *95.35 ppm* | 0.04 | *25.16 ppm* | 0.00 | 0.00 | 0.00 |
| $SO_3$ | 0.79 | 0.50 | 0.34 | 0.19 | 0.14 | 0.52 | 0.19 | 0.34 | 0.12 | 0.59 | 0.16 | 0.23 | 0.29 | 0.34 | 0.36 | 0.25 |
| Sum | 98.26 | 99.06 | 98.77 | 98.74 | 98.94 | 98.84 | 98.83 | 98.70 | 99.21 | 99.10 | 99.22 | 99.11 | 99.15 | 98.74 | 98.89 | 98.92 |
| Trace ele. | | | | | | | *19+600* agg. sh. | | | | | | | | | |
| Be | 0.50 | 0.33 | 0.54 | 0.73 | 0.68 | 0.51 | 1.72 | 0.88 | 0.65 | | 1.82 | 0.83 | 1.18 | | 1.01 | |
| Sc | 6.27 | 4.53 | 5.11 | 6.84 | 6.61 | 5.78 | 13.5 | 7.38 | 7.13 | | 13.8 | 8.96 | 9.96 | | 8.88 | |
| V | 66.9 | 29.3 | 73.0 | 107 | 85.4 | 72.4 | 127 | 111 | 70.2 | | 115 | 81.2 | 86.7 | | 107 | |
| Cr | 565 | 269 | 1079 | 1720 | 1133 | 1114 | 242 | 1787 | 714 | | 206 | 631 | 754 | | 1473 | |
| Co | 12.5 | 7.47 | 11.5 | 15.8 | 13.3 | 18.1 | 19.9 | 17.1 | 11.4 | | 7.34 | 8.39 | 25.1 | | 17.4 | |
| Ni | 27.3 | 20.7 | 28.0 | 40.3 | 42.3 | 36.3 | 35.6 | 46.1 | 30.8 | | 32.8 | 27.3 | 40.8 | | 91.2 | |
| Cu | 9.49 | 4.39 | 10.5 | 15.0 | 11.8 | 12.0 | 45.0 | 15.5 | 11.9 | | 28.4 | 15.7 | 17.5 | | 20.2 | |
| Zn | 55.4 | 33.3 | 38.1 | 44.7 | 48.7 | 37.4 | 117 | 48.4 | 43.6 | | 85.8 | 56.4 | 108 | | 55.9 | |
| Ga | 6.70 | 3.05 | 5.33 | 7.97 | 8.13 | 5.10 | 16.2 | 8.53 | 7.94 | | 16.2 | 10.3 | 11.1 | | 11.2 | |
| Rb | 37.5 | 10.7 | 29.1 | 49.8 | 47.9 | 26.8 | 86.6 | 55.1 | 46.0 | | 119 | 61.4 | 62.4 | | 70.5 | |
| Sr | 240 | 1544 | 703 | 289 | 269 | 674 | 429 | 264 | 358 | | 95.4 | 104 | 60.8 | | 263 | |
| Y | 20.0 | 18.8 | 13.0 | 13.1 | 17.1 | 14.4 | 17.9 | 14.6 | 13.8 | | 23.9 | 18.1 | 27.4 | | 15.8 | |
| Zr | 162 | 123 | 149 | 135 | 232 | 228 | 107 | 149 | 219 | | 193 | 229 | 211 | | 281 | |
| Nb | 6.97 | 4.41 | 6.22 | 7.05 | 7.70 | 5.49 | 8.63 | 7.36 | 7.26 | | 11.3 | 8.34 | 8.90 | | 8.86 | |
| Cs | 1.93 | 0.74 | 1.60 | 3.33 | 2.34 | 1.37 | 4.63 | 3.21 | 2.36 | | 7.58 | 3.62 | 3.88 | | 3.77 | |
| Ba | 93.3 | 31.3 | 65.5 | 118 | 120 | 67.4 | 294 | 135 | 114 | | 270 | 149 | 153 | | 173 | |
| La | 19.3 | 16.7 | 15.3 | 19.3 | 22.1 | 15.4 | 32.4 | 16.7 | 17.9 | | 30.8 | 22.1 | 20.9 | | 20.3 | |
| Ce | 35.3 | 22.9 | 25.9 | 34.1 | 39.5 | 27.1 | 57.9 | 29.7 | 32.7 | | 57.3 | 40.3 | 39.1 | | 37.5 | |
| Pr | 5.13 | 3.81 | 3.69 | 4.56 | 5.12 | 3.79 | 7.77 | 4.02 | 4.42 | | 7.49 | 5.31 | 5.16 | | 4.92 | |
| Nd | 20.6 | 15.4 | 13.5 | 16.2 | 18.6 | 14.0 | 28.9 | 14.3 | 15.7 | | 26.7 | 18.8 | 19.1 | | 17.3 | |
| Sm | 4.51 | 3.82 | 2.85 | 3.13 | 3.54 | 3.22 | 4.88 | 2.99 | 2.95 | | 4.96 | 3.58 | 4.42 | | 3.36 | |
| Eu | 0.97 | 0.82 | 0.69 | 0.66 | 0.70 | 0.89 | 0.84 | 0.74 | 0.63 | | 0.93 | 0.72 | 1.11 | | 0.82 | |
| Gd | 3.59 | 3.28 | 2.44 | 2.66 | 2.95 | 2.78 | 3.95 | 2.75 | 2.51 | | 4.29 | 3.14 | 4.52 | | 3.06 | |
| Tb | 0.60 | 0.55 | 0.39 | 0.43 | 0.52 | 0.46 | 0.61 | 0.47 | 0.41 | | 0.73 | 0.53 | 0.84 | | 0.52 | |
| Dy | 3.32 | 2.92 | 2.09 | 2.29 | 2.96 | 2.52 | 3.45 | 2.68 | 2.35 | | 4.27 | 3.05 | 4.63 | | 2.84 | |
| Ho | 0.64 | 0.56 | 0.42 | 0.45 | 0.59 | 0.48 | 0.66 | 0.51 | 0.48 | | 0.87 | 0.62 | 0.92 | | 0.56 | |
| Er | 1.73 | 1.54 | 1.22 | 1.31 | 1.67 | 1.33 | 1.89 | 1.41 | 1.43 | | 2.48 | 1.77 | 2.41 | | 1.68 | |
| Tm | 0.25 | 0.21 | 0.18 | 0.19 | 0.24 | 0.19 | 0.29 | 0.20 | 0.22 | | 0.37 | 0.27 | 0.33 | | 0.26 | |
| Yb | 1.76 | 1.56 | 1.30 | 1.43 | 1.79 | 1.33 | 2.18 | 1.45 | 1.59 | | 2.63 | 1.92 | 2.35 | | 1.91 | |
| Lu | 0.28 | 0.24 | 0.23 | 0.23 | 0.28 | 0.21 | 0.35 | 0.23 | 0.27 | | 0.43 | 0.32 | 0.38 | | 0.33 | |
| Hf | 4.56 | 3.45 | 4.25 | 3.86 | 6.65 | 6.48 | 3.13 | 3.97 | 6.02 | | 5.55 | 6.33 | 5.96 | | 8.11 | |
| Ta | 0.50 | 0.27 | 0.41 | 0.47 | 0.57 | 0.34 | 0.63 | 0.50 | 0.52 | | 0.84 | 0.60 | 0.64 | | 0.65 | |
| Pb | 15.8 | 8.68 | 6.95 | 7.14 | 5.50 | 15.4 | 22.0 | 8.45 | 10.8 | | 21.3 | 13.3 | 11.2 | | 11.7 | |
| Th | 6.40 | 3.25 | 4.97 | 6.15 | 7.17 | 4.56 | 9.01 | 6.31 | 6.19 | | 11.5 | 7.63 | 7.92 | | 8.30 | |
| U | 1.61 | 1.67 | 1.35 | 1.46 | 1.82 | 1.31 | 1.90 | 1.54 | 1.68 | | 2.44 | 1.90 | 2.16 | | 2.30 | |

Note: sample no. indicate milestone at the sampling locality along highway no.12

**Table A-3.** Concentration of major elements (in wt%) and trace elements (in ppm) for molasse sequence, Nam Duk Formation.

| Formation | Molasse sequence/Nam Duk Formation | | | | | | | | | | | | | |
|---|---|---|---|---|---|---|---|---|---|---|---|---|---|---|
| Sample | *34+600* | *34+750* | *35+150* | *35+175* | *36+150* | *36+600* | *36+600* | *36+650* | *36+700* | *40+400* | *40+400* | *40+450* | *40+450* | *40+560* |
| Rock / Major ele. | sandstone | sandstone | sandstone | sandstone | sandstone | sandstone | shale | sandstone | sandstone | sandstone | shale | sandstone | shale | shale |
| $SiO_2$ | 55.23 | 42.55 | 55.95 | 50.92 | 60.38 | 49.67 | 51.56 | 52.49 | 69.01 | 55.25 | 55.33 | 54.48 | 47.06 | 22.14 |
| $TiO_2$ | 1.42 | 1.36 | 1.08 | 0.87 | 1.23 | 1.32 | 1.97 | 1.58 | 1.54 | 1.00 | 2.06 | 1.91 | 1.21 | 0.77 |
| $Al_2O_3$ | 8.47 | 7.04 | 7.20 | 7.12 | 9.53 | 7.11 | 10.05 | 8.45 | 8.70 | 5.61 | 11.11 | 11.74 | 5.71 | 3.10 |
| $Fe_2O_3$ | 18.69 | 19.71 | 21.06 | 25.31 | 23.43 | 22.62 | 19.42 | 14.84 | 14.41 | 25.03 | 22.18 | 21.49 | 25.46 | 7.67 |
| MnO | 0.22 | 0.31 | 0.22 | 0.33 | 0.22 | 0.24 | 0.19 | 0.33 | 0.04 | 0.35 | 0.12 | 0.21 | 0.69 | 0.09 |
| MgO | 0.48 | 0.58 | 0.38 | 0.49 | 0.33 | 0.63 | 0.53 | 0.24 | 0.32 | 0.43 | 0.41 | 0.42 | 0.64 | 0.13 |
| CaO | 11.09 | 24.55 | 10.30 | 11.55 | 1.18 | 14.50 | 8.52 | 17.70 | 1.07 | 9.36 | 2.74 | 3.32 | 15.94 | 63.46 |
| $Na_2O$ | 0.00 | 0.00 | 0.00 | *39.62ppm* | 0.00 | 0.00 | 0.00 | *51.36 ppm* | 0.00 | 0.00 | 0.00 | 0.00 | 0.00 | 0.00 |
| $K_2O$ | 3.10 | 2.53 | 2.11 | 1.95 | 2.78 | 2.43 | 5.31 | 3.40 | 3.82 | 1.63 | 4.68 | 5.18 | 2.04 | 1.36 |
| $P_2O_5$ | 0.05 | *83.68 ppm* | 0.03 | 0.03 | 0.10 | 0.03 | 0.05 | 0.09 | 0.13 | 0.02 | 0.04 | 0.06 | 0.00 | 0.00 |
| $SO_3$ | 0.24 | 0.68 | 0.51 | 0.48 | 0.10 | 0.54 | 0.99 | 0.12 | 0.13 | 0.29 | 0.33 | 0.28 | 0.24 | 0.53 |
| Sum | 98.99 | 99.31 | 98.84 | 99.05 | 99.28 | 99.09 | 98.59 | 99.24 | 99.17 | 98.70 | 99.00 | 99.09 | 99.09 | 99.25 |
| Trace ele. | | | | | | | | | | | | | | |
| Be | 1.43 | | 1.08 | 1.23 | | 1.09 | 2.19 | | 0.99 | 0.83 | 2.04 | 0.93 | 2.12 | 0.77 |
| Sc | 8.64 | | 7.78 | 7.88 | | 7.80 | 15.9 | | 7.93 | 8.18 | 17.5 | 7.50 | 13.9 | 6.11 |
| V | 82.7 | | 106 | 103 | | 81.6 | 109 | | 62.3 | 124 | 114 | 78.1 | 101 | 47.3 |
| Cr | 879 | | 1692 | 1611 | | 815 | 287 | | 178 | 2184 | 330 | 815 | 322 | 136 |
| Co | 13.3 | | 14.2 | 15.2 | | 12.5 | 15.1 | | 5.76 | 21.5 | 17.0 | 14.2 | 14.4 | 7.45 |
| Ni | 37.5 | | 49.7 | 48.1 | | 41.9 | 55.0 | | 21.7 | 53.9 | 40.4 | 27.0 | 220 | 17.1 |
| Cu | 19.9 | | 23.6 | 18.2 | | 14.5 | 41.2 | | 9.95 | 19.3 | 37.9 | 12.4 | 43.2 | 6.51 |
| Zn | 74.5 | | 85.6 | 69.0 | | 55.9 | 108 | | 37.8 | 54.1 | 87.5 | 42.4 | 94.8 | 38.4 |
| Ga | 12.9 | | 10.1 | 10.3 | | 11.0 | 18.8 | | 11.3 | 9.63 | 18.4 | 8.34 | 17.2 | 6.17 |
| Rb | 67.5 | | 50.4 | 50.5 | | 57.0 | 132 | | 62.7 | 42.2 | 110 | 50.0 | 118 | 44.0 |
| Sr | 132 | | 97.2 | 137 | | 138 | 118 | | 60.5 | 104 | 124 | 214 | 133 | 961 |
| Y | 21.5 | | 19.1 | 19.2 | | 22.7 | 26.2 | | 17.6 | 18.4 | 29.8 | 21.4 | 28.7 | 14.3 |
| Zr | 220 | | 231 | 191 | | 243 | 170 | | 230 | 168 | 324 | 238 | 211 | 88.3 |
| Nb | 9.89 | | 9.12 | 7.77 | | 9.51 | 11.8 | | 10.2 | 7.58 | 13.1 | 8.33 | 11.4 | 5.18 |
| Cs | 4.07 | | 2.93 | 2.83 | | 3.32 | 10.2 | | 2.86 | 3.51 | 9.63 | 3.68 | 11.1 | 3.47 |
| Ba | 213 | | 152 | 158 | | 170 | 327 | | 180 | 119 | 259 | 125 | 264 | 109 |
| La | 25.3 | | 17.8 | 18.5 | | 24.1 | 33.9 | | 26.8 | 20.1 | 35.8 | 21.3 | 32.9 | 14.1 |
| Ce | 48.1 | | 33.3 | 35.0 | | 45.8 | 65.4 | | 49.9 | 37.4 | 68.2 | 38.3 | 63.4 | 23.5 |
| Pr | 6.05 | | 4.32 | 4.64 | | 5.89 | 8.29 | | 6.31 | 4.96 | 8.63 | 4.88 | 8.16 | 3.32 |
| Nd | 22.4 | | 16.0 | 17.3 | | 21.9 | 30.9 | | 22.6 | 18.7 | 32.7 | 17.5 | 30.9 | 13.1 |
| Sm | 4.57 | | 3.37 | 3.87 | | 4.45 | 5.95 | | 4.09 | 4.37 | 6.35 | 3.84 | 6.04 | 2.96 |
| Eu | 0.95 | | 0.82 | 1.02 | | 1.08 | 1.15 | | 0.81 | 1.05 | 1.22 | 0.87 | 1.18 | 0.81 |
| Gd | 4.11 | | 3.23 | 3.70 | | 4.09 | 4.93 | | 3.25 | 3.98 | 5.29 | 4.13 | 5.01 | 2.39 |
| Tb | 0.70 | | 0.59 | 0.66 | | 0.71 | 0.79 | | 0.53 | 0.69 | 0.90 | 0.72 | 0.86 | 0.40 |
| Dy | 3.99 | | 3.48 | 3.61 | | 4.09 | 4.47 | | 3.04 | 3.59 | 5.21 | 3.76 | 5.02 | 2.17 |
| Ho | 0.77 | | 0.69 | 0.69 | | 0.78 | 0.93 | | 0.62 | 0.69 | 1.10 | 0.72 | 1.02 | 0.44 |
| Er | 2.08 | | 1.91 | 1.86 | | 2.16 | 2.59 | | 1.79 | 1.83 | 3.02 | 1.92 | 2.88 | 1.20 |
| Tm | 0.31 | | 0.32 | 0.27 | | 0.36 | 0.41 | | 0.30 | 0.29 | 0.47 | 0.32 | 0.45 | 0.17 |
| Yb | 2.29 | | 2.14 | 2.04 | | 2.34 | 2.82 | | 2.02 | 1.87 | 3.29 | 2.04 | 3.07 | 1.16 |
| Lu | 0.35 | | 0.34 | 0.32 | | 0.37 | 0.47 | | 0.31 | 0.30 | 0.57 | 0.34 | 0.49 | 0.19 |
| Hf | 6.30 | | 6.88 | 5.49 | | 7.01 | 4.89 | | 6.41 | 5.10 | 9.32 | 6.95 | 6.12 | 2.41 |
| Ta | 0.76 | | 0.73 | 0.57 | | 0.73 | 0.95 | | 0.81 | 0.55 | 1.05 | 0.61 | 0.92 | 0.33 |
| Pb | 18.1 | | 11.8 | 9.15 | | 15.3 | 21.7 | | 11.4 | 15.3 | 20.6 | 9.93 | 23.6 | 8.11 |
| Th | 10.2 | | 8.04 | 7.14 | | 9.04 | 12.9 | | 10.00 | 7.44 | 13.8 | 7.78 | 12.5 | 4.53 |
| U | 2.59 | | 2.00 | 1.73 | | 2.17 | 2.76 | | 2.15 | 1.89 | 3.18 | 2.06 | 2.81 | 1.47 |

Note: sample no. indicate milestone at the sampling locality along highway no.12

**Table A-4.** Concentration of major elements (in wt%) and trace elements (in ppm) for Late Paleozoic siliciclastic sediments from Loei and Saraburi area.

| Formation | Late Paleozoic Siliciclastic sediments from Loei and Saraburi area | | | | | | | | | | | |
|---|---|---|---|---|---|---|---|---|---|---|---|---|
| Sample | *THL 01* | *THL 04* | *THL 05* | *THL 06* | *THL 07* | *THL 08* | *THL 09* | *THS 10* | *THS 11* | *THS 12* | *THP 13* | *THS 15* |
| Major ele. \ Rock | sandstone | sandstone | sandstone | sandstone | sandstone | shale | sandstone | sandstone | shale | chert | sandstone | shale |
| $SiO_2$ | 41.41 | 67.62 | 48.86 | 48.25 | 54.86 | 59.79 | 46.16 | 44.25 | 49.70 | 86.72 | 60.85 | 46.92 |
| $TiO_2$ | 2.05 | 2.61 | 1.82 | 1.25 | 1.33 | 2.05 | 1.42 | 1.52 | 1.83 | 0.38 | 1.54 | 1.70 |
| $Al_2O_3$ | 7.15 | 12.72 | 7.49 | 5.69 | 6.09 | 11.56 | 7.03 | 6.93 | 12.30 | 3.50 | 8.48 | 9.59 |
| $Fe_2O_3$ | 14.37 | 3.90 | 19.99 | 18.88 | 17.87 | 16.75 | 24.60 | 16.97 | 28.36 | 6.35 | 19.86 | 21.78 |
| MnO | 0.42 | 0.02 | 0.21 | 0.72 | 0.38 | 0.18 | 0.28 | 0.26 | 0.08 | 0.10 | 0.10 | 0.24 |
| MgO | 0.28 | 0.10 | 0.49 | 0.56 | 0.51 | 0.30 | 0.43 | 0.24 | 0.74 | 0.06 | 0.45 | 0.65 |
| CaO | 30.27 | 5.95 | 17.78 | 20.30 | 15.12 | 1.62 | 17.07 | 26.62 | 2.77 | 0.64 | 4.06 | 13.07 |
| $Na_2O$ | 0.09 | 0.00 | *57.18 ppm* | 0.00 | 0.07 | 0.00 | 0.00 | 0.00 | 0.02 | 0.03 | 0.00 | 0 |
| $K_2O$ | 2.97 | 5.94 | 2.24 | 2.46 | 2.38 | 6.55 | 2.19 | 2.31 | 2.66 | 1.31 | 3.58 | 4.58 |
| $P_2O_5$ | 0.05 | 0.00 | 0.04 | 0.00 | 0.02 | 0.11 | 0.04 | *96.66 ppm* | 0.00 | 0.00 | 0.13 | 0 |
| $SO_3$ | 0.03 | 0.19 | 0.10 | 0.83 | 0.38 | 0.16 | 0.08 | 0.11 | 0.11 | 0.31 | 0.10 | 0.65 |
| Sum | 99.09 | 99.05 | 99.02 | 98.94 | 99.01 | 99.07 | 99.30 | 99.21 | 98.57 | 99.40 | 99.15 | 99.54 |
| Trace ele. | | | | | | | | | | | | |
| Be | 1.10 | 1.47 | 0.84 | 1.05 | 0.94 | 2.27 | 1.00 | 1.12 | 1.42 | 0.55 | 1.43 | 2.38 |
| Sc | 10.1 | 10.3 | 10.8 | 7.22 | 8.17 | 16.7 | 10.5 | 6.88 | 23.0 | 3.47 | 13.0 | 15.0 |
| V | 76.9 | 70.3 | 95.6 | 96.7 | 89.1 | 143 | 83.7 | 61.9 | 81.7 | 38.2 | 99.2 | 107 |
| Cr | 360 | 173 | 541 | 1326 | 1103 | 104 | 519 | 355 | 40.7 | 602 | 396 | 226 |
| Co | 9.12 | 2.78 | 13.8 | 15.6 | 13.7 | 7.99 | 10.5 | 11.4 | 7.69 | 5.63 | 13.2 | 13.2 |
| Ni | 31.6 | 80.3 | 32.2 | 41.6 | 44.2 | 32.3 | 35.9 | 26.6 | 7.42 | 22.4 | 51.2 | 35.9 |
| Cu | 12.5 | 9.02 | 15.4 | 16.3 | 15.6 | 46.6 | 18.0 | 9.23 | 83.1 | 9.65 | 12.2 | 35.4 |
| Zn | 55.2 | 24.7 | 56.9 | 47.8 | 49.1 | 84.5 | 53.1 | 56.7 | 83.4 | 17.3 | 72.1 | 80.1 |
| Ga | 11.0 | 15.4 | 11.7 | 9.67 | 9.97 | 21.2 | 12.4 | 9.61 | 20.4 | 5.24 | 14.7 | 18.8 |
| Rb | 57.8 | 94.0 | 47.8 | 63.3 | 56.9 | 149 | 58.3 | 57.7 | 38.6 | 16.9 | 63.9 | 142 |
| Sr | 158 | 63.1 | 146 | 175 | 144 | 103 | 79.1 | 96.9 | 411 | 14.7 | 108 | 126 |
| Y | 23.5 | 22.6 | 27.2 | 18.2 | 21.8 | 27.4 | 20.8 | 23.6 | 41.3 | 16.2 | 18.6 | 29.3 |
| Zr | 167 | 520 | 469 | 281 | 313 | 162 | 163 | 266 | 176 | 74.2 | 218 | 184 |
| Nb | 8.19 | 11.2 | 9.01 | 8.86 | 9.32 | 12.2 | 9.18 | 8.93 | 6.40 | 4.31 | 8.05 | 13.1 |
| Cs | 2.82 | 4.76 | 3.19 | 2.95 | 2.88 | 9.22 | 2.88 | 3.31 | 1.76 | 0.63 | 3.66 | 9.20 |
| Ba | 173 | 262 | 159 | 166 | 173 | 352 | 146 | 210 | 714 | 189 | 212 | 325 |
| La | 20.9 | 34.0 | 27.4 | 23.2 | 23.6 | 37.6 | 23.9 | 26.3 | 67.7 | 20.4 | 27.8 | 36.0 |
| Ce | 37.7 | 65.7 | 50.8 | 43.5 | 44.6 | 71.0 | 43.8 | 51.2 | 34.5 | 28.0 | 49.4 | 70.2 |
| Pr | 5.03 | 8.63 | 6.64 | 5.62 | 5.76 | 9.11 | 5.74 | 6.63 | 24.2 | 6.01 | 6.40 | 9.05 |
| Nd | 18.9 | 30.5 | 24.3 | 20.0 | 20.5 | 33.4 | 21.0 | 24.8 | 89.5 | 22.8 | 23.0 | 33.8 |
| Sm | 4.16 | 5.75 | 4.78 | 3.87 | 3.93 | 6.17 | 4.26 | 5.10 | 17.1 | 4.19 | 4.48 | 6.61 |
| Eu | 0.98 | 1.13 | 0.98 | 0.89 | 0.89 | 1.26 | 0.98 | 1.12 | 3.42 | 0.85 | 0.89 | 1.30 |
| Gd | 3.92 | 4.41 | 4.40 | 3.50 | 3.71 | 5.21 | 3.86 | 4.72 | 11.5 | 3.04 | 3.92 | 5.60 |
| Tb | 0.67 | 0.71 | 0.75 | 0.56 | 0.62 | 0.83 | 0.62 | 0.80 | 1.90 | 0.53 | 0.65 | 0.94 |
| Dy | 3.67 | 4.00 | 4.15 | 3.16 | 3.67 | 4.81 | 3.39 | 4.20 | 9.67 | 2.76 | 3.56 | 5.38 |
| Ho | 0.76 | 0.81 | 0.89 | 0.65 | 0.78 | 1.02 | 0.70 | 0.77 | 1.59 | 0.52 | 0.66 | 1.08 |
| Er | 1.99 | 2.26 | 2.44 | 1.80 | 2.11 | 2.72 | 1.89 | 2.10 | 4.25 | 1.48 | 1.88 | 2.99 |
| Tm | 0.29 | 0.35 | 0.36 | 0.26 | 0.32 | 0.39 | 0.28 | 0.30 | 0.60 | 0.21 | 0.28 | 0.45 |
| Yb | 2.12 | 2.59 | 2.72 | 2.00 | 2.42 | 2.96 | 1.99 | 2.11 | 4.09 | 1.46 | 1.95 | 3.27 |
| Lu | 0.35 | 0.44 | 0.45 | 0.34 | 0.40 | 0.49 | 0.34 | 0.34 | 0.64 | 0.22 | 0.32 | 0.54 |
| Hf | 4.88 | 13.9 | 12.9 | 8.02 | 9.02 | 4.75 | 4.59 | 7.46 | 5.48 | 1.96 | 6.47 | 5.83 |
| Ta | 0.57 | 0.88 | 0.64 | 0.66 | 0.69 | 0.94 | 0.66 | 0.69 | 0.42 | 0.22 | 0.60 | 1.12 |
| Pb | 8.55 | 17.2 | 13.0 | 10.6 | 10.1 | 10.2 | 8.81 | 12.3 | 19.4 | 5.80 | 10.3 | 22.7 |
| Th | 6.78 | 13.0 | 9.78 | 8.26 | 8.40 | 14.9 | 8.42 | 8.91 | 6.51 | 1.72 | 11.2 | 14.9 |
| U | 1.78 | 3.05 | 2.66 | 2.11 | 2.28 | 3.04 | 2.18 | 2.77 | 1.85 | 0.52 | 2.38 | 3.04 |

# APPENDIX B
# GLOSSARY

# Glossary of Thai Geographic Terms

| | | |
|---|---|---|
| Changwat | = | Province, city |
| Amphoe | = | Sub-province, town, district |
| Ban | = | Village, small community |
| Doi | = | Mount, mountain, a proiment peak of a mountain |
| Huai | = | Gully, creek |
| Khao | = | Hill, isolated mountain |
| Khlong | = | Stream, canal |
| Mae | = | River |
| Mae Nam | = | Large River |
| Phu | = | Hill or mountain (especially northeastern Thailand) |
| Phu Khao | = | A mountain range |
| Wat | = | Temple |

# BIOGRAPHY

Mr. Kitsana Malila was born on February 3, 1978 in Suhkothai province, Thailand. He is the older brother of three member's family. He began his first education at the age of six and completed the Primary School from Wat Bumpenneau School, Bangkok. He continued with his High School in Triam-Udomsuksa-Nomklao School. In May 1995, he passed the national entrance examination to study in the School of Geotechnology, Institute of Engineering, Suranaree University of Technology (SUT), Nakhon Ratchasima. After graduation, he served in position of assistant geotechnical engineer at the GMT Co., Ltd. between January – April, 1999. Afterward, he continued with his graduate studied in SUT and earned his Master's Degree in Geotechnology in May 2002. Currently, he is a Ph.D. candidate in Geotechnology, SUT.